主論文

Design of New Reactions and Ligands for Oxidative Coupling

酸化的カップリングのための新しい反応と配位子の設計

Kazuhiro Hata

秦　　一　博

Department of Chemistry, Graduate School of Science
Nagoya University

2015

Preface

The studies in this thesis have been carried out under the direction of Prof. Dr. Kenichiro Itami at Nagoya University between April 2010 and March 2015. The studies are concerned with design of new reactions and ligands for oxidative coupling.

I like to express my sincerest gratitude to:

Prof. Dr. Kenichiro Itami for his continuous advice, helpful discussions, valuable support, earnest guidance and hearty encouragement during these days. Associate Prof. Dr. Junichiro Yamaguchi for his technical assistance, valuable advice, various suggestion and warm encouragement during these days. WPI Associate Prof. Dr. Shinya Hagihara for his continuous advice, many discussions, heartfelt encouragement. JST-ERATO Designated Associate Prof. Dr. Yasutomo Segawa for his technical advice, various support, and measurement of X-ray crystallography. Dr. Hideto Ito for his continuous advice, technical advice, sincere guidance and helpful discussion. Assistant Dr. Kei Murakami for his various advice, helpful discussions and hearty.

Prof. Dr. Armido Studer (Westfälische Wilhelms-Universität, Münster, Germany), for his kindly accepting as a visiting student during October 2012 to May 2013, sincere guidance, helpful discussions and fantastic collaboration. Dr. Zhiheng He for his helpful discussions. Dr. Constantin Gabriel Daniliuc for his measurement of X-ray crystallography. Prof. Dr. Kazuyuki Tatsumi, Ms. Kihara for their kind support throughout this collaboration. Prof. Dr. Shigehiro Yamaguchi for his kind support throughout this collaboration, brilliant advice and excellent discussions. Dr. Ulrich Hennecke, Dr. Ludger Tebben, Ms. Sandra, Thüer and Ms. Martina Prekel for their help.

Dr. Christoph Rosorius, and Mr. Tetsushi Yoshidomi for their active collaboration and constant discussions.

Prof. Dr. Masato Kitamura, Associate Prof. Dr. Susumu Saito, Associate Prof. Dr. Aiko Fukazawa, WPI Associate Prof. Dr. Masayasu Taki, Associate Prof. Dr. Yasuhiro

Ohki, Dr. Hiroshi Naka, Dr. Shohei Saito Dr. Shinji Tanaka, Dr. Jun Shimokawa Dr. Masakazu Nambo, Dr. Haruka Omachi and Dr. Shunsuke Oishi for their help and brilliant advice.

Mr. Toshiaki Noda, Ms. Hideko Natsume, Mr. Hisakazu Okamoto for excellent works of scientific glassware. Dr. Kin-ichi Oyama for the assistance in mass spectrometry and measurement of elemental analysis. Mr. Yutaka Maeda for his support in NMR analysis. Dr. Keiko Kuwata for the assistance in mass spectrometry.

Ms. Rika Kato, Ms. Yui Ueyama, Ms. Hiromi Yamaguchi, Ms, Akemi Saito and Ms. Nanako Kato for their kind assistance and help.

Dr. Shuichi Yanagisawa
Ms. Akiko Katsura
Mr. Takehisa Maekawa
Dr. Debasis Mandal
Dr. Sylvia Kirchberg
Mr. Kei Muto
Ms. Hiromi Yoshida
Dr. Kazuya Yamaguchi
Mr. Yuki Ishii
Ms. Keika Hattori
Mr. Hiroki Kamiya
Mr. Takao Fujikawa
Ms. Yuko Kamada
Mr. Shin Suzuki
Ms. Friederike Sibbel
Mr. Masahiko Yoshimura
Mr. Kenta Kato
Dr. Eiji Yamaguchi
Dr. Hua Zhang
Dr. Jiao Jiao
Dr. Kirika Ueda
Mr. Toshiki Kojima
Mr. Atsushi Yamaguchi
Dr. Kenji Mochida
Mr. Kazuma Amaike
Mr. Katsuma Matsui
Dr. Petr Šenel
Mr. Kyohei Ozaki
Mr. Takahiro Uehara
Ms. Yukari Mitamura
Dr. Shuhua Chou
Mr. Hiroki Kondo
Ms. Natsumi Kubota
Mr. Ryosuke Takise
Mr. Shin Miyamura
Mr. Tsuyoshi Oshima
Ms. Kaho Maeda
Dr. Ziadi Asraa
Mr. Yasuto Hatakeyama
Ms. Eva Koch
Mr. Takuya Yamamoto
Mr. Satoshi Tani
Ms. Sanae Matsuura
Dr. Katsuaki Kawasumi
Mr. Hiroyuki Ishikawa
Ms. Akiko Yagi
Dr. Anna Junker
Mr. Kazuki Kimura
Mr. Tomonori Kajino
Dr. Lilia Lohley
Dr. Venkata Gandikota
Ms. Misaho Araki
Mr. Yutaro Saito
Mr. Richard Maceiczyk
Mr. Nils Schöler
Mr. Jun Orii
Mr. Shun Yamashita
Mr. Kakishi Uno
Mr. Dominik Bergman
Mr. Artur Kokornaczyk

Ms. Katie Chepiga | Ms. Mari Shibata | Mr. Kento Otani
Mr. Keishu Okada | Mr. Takahiro Kawakami | Ms. Chisa Kobayashi
Mr. Keiichiro Murai | Ms. Manami Muraki | Mr. Shuya Yamada
Mr. Michel Wade | Ms. Humin Dai | Mr. Takeshi Kaneda
Ms. Masako Fushimi | Dr. Lingkui Meng | Dr. Guillaume Povie
and all other past present members of Prof. Itami's group for their enthusiasm, kind consideration, great discussions and excellent relationship.

All other member of WPI ITbM, JST-ERATO Itami Molecular Nanocarbon Project, Prof. Studer's group, Prof. Yamaguchi's group Prof. Noyori's group, Prof. Kitamura's group and IRTG Nagoya-Münster for their kind support and encouragement.

The Japan Society for the Promotion of Science (JSPS) for the research fellowship for young scientist (DC2) and for Strategic Young Researcher Overseas Visits Program for Accelerating Brain Circulation, and Integrative Graduate Education and Research Program in Green Natural Science (IGER) for financial support.

Finally, I express my deep appreciate to my family, Mr. Yasufumi Hata, Ms. Mie Hata and Ms. Machiko Hata for their constant assistance and encouragement.

Kazuhiro Hata

Department of Chemistry
Graduate School of Science
Nagoya University
2015

Contents

General Introduction

1. Transition Metal-Catalyzed Oxidative Coupling of Aromatic Compounds

Classical Coupling Reaction and Oxidative Coupling Reaction. Transition metal-catalyzed coupling reaction is one of the most important reactions to obtain synthetically valuable compounds. Especially for several decades, coupling reaction between aromatic compounds has been well developed by many researchers for the construction of biaryls, which are quite important materials in the field of organic synthesis, physical organic chemistry and natural product synthesis as well as materials science. In general, syntheses of biaryl compounds are achieved by cross-coupling between aryl halides or aryl sulfonates and arylmetal compounds in the presence of transition metal catalysts. For example, palladium-catalyzed cross-coupling of aryl halides with arylmetals, such as aryllithium (Murahashi coupling),[1] arylmagnesium (Kumada–Tamao–Corriu coupling),[2] arylstannane (Migita–Kosugi–Stille coupling),[3] arylzinc (Negishi coupling),[4] arylboron (Suzuki–Miyaura coupling),[5] arylsilane (Hiyama coupling),[6] are well known as general cross-coupling methods (Figure 1).

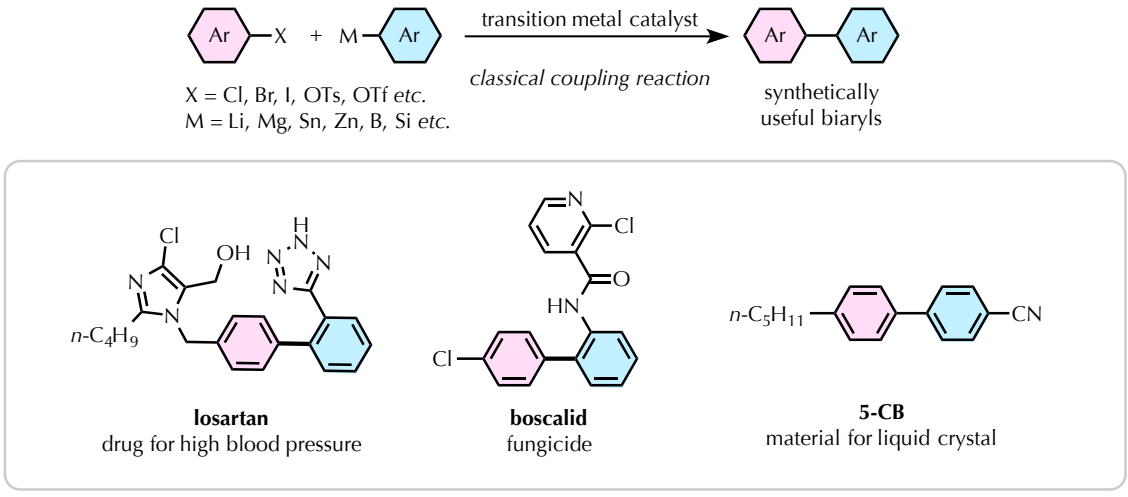

Figure 1. Classical coupling reaction for synthesis of biaryls. X = leaving groups, M = metal or electropositive element.

In recent years, oxidative coupling reaction is in the limelight and has been vigorously investigated as one of efficient and alternative approach to obtain biaryls. In contrast to the classical coupling reactions (C–X/C–M type) that couple electrophiles

(aryl halides) and nucleophiles (arylmetals), oxidative coupling reactions achieve the coupling between nucleophiles (Figure 2). In most of cases, this type of transformation can be achieved in the presence of transition metal catalyst (TM) and external oxidant (Ox) with two nucleophiles such as arylmetals. While a number of transition metal-catalyzed oxidative coupling reactions are reported, many problems still remain unsolved. For example, harsh oxidative reaction conditions and narrow scope of applicable substrates limit the opportunity to apply oxidative coupling to organic synthesis. Therefore practical and efficient transformation is strongly demanded for the further development of oxidative coupling reaction.

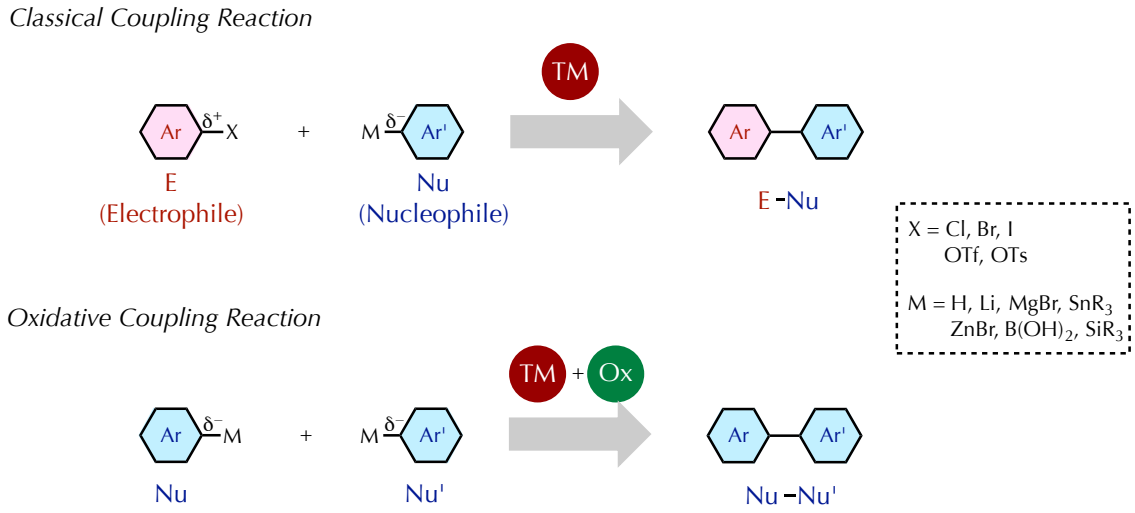

Figure 2. Classical coupling reaction and oxidative coupling reaction. TM = transition metal catalyst, Ox = oxidant.

In the transition metal-catalyzed oxidative coupling, oxidant plays a quite important role to oxidize the inactive low-valent transition metal to provide active and strongly electrophilic high-valent metal species (Figure 3). This high-valent metal species shows higher reactivities toward coupling reaction on metal *via* transmetalation and/or C–H metalation. The thus-formed arylmetal intermediate is active enough for various subsequent reactions, such as transmetalation, C–H metalation, carbometalation, and π-complexation, resulting in the formation of biaryls through reductive elimination or further coupling reaction along with regeneration of low-valent transition metal.

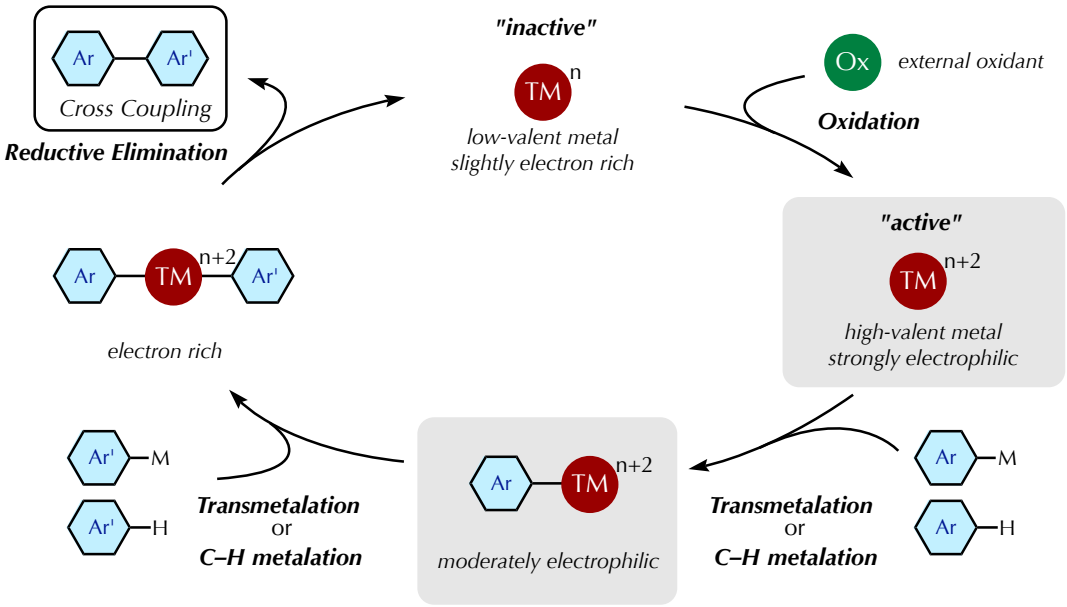

Figure 3. Catalytic cycle in transition metal-catalyzed oxidative coupling to afford biaryls.

In oxidative coupling reactions, the generation and controlling the activity of high-valent metal species are assumed to be a key in the catalytic cycle. Therefore, the appropriate design of new reactions and catalysts as well as ligands would be needed for not only overcoming intrinsic synthetic problems but also achieving otherwise-difficult new transformation.

Along this line, in this thesis, the author focused on the development of new oxidative coupling methodologies and new ligands that enable efficient oxidative reactions.

2. Transition Metal-Catalyzed Oxidative C–H Arylation and Multi-Component Coupling

2.1 Oxidative C–H Arylation

Classical transition metal-catalyzed coupling reactions involving oxidative addition and transmetalation processes require the preparation of each coupling partner from non-functionalized arenes (Figure 4). For example, aryl halides or arylmetal agents have to be prepared by halogenation, lithiation, borylation, silylation, zincation, stanylation and magnesiation of the corresponding arenes, resulting in multi-step synthesis (path A). On the other hand, direct C–H arylation[7-9] through oxidative coupling allows the short-step synthesis of biaryls (path B).

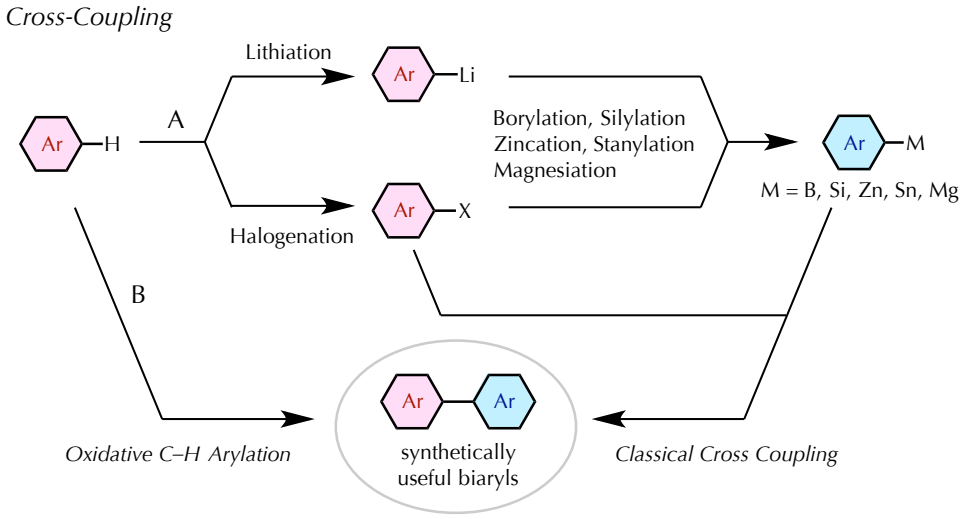

Figure 4. Possible reaction pathways to afford biaryl in cross coupling reaction

Oxidative C–H/C–H Coupling. One of the ultimate and ideal biaryl-forming reactions is thought to be Ar–H/Ar–H coupling, so-called cross-dehydrogenative coupling (CDC), because installation of functionalities on substrates is not required (Figure 5).

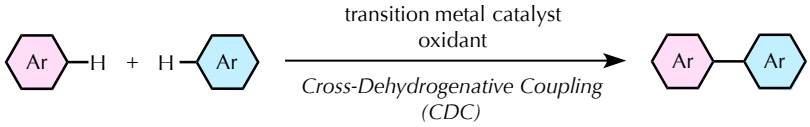

Figure 5. Ar–H/Ar–H coupling (cross-dehydrogenative coupling).

Various approaches for CDC reactions have been developed by employing reactants having different electronic properties (Figure 6). The Fagnou group revealed that indoles and benzene undergo CDC reaction to afford phenylindoles in high yields.[10] They also demonstrated that the regioselectivity at C2/C3 can be switched by the adjustment of reaction conditions. While the coupling reaction occurred at the C3 position of indoles with $Cu(OAc)_2$ as an oxidant, the use of $Ag(OAc)_2$ as an oxidant resulted in the generation of C2-coupling product. Su and co-workers studied CDC reaction between simple arenes. They utilized the electron-deficiency of perfluoroarenes to achieve CDC reaction with benzene.[11] More recently, Itami and co-workers demonstrated the regioselective mesitylation of polycyclic aromatic hydrocarbons (PAHs) with an *o*-chloranil oxidant.[12]

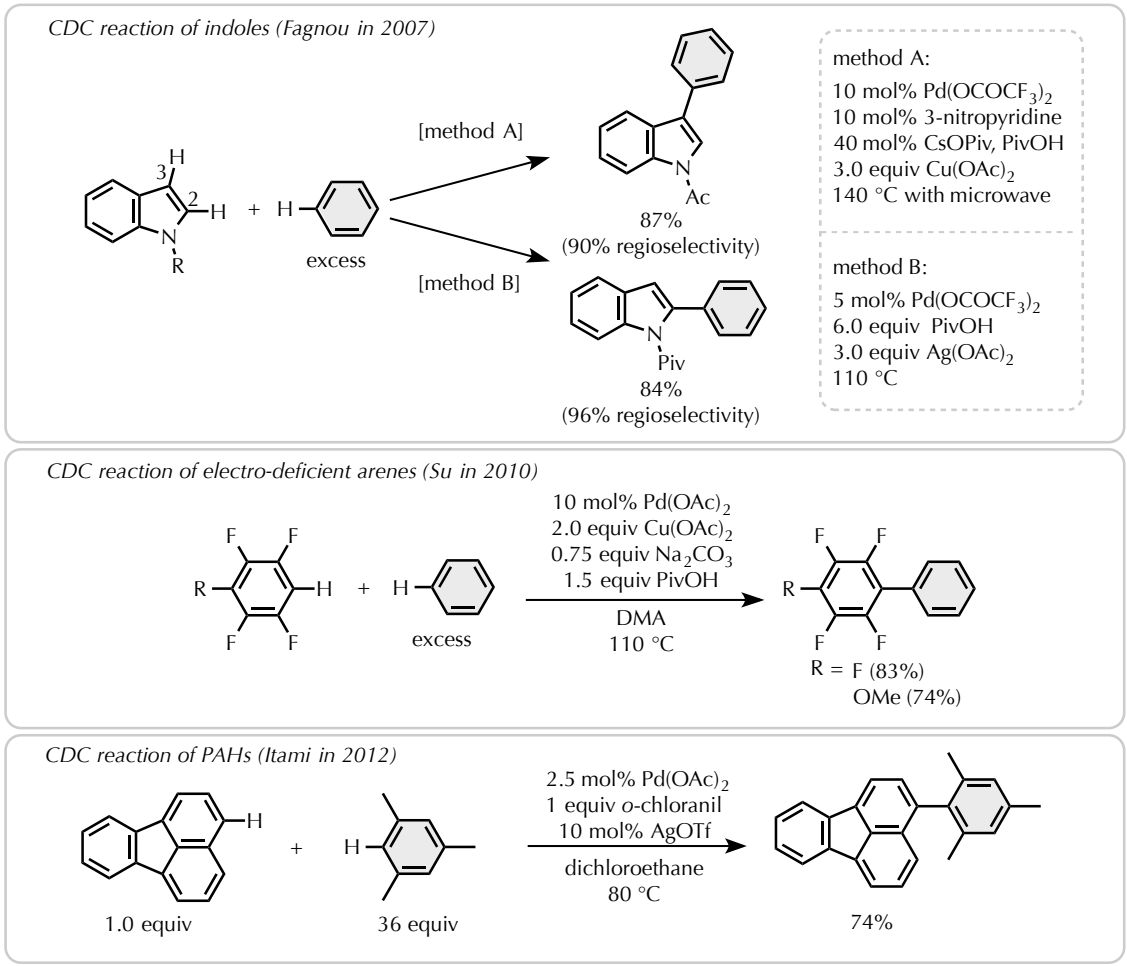

Figure 6. Pd-catalyzed CDC reactions controlled by different electronic properties of reactants.

Although CDC reactions involving Ar–H/Ar–H coupling have been well investigated, there are still some problems such as the requirement of excess amount of arenes, low regioselectivity and reactivity, harsh reaction conditions, and limited substrate scope.

Oxidative C–H Arylation with Arylmetal Agents. Alternative method to obtain biaryls is to employ arylmetal (Ar–M) instead of Ar–H as one of coupling partners (Figure 7). Practical and regioselective oxidative C–H arylation with arylmetal agents without directing group have been disclosed recently.[13]

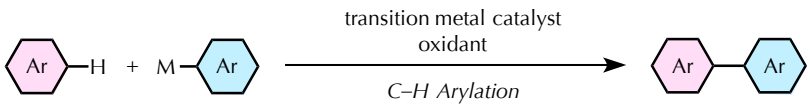

Figure 7. Ar–H/Ar–M cross-coupling (C–H arylation).

A variety of arylmetal agents are available in oxidative Ar–H/Ar–M coupling reaction (Figure 8). In 2008, Shi and co-workers achieved C–H arylation of simple arenes and heteroarenes with arylboronic acids. In this coupling reaction, oxygen is used as an oxidant for re-oxidation of palladium catalyst.[14] Furthermore, the arylation proceeds even at room temperature to give coupling products in high yield with high regioselectivity. Oi and Inoue reported that arylstannanes and arylsilanes can be utilized as arylation agents.[15]

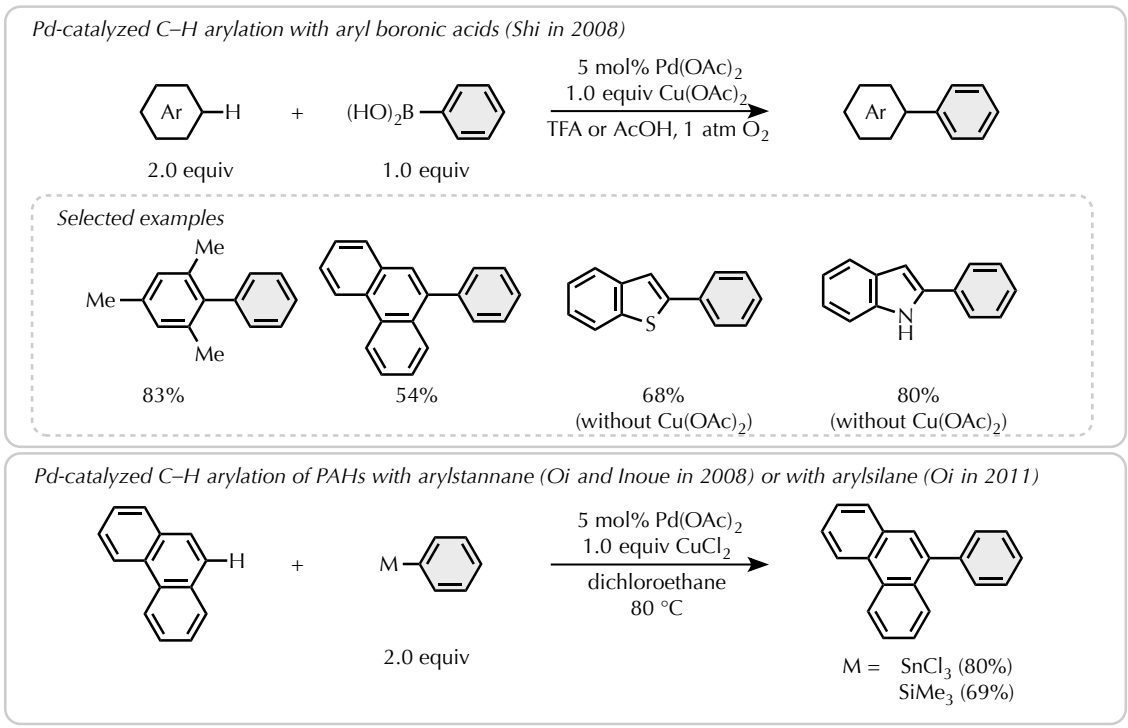

Figure 8. Pd-catalyzed C–H arylation with arylmetal agents.

Recently, silver, iron and gold were also found to be applicable to oxidative coupling as catalysts (Figure 9). Baran and co-workers reported silver-catalyzed C–H arylation of azines and azoles.[16] They employed potassium persulfate as a re-oxidant for silver catalyst. Shirakawa and Hayashi discovered iron-catalyzed C–H arylation of simple arenes in the presence of di-*tert*-butyl peroxide.[17] Gold-catalyzed C–H arylation of stoichiometric amount of simple arenes with arylsilanes using iodine (III) as oxidant for gold complex was developed by Lloyd-Jones and Russell.[18]

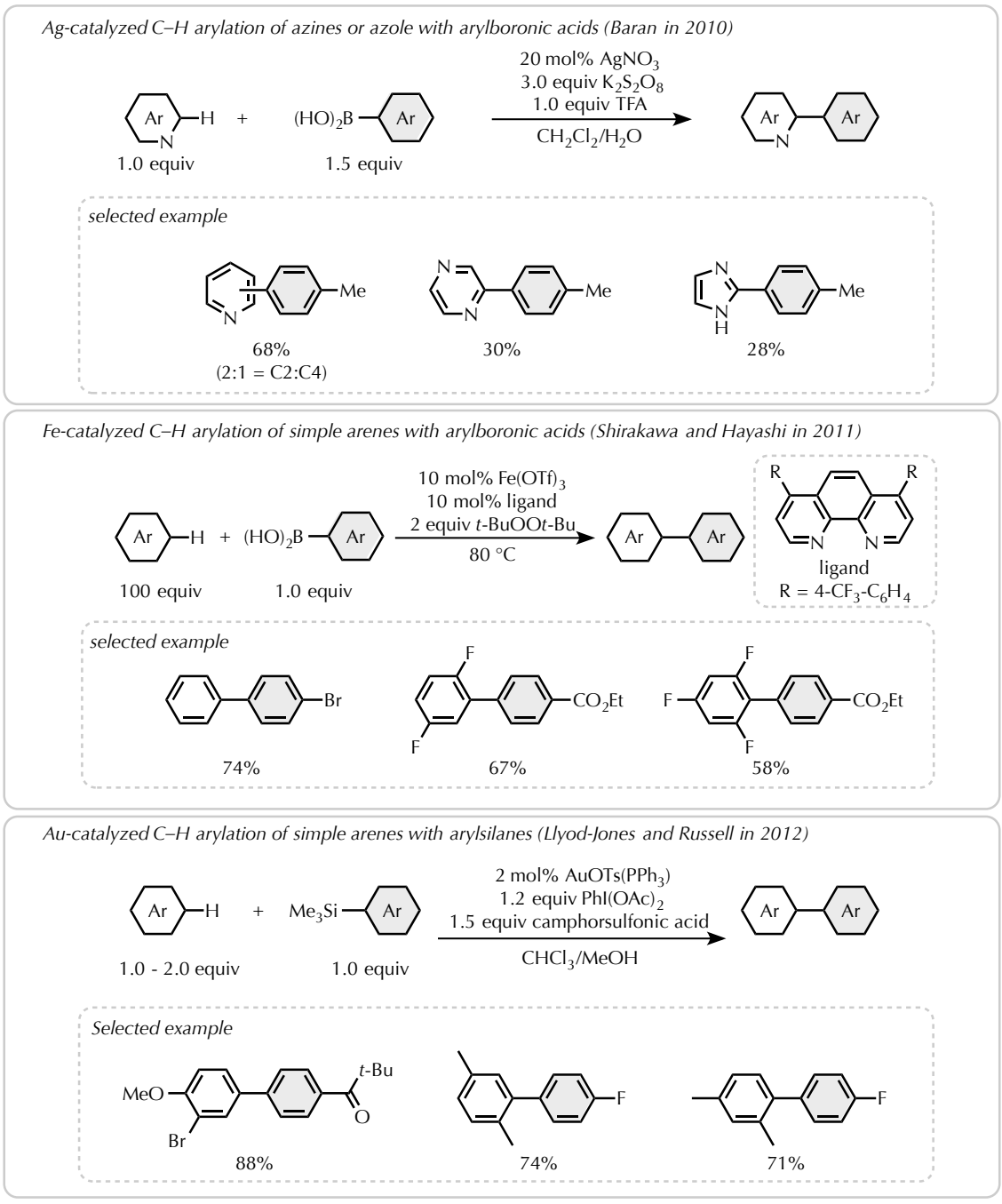

Figure 9. C–H arylation with other transition metal catalyst.

Ligand Effect in Oxidative C–H Arylation. In this section, the ligand effects are reviewed by introducing the examples of using ligand in the oxidative coupling reaction. In the iron-catalyzed oxidative C–H arylation of benzene with arylboronic acid, bipyridyl ligands play significant roles toward reactivity and chemoselectivity (Figure 10).[17] When iron tris(trifluoromethansulfonate) catalyst was used alone in the reaction,

the coupling product was obtained in only 21%. This result is ascribed to the high Lewis acidity of catalyst that induce side reactions and full consumption of an oxidant before the full conversion of a substrate. These problems were overcome by employing phenanthroline ligand to reduce the activity of catalyst, resulting in the increase of yield of the desired product. Further improvement in yield was found in the case of using an electronically modified phenanthroline ligand.

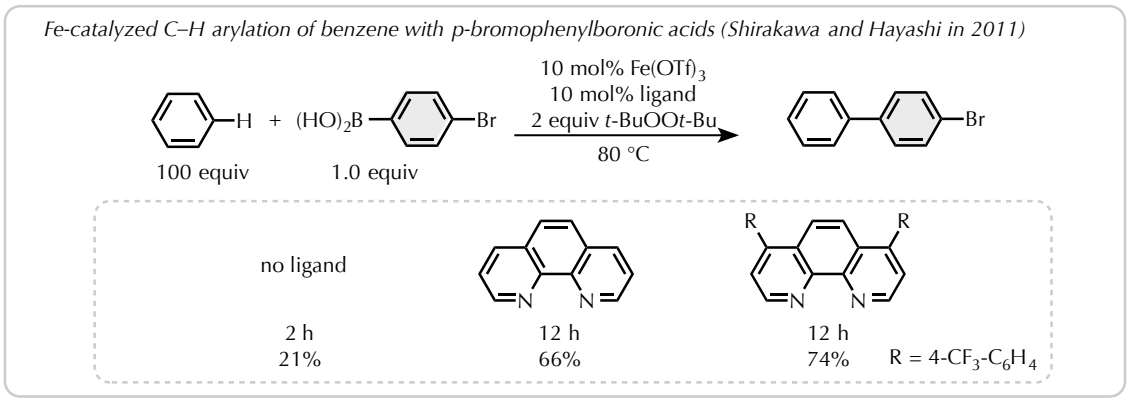

Figure 10. Ligand effects in iron-catalyzed oxidative C–H arylation of benzene.

In 2012, Itami and Yamaguchi reported the C–H arylation of heteroarenes such as thiophenes with hindered arylboronic acids catalyzed by palladium and pyridine-oxazoline or bisoxazoline ligands (Figure 11). In this reaction, no product was observed without ligands. They also demonstrated enantioselective C–H arylation with a chiral bisoxazoline ligand.[19] These results strongly indicate that ligand plays critical roles in the reactivity and selectivities in the coupling reaction.

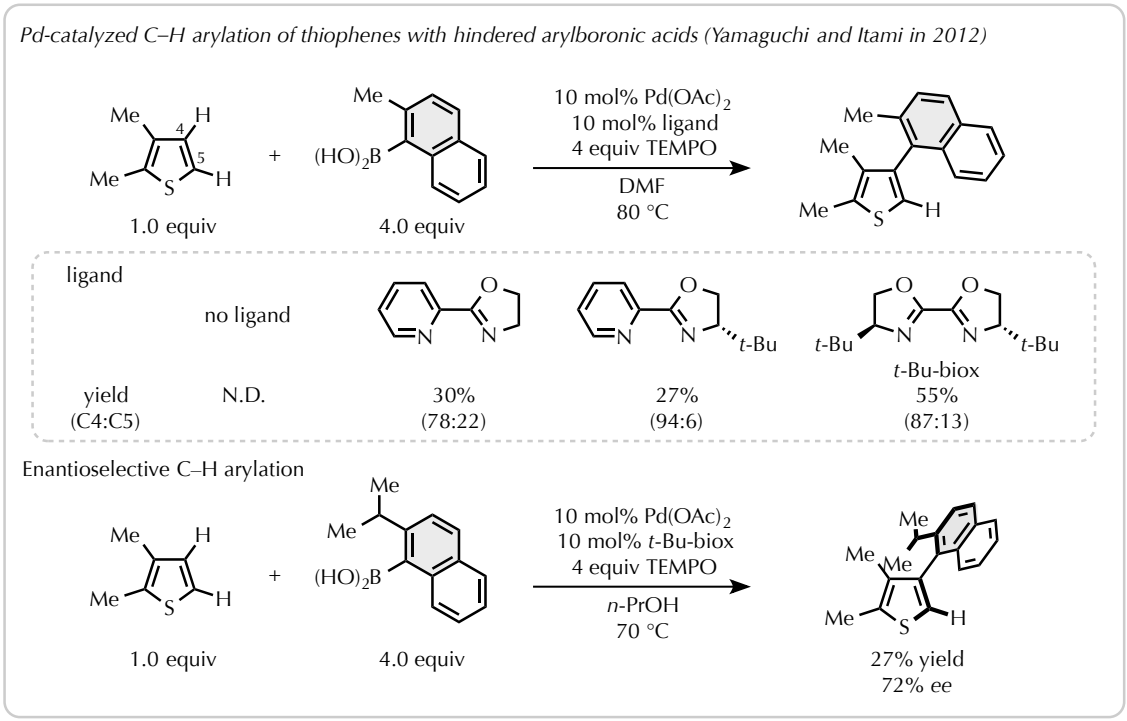

Figure 11. Ligand effects in palladium-catalyzed oxidative C–H arylation of thiophenes.

In most of transition metal-catalyzed organic reactions, ligand plays important roles and affects the activity and stability of the catalyst, chemo-, regio-, stereo- and enantioselectivities. In oxidative C–H arylation, there are many examples that reaction proceeds with metal catalyst not bearing any organic ligands such as phosphine, amine and carbene. Fundamentally, those electronically enriched organic ligands are expected not to tolerate the oxidative conditions. These less availability of ligands will lose the opportunity for further development of novel, practical, efficient and selective oxidative coupling reaction. Thus, the application of appropriate combination of ligand and metal catalyst as well as their precise design and synthesis is quite essential and demanded for oxidative C–H arylation.

2.2 Oxidative Multi-Component Coupling

Among various types of oxidative coupling reactions, multi-component coupling is also attractive and regarded as one of efficient methods to shorten multi-step reactions (Figure 12).

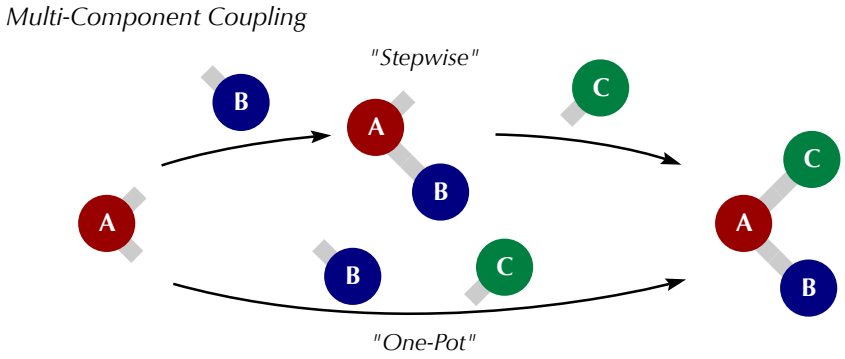

Figure 12. Stepwise and one-pot multi-component couplings

In the oxidative multi-component coupling, three or more nucleophiles can be used and coupled each other in one-pot. While there are a few examples of multi-component coupling under oxidative conditions, it is easily expected to access a range of structurally complicated and synthetically useful compounds that are otherwise-difficult to synthesize by the other methods (Figure 13).

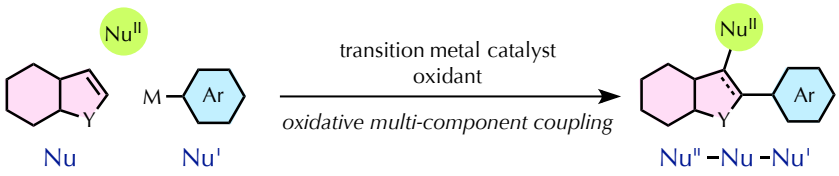

Figure 13. Oxidative three-component coupling between heterocycles, arylmetals and other nucleophiles.

During the course of investigation on palladium-catalyzed C–H arylation of indole derivatives with arylboronic acids, Studer and co-workers found that the employment of 2,2,6,6-tetramethylpiperidine *N*-oxyl (TEMPO) as an oxidant resulted in nitroxyarylation products (Figure 14).[20] In this reaction, TEMPO works not only as an oxidant but also as one of the coupling components.

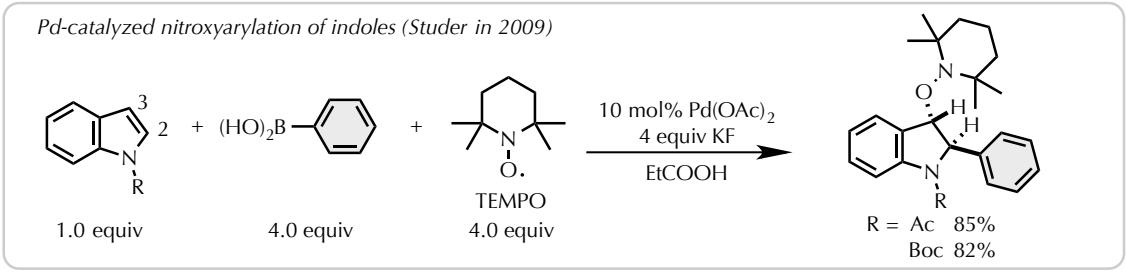

Figure 14. Three-component coupling between indoles, phenyl with boronic acid and TEMPO under the oxidative conditions.

In 2013, palladium-catalyzed multi-component coupling between indoles, arylboronic acids and β-ketoester in the presence of peroxide was discovered by Pihko (Figure 15).[21] In this reaction, C–H arylation at C2 position and C–C bond formation at C3 position occur to give a multi-component coupling product in high yield.

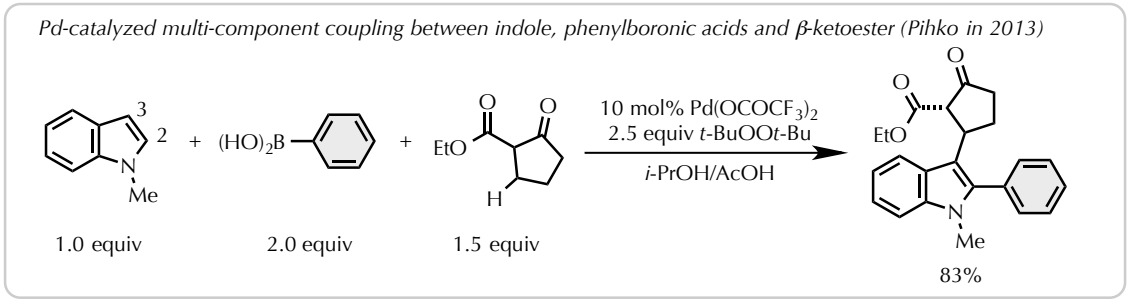

Figure 15. Three-component coupling between indole, phenylboronic acid and β-ketoester under the oxidative conditions.

Multi-component coupling has potential to synthesize structurally complicated compounds in one-pot, leading to a step-economical synthesis and a rapid discovery of pharmaceuticals. However, the variation of these reactions is rare by the oxidative method so that the further developments and improvements are still needed.

3. A Scenario for Efficient Oxidative Coupling

In oxidative coupling, the oxidation of low-valent metal to high-valent metal is key process for the catalytic reaction. In general, the oxidation to the higher oxidation state is unfavorable because of the instability of active high-valent metal species (high oxidation potential). To promote this sluggish oxidation process, the use of electron-donating ligand is one of the solutions. Electron-donating ligand bound to the low-valent metal species will lower the oxidation potential to high-valent metal, facilitating the oxidation. Furthermore, ligand could potentially stabilize the unstable high-valent metal species. To understand the effect of ligand in the oxidation process, it is quite important to investigate the oxidation process of low-valent metal to high-valent metal. Electron-rich *N*-heterocyclic carbene (NHC) ligand is expected to operate easy oxidation process and maintain high-valent state. Therefore, the design and application of new NHC ligand having high electron-donating property will be important for the development of efficient oxidative coupling.

As described in Sections 2, oxidative multi-component coupling is on the road to development. Further expansion of applicability of oxidative multi-component coupling is thought to be valuable to investigate because that would enable shortening the reaction steps and accessing synthetically useful structures that cannot be synthesized by the other methods.

4. Survey of This Thesis

In this thesis, the author focuses on the design of new reaction and ligand for oxidative coupling.

Chapter 1 describes the palladium-catalyzed oxidative three-component coupling of benzofurans, arylboronic acids and carboxylic acids (Figure 16). Dihydrobenzofuran structures have been often seen in many natural products and pharmaceutical compounds. The author found that the novel three-component coupling readily affords functionalized dihydrobenzofuran derivatives under the oxidative conditions with 2,2,6,6-tetramethylpipelidine *N*-oxyl (TEMPO).

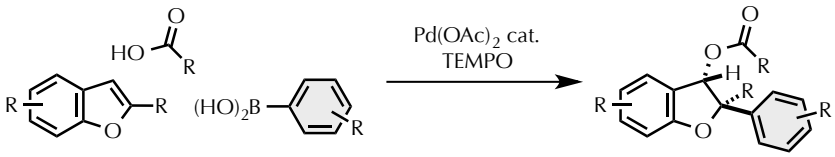

Figure 16. Oxidative three-component coupling between benzofurans, arylboronic acids and carboxylic acids by palladium catalyst.

Chapter 2 describes the design, synthesis and metal complexation of 1,3,5-triaryl-2-pyridylidene as an abnormal NHC ligand (Figure 17). The author observed the generation of pyridylidene as a free carbene by deprotonation of the corresponding pyridinium salt. The complexation with $AuCl(SMe_2)$ afforded the novel and stable triarylpyridylidene-gold complex and it was revealed that triarylpyridylidene showed the strongest electron-donating ability among other reported NHCs.

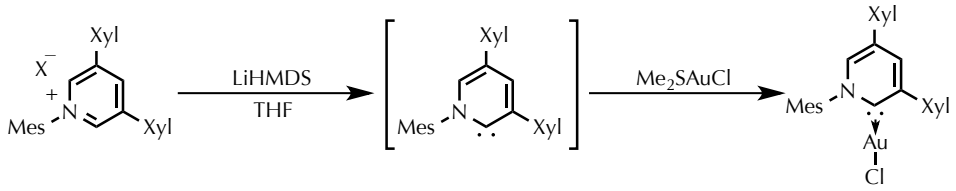

Figure 17. Synthesis and complexation of 1,3,5-triaryl-2-pyridylidene as an abnormal *N*-heterocyclic carbene.

Chapter 3 describes the application of (1,3,5-triaryl-2-pyridylidene)gold complex to the oxidative C–H arylation of heterocycles with arylsilanes (Figure 18). Triarylpyridylidene-gold complex effectively catalyzed C–H arylation of isoxazoles, indole derivative and benzothiophene to give a series of heterobiaryls. Through the investigations on ligand effects, triarylpyridylidene ligand was found to facilitate the oxidative process in gold-catalyzed C–H arylation.

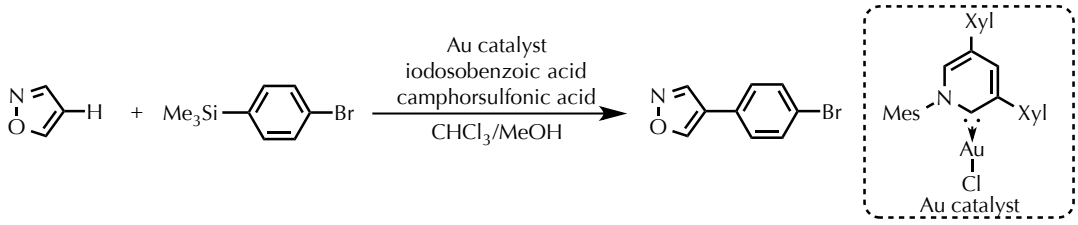

Figure 18. Application of 1,3,5-triaryl-2-pyridylidene-gold complex to the oxidative C–H arylation of heterocycles with arylsilanes.

5. References

[1] For early examples on organolithium compounds, see: M. Yamamura, I. Moritani and S. Murahashi, *J. Organomet. Chem.*, 1975, **91**, C39.

[2] For early examples on organomagnesium compounds, see: (a) K. Tamao, K. Sumitani and M. Kumada, *J. Am. Chem. Soc.*, 1972, **94**, 4374; (b) R. J. Corriu and J. P. Masse, *J. Chem. Soc., Chem. Commun.*, 1972, 144.

[3] For early examples on organotin compounds, see: (a) M. Kosugi, K. Sasazawa, Y. Shimizu and T. Migita, *Chem. Lett.*, 1977, 301; (b) D. Milstein and J. K. Stille, *J. Am. Chem. Soc.*, 1978, **100**, 3636.

[4] For early examples on organozinc compounds, see: (a) E. Negishi, A. O. King and N. Okukado, *J. Org. Chem.*, 1977, **42**, 1821; (b) A. O. King, N. Okukado and E. Negishi, *J. Chem. Soc., Chem. Commun.*, 1977, 683.

[5] For early examples organoboron compounds, see: (a) N. Miyaura and A. Suzuki, *J. Chem. Soc., Chem. Commun.*, 1979, 866; (b) N. Miyaura, K. Yamada and A. Suzuki, *Tetrahedron Lett.*, 1979, **20**, 3437.

[6] For early examples on organosilicon compounds, see: Y. Hatanaka and T. Hiyama, *J. Org. Chem.*, 1988, **53**, 918.

[7] For early examples on C–H arylation, see: (a) D. E. Ames and D. Bull, *Tetrahedron*, 1982, **38**, 383; (b) D. E. Ames, and A. Opalko, *Synthesis*, 1983, 234; (c) D. E. Ames, and A. Opalko, *Tetrahedron*, 1984, **40**, 1919; (d) N. Nakamura, Y. Tajima and K. Sakai, *Heterocycles*, 1982, **19**, 235.

[8] Recent selected reviews on C–H arylation, see: (a) L. Ackermann, R. Vicente and A. R. Kapdi, *Angew. Chem., Int. Ed.,* 2009, **48**, 9792; (b) L.-C. Campeau, D. R. Styart and K. Fagnou, *Aldrichimica Acta*, 2007, **40**, 25; (c) D. Alberico, M. E. Scott and M. Lautens, *Chem. Rev.*, 2007, **107**, 174; (d) M. Miura and M. Nomura, *Top. Curr. Chem.*, 2002, **219**, 211; (e) L. Ackermann and R. Vicente, *Top. Curr. Chem.*, 2010, **292**, 211; (f) N. Kuhl, M. N. Hopkinson, J. Wencel-Delord and F. Glourius, *Angew. Chem., Int. Ed.*, 2012, **51**, 10236.

[9] For reviews on synthesis-oriented C–H functionalization, see: (a) J. Yamaguchi, A. D. Yamaguchi and K. Itami, *Angew. Chem., Int. Ed.*, 2012, **51**, 8960; (b) Y. Segawa, T. Maekawa and K. Itami, *Angew. Chem., Int. Ed.*, 2015, **54**, 66.

[10] D. R. Stuart and K. Fagnou, *Science*, 2007, **316**, 1172.

[11] Y. Wei and W. Su, *J. Am. Chem. Soc*., 2010, **132**, 16377.

[12] K. Kawasumi, K. Mochida, T. Kajino, Y. Segawa and K. Itami, *Org. Lett*., 2012, **14**, 418.

[13] For selected review of C–H arylation with organometallics, see: C.-L. Sun, B.-J. Li and Z.-J. Shi, *Chem. Commun*., 2010, **46**, 677.

[14] S.-D. Yang, C.-L. Sun, Z. Fanf, B.-J. Li, Y.-Z. Li and Z.-J. Shi, *Angew. Chem., Int. Ed*., 2008, **47**, 1473.

[15] (a) H. Kawai, Y. Kobayashi, S. Oi and Y. Inoue, *Chem. Commun*., 2008, 1464; (b) K. Funaki, H. Kawai, T. Sato and S. Oi, *Chem. Lett*., 2011, **40,** 1050.

[16] Y. Fujiwara, J. A. Dixon, F. O'Hara, E. D. Funder, D. D. Dixon, R. A. Rodriguez, R. D. Baxter, B. Herlé, N. Sach, M. R. Collins, Y. Ishihara and P. S. Baran, *Nature*, 2012, **492**, 95.

[17] N. Uchiyama, E. Shirakawa, R. Nishikawa and T. Hayashi, *Chem. Commun*., 2011, **47**, 11671.

[18] L. T. Ball, G. C. Lloyd-Jones and C. A. Russell, *Science*, 2011, **337**, 1644.

[19] (a) K. Yamaguchi, J. Yamaguchi, A. Studer and K. Itami, *Chem. Sci*., 2012, **3**, 2165; (b) K. Yamaguchi, H. Kondo, J. Yamaguchi and K. Itami, *Chem. Sci*., 2013, **4**, 3753.

[20] S. Kirchberg, R. Fröhlich and A. Studer, *Angew. Chem., Int. Ed*., 2009, **48**, 4235.

[21] R. Y. Nimje, M. V. Lekinen and P. M. Pihko, *Angew. Chem., Int. Ed*., 2013, **52**, 4818.

Chapter 1

Synthesis of Dihydrobenzo[*b*]furans by Palladium-Catalyzed Oxidative Three-Component Coupling

Abstract

The synthesis of 2,3-dihydrobenzo[*b*]furans by palladium-catalyzed oxidative three-component coupling between benzo[*b*]furans, arylboronic acids and carboxylic acids is described. The three-component coupling proceeds through dearomatizing acyloxyarylation of benzofurans with high regio- and diastereoselectivity under room temperature to give 3-acyloxyl-2-aryl-2,3-dihydrobenzofuans in good yields.

1. Introduction

2,3-Dihydrobenzofuran and its derivatives are often found in many natural products and pharmaceutically relevant compounds (Figure 1). Thus, the development of direct approach from readily available benzofurans to 2,3-dihydrobenzofurans is thought to be useful and important. Along these lines, the functionalization at C2 and/or C3 position of benzofurans and subsequent hydrogenation is an obvious route to synthesize substituted 2,3-dihydrobenzofurans.[1] However, these synthetic routes require multi-step sequence involving prior installation of substituents onto benzofurans. More direct and straightforward method to obtain 2,3-dihydrobenzofurans having two substituents at C2 and C3 positions would be required. In this regard, oxidative three-component coupling involving dearomatization of benzofurans would offer great potential as efficient and one-pot transformation for the synthesis of natural products and pharmaceutical compounds having benzofuran as a core structure.[2]

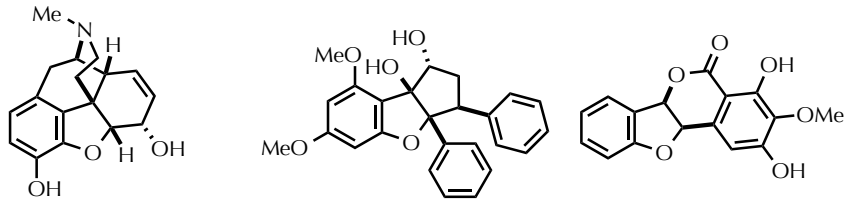

Morphine — opiate analgesic drug

Rocaglaol — cytotoxicity against HT-29

(+)-Platyphyllarin A — antiplatelet activities

Figure 1. Natural products bearing dihydrobenzo[*b*]furan structure.

Recently, Studer and co-workers reported an interesting work on palladium-catalyzed oxidative three-component coupling involving aminoxyarylation/dearomatization of benzofuran with arylboronic acids and (2,2,6,6-tetramethylpiperidine 1-oxyl) TEMPO[3] (Figure 2).[4] They obtained aminoxyarylation products in excellent yields with high diastereoselectivities under mild conditions. However, the utility of TEMPO-substituted products is low owing to the difficulty of cleaving the N–O bond that will produce synthetically useful alcohols. Therefore, installation of other transformable functional groups such as an acyloxyl group is strongly required.

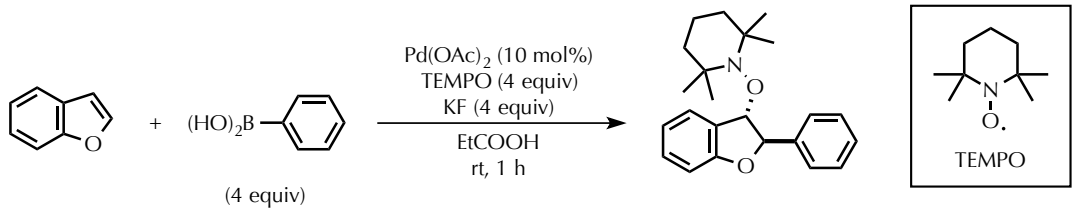

Figure 2. Palladium-catalyzed diastereoselective aminoxyarylation of benzo[*b*]furan with arylboronic acids and TEMPO.[4]

Transition metal-catalyzed acyloxyarylation of carbon–carbon double bonds has been successfully used for vicinal alkene difunctionalization.[5–7] The acyloxy group in the products can be further modified, rendering this approach synthetically highly valuable. While acyloxyarylation of terminal[6] or internal[7] olefins has been developed, the vicinal acyloxyarylation of aromatic compounds has not been reported to date. Herein the author reports palladium-catalyzed oxidative three-component coupling between various 2-substituted benzofurans, arylboronic acid and carboxylic acids involving dearomatizing acyloxyarylation of benzofurans (Figure 3).

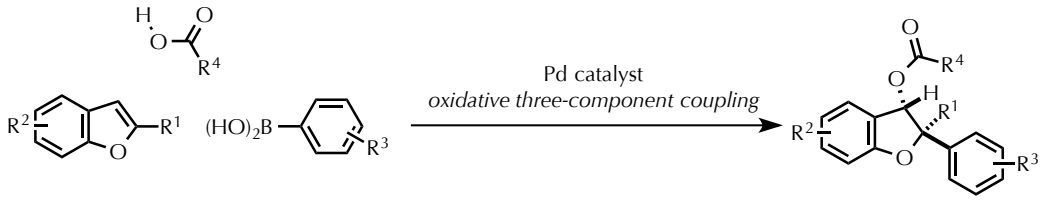

Figure 3. Palladium-catalyzed oxidative three-component coupling of benzo[*b*]furan with arylboronic acids and carboxylic acids.

2. Results and Discussion

Initial Investigation of Acyloxyarylation

After extensive investigation, the author found that the treatment of 2-methylbenzofuran (**1a**) with phenylboronic acid (**2a**: 1.5 equiv.) and acetic acid (**3a**: solvent) in the presence of palladium acetate (5 mol%) and 2,2,6,6-tetramethylpiperidine *N*-oxyl (TEMPO: 3 equiv.) for 5 hours at room temperature gave the target 2,3-difunctionalized product. Thus, 2-methyl-2-phenyl-2,3-dihydrobenzofuran-3yl acetate (**4aaa**) was obtained in high yield (93%) and good diastereoselectivity (93:7 dr). Notably, the acyloxyarylation reaction showed virtually complete regioselectivity; 3-aryl-2-acyloxylated products were not observed. The reaction with extended time (12 hours) did not improve the

diastereoselectivity (95%, 93:7 dr). The result indicates that no epimerization occurs under the reaction conditions. Addition of KF to the reaction led to excellent diastereoselectivity (95%), albeit in a lower yield (47%). Employment of $Pd(OCOCF_3)_2$ instead of $Pd(OAc)_2$ as a precatalyst afforded a similar result. Homo-coupling product of phenylboronic acid (**2a**) was not detected under the present reaction conditions unlike the related direct C–H arylation with arylboronic acids under oxidative conditions.[8]–[9] The acetoxy group on **4aaa** is possible to be transformed into hydroxy group (**5aa**) in 90% yield by hydrolysis under basic conditions without epimerization (see experimental section for details). The following mechanism to explain the regio- and diastereoselective acyloxyarylation is proposed in Figure 4. Transmetalation of palladium acetate with phenylboronic acid (**2a**) generates the Ph–Pd–OAc species, and the subsequent electrophilic palladation at the C2 position of 2-methylbenzofuran (**1a**) gives the benzylic cation intermediate **A**. Diastereoselective trapping of the cation species with carboxylic anion at the C3 position produces the diorganopalladium intermediate **B**. Reductive elimination of product **4aaa** provides Pd(0), which is then oxidized by TEMPO in acetic acid (**3a**) to regenerate $Pd(OAc)_2$. The presence of TEMPO is critically important in this reaction because no acyloxyarylation product was formed with other oxidants such as peroxides.

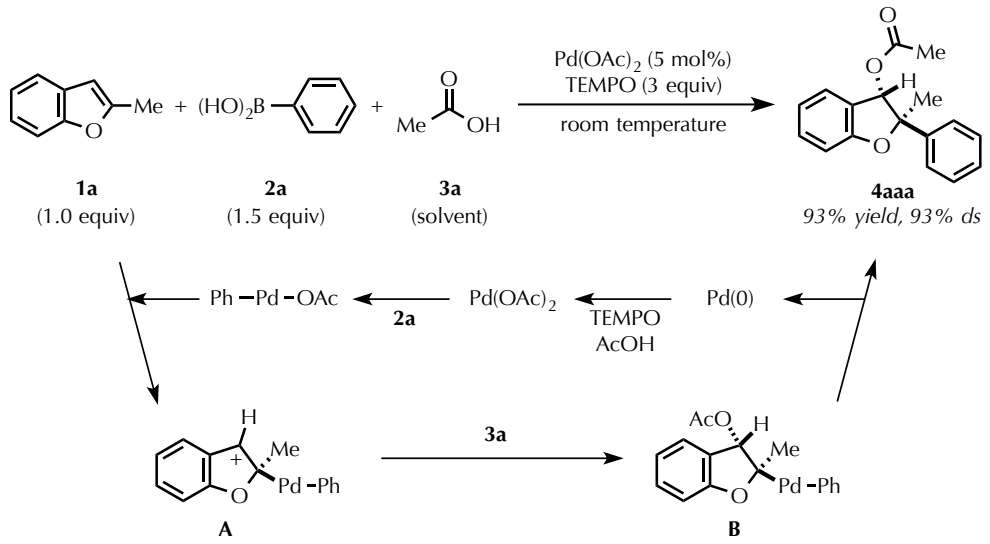

Figure 4. Discovery of Pd/TEMPO-catalyzed oxidative three-component coupling between 2-methylbenzofurans (**1a**), phenylboronic acids (**2a**) and acetic acids (**3a**).

Substrate Scope

With optimized conditions in hand, the scope of acyloxyarylation was examined by using several sterically or electronically diverse benzofurans (**1**), aryboronic acids (**2**) and carboxylic acids (**3**) (Table 1). 2-*n*-Butylbenzofuran (**1b**) was transformed into the corresponding product **4baa** in high yield and diastereoselectivity. The major isomer was isolated by recrystallization as a colorless crystal, and the relative configuration was determined by X-ray crystallography, which showed that the acetoxy group and the phenyl group are *trans* oriented (Figure 5). The substituents at the C2 position of benzofurans influence the outcome of acyloxyarylation. For example, the reaction of benzofuran (**1j**: R^1 = H) with phenylboronic acid (**2a**) and acetic acid (**3a**) under optimized conditions generated 2-phenylbenzofuran as the major product of direct C–H arylation in 82% yield (Figure 6). Subjection of propionic acid (**3b**) instead of acetic acid (**3a**) furnished the corresponding propionyloxyarylation product (**4aab**, 62%, 85:15 dr) in good yield with moderate diastereoselectivity. Substituents at the C4–7 positions of benzofuran were tolerated to the acyloxyarylation. The desired products were isolated in good yields with moderate to good diastereoselectivities (**4caa**–**4iaa**, 66–96%, 74:24–94:6 dr). Substituents at the *para* position were tolerated but the products **4aba**–**4aga** were obtained in lower yields. Whereas moderate to good yields were achieved with the halides, the electron rich *para*-methoxy congener gave a significantly lower yield (see **4aga**). (**4aba**–**4aga**, 28–84%). *meta*-Substituted arylboronic acids were suitable substrates as documented for the successful acyloxyarylation of **1a** with *m*-$MeC_6H_4B(OH)_2$ (see **4afa**); however, the reaction with sterically more hindered boronic acids such as 2-methylphenyl or 1-naphthylboronic acid failed.

Table 1. Scope of Pd/TEMPO-catalyzed oxidative three-component coupling between benzofurans, phenylboronic acids and acetic acids.

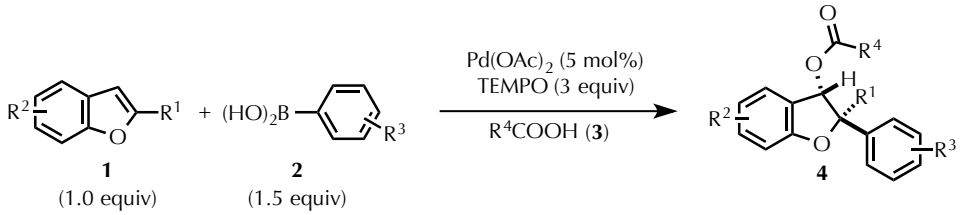

1 (1.0 equiv) + **2** (1.5 equiv) → **4**

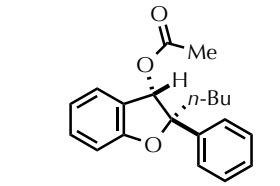

4baa
89% (89:11 dr)

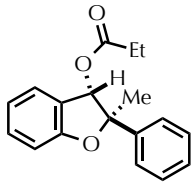

4aab
62% (85:15 dr)

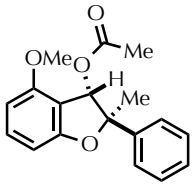

4caa
87% (85:15 dr)

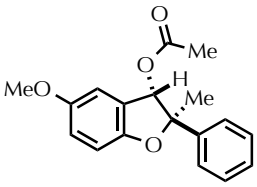

4daa
96% (89:11 dr)

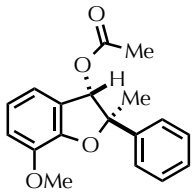

4eaa
89% (91:9 dr)

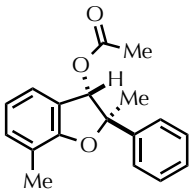

4faa
90% (94:6 dr)

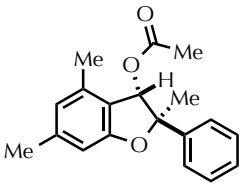

4gaa
86% (90:10 dr)

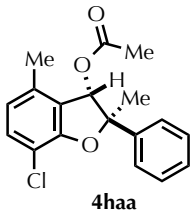

4haa
66% (76:24 dr)

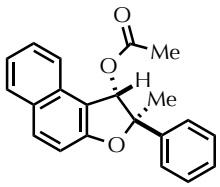

4iaa
88% (78:22 dr)

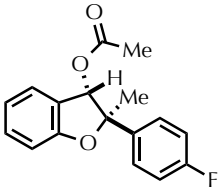

4aba
84% (93:7 dr)

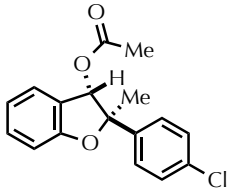

4aca
48% (89:11 dr)

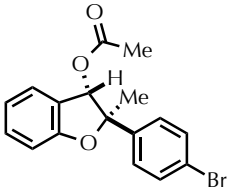

4ada
55% (89:11 dr)

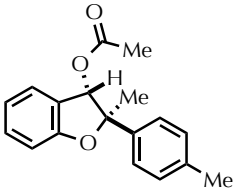

4aea
58% (88:12 dr)

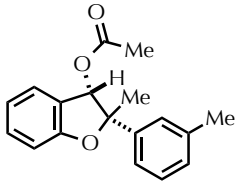

4afa
51% (86:14 dr)

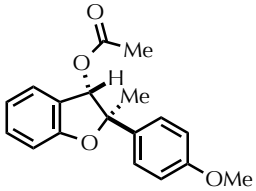

4aga
28% (83:17 dr)

a) Condition: **1** (0.20 mmol), **2** (0.30 mmol), **3** (0.4 mL), $Pd(OAc)_2$ (5 mol%), TEMPO (0.60 mmol), room temperature. b) isolated yield, diastereoselectivity was determined by ^1H NMR.

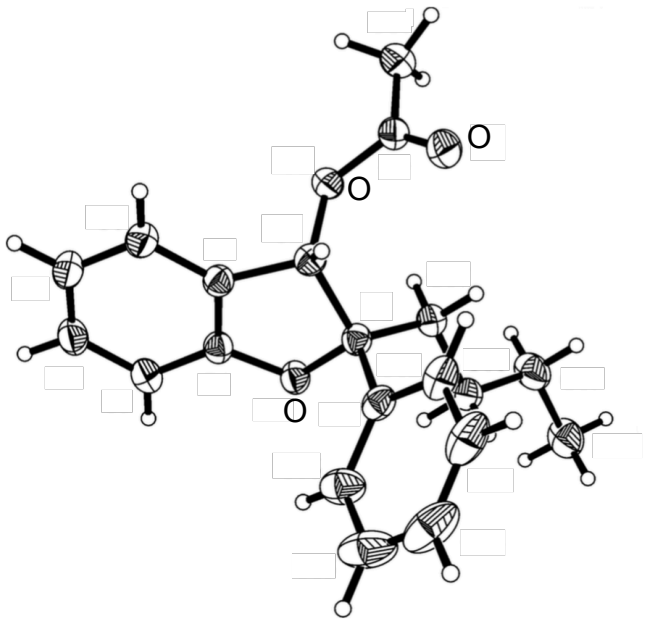

Figure 5. X-ray crystal structure of **4baa** (thermal ellipsoids are shown with 30% probability).

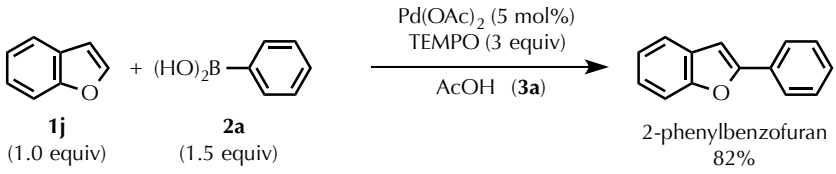

Figure 6. Operation of acyloxyarylation with benzofuran (**1j**) under optimized conditions.

3. Conclusion

Single-step synthesis of functionalized dihydrobenzofurans by palladium-catalyzed oxidative three-component coupling between benzofurans, arylboronic acids and carboxylic acids under mild conditions has been developed. A range of benzofuran derivatives and arylboronic acids can be used in the dearomatizing acyloxyarylation. Acyloxy groups and aryl groups are introduces at the C3- and C2-positions of the benzofuran core, respectively, with perfect regioselectivity and high diastereoselectivity. Remarkably, the reaction allows the formation of quaternary C-center at the C2 position. The thus-formed acyloxyarylation products can be converted into the corresponding alcohols without epimerization by simple hydrolysis to produce 2-aryl-3-oxy-duhydrobenzofurans.[10]

4. Experimental

General

All reactions involving air- or moisture-sensitive reagents or intermediates were carried out in heat-gun-dried glassware under an argon atmosphere and were performed using standard Schlenk techniques. All solvents for extraction and flash chromatography were distilled before use. Acetic acid was purchased from *Acros* and used as received.

^{1}H NMR and ^{13}C NMR spectra were recorded on a *Bruker DPX 300* spectrometer. Chemical shifts δ in ppm are referenced to the TMS peak as an internal standard. TLC was carried out on *Merck* silica gel 60 F_{254} plates; detection by UV or dipping into a solution of $Ce(SO_4)_2 \cdot H_2O$ (10 g), phosphormolybdic acid hydrate (25 g), conc. H_2SO_4 (60 mL) and H_2O (0.94 L) or $NaHCO_3$ (5.0 g), $KMnO_4$ (1.5 g) and H_2O (0.20 L) followed by heating. Flash chromatography (FC) was carried out on *Merck* or *Fluka* silica gel 60 (40–63 μm) with an argon pressure of about 1.1–1.5 bar. ESI-MS and HRMS were performed using a *Bruker MicroTof*. Melting points were determined on a *Stuart SMP10* and are uncorrected. IR spectra were recorded on a *Digilab* Varian 3100 FT-IR Excalibur Series.

The reactants or reagents are purchased or prepared by following literatures. 2-methylbenzofuran (*Aldrich*), 2-*n*-butylbenzofuran (*Aldrich*), phenyl boronic acid (*Aldrich*), 4-fluorophenylboronic acid (*Alfa Aesar*), 4-chlorophenylboronic acid (*Alfa Aesar*), 4-bromophenylboronic acid (*Alfa Aesar*), 4-methylphenylboronic acid (*Alfa Aesar*), 3-methylphenylboronic acid (*Alfa Aesar*), 4-methoxyphenylboronic acid (*ABCR*), palladium acetate (*TCI*), palladium trifluoroacetate (*Aldrich*), acetic acid (*Acros*), propionic acid (*Acros*), potassium fluoride (*Aldrich*), 2,2,6,6-tetramethylpiperidin-*N*-oxyl radical (TEMPO, *CIBA*, *Specialty Chemicals*), 4-methoxyl-2-methy-benzofuran,[11] 5-methoxyl-2-methy-benzofuran,[11,12] 7-methoxyl-2-methy-benzofuran,[11] 2,7-dimethylbenzofuran,[11] 2,4,6-trimethylbenzofuran,[13] 2-methylnaphtho[2,1-*b*]furan.[11]

General Procedure for the Acyloxyarylation of Benzofurans

An arylboronic acid (0.30 mmol, 1.5 equiv), TEMPO (94 mg, 0.60 mmol, 3.0 equiv), palladium acetate (2.2 mg, 0.010 mmol, 5 mol%), benzofuran derivative (0.20 mmol, 1.0 equiv) and acetic acid (0.40 mL) were stirred in a sealed tube at room temperature for 5 h. A saturated aqueous solution of K_2CO_3 (2.0 mL) was added and the mixture was extracted with CH_2Cl_2 (3 × 4.0 mL). The combined organic layers were dried over $MgSO_4$ and filtrated, and the volatiles were removed under reduced pressure. The residue was purified by FC.

*2-Methyl-2-phenyl-2,3-dihydrobenzofuran-3-yl acetate (**4aaa**)*

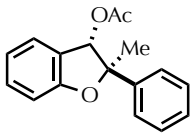

According to the general procedure with 2-methylbenzofuran (26 mg, 0.20 mmol) and phenylboronic acid (37 mg, 0.30 mmol). FC (pentane/Et_2O 200:1 to 10:1) gave **4aaa** as a colorless oil (46 mg, 0.17 mmol, 86%, dr 93:7).

^{1}H NMR ($CDCl_3$, 300 MHz) δ 7.57 (dd, *J* = 8.4, 1.2 Hz, 2H), 7.38–7.27 (m, 5H), 7.05 (d, *J* = 8.4 Hz, 1H), 6.94 (t, *J* = 7.5 Hz, 1H), 6.37 (d, *J* = 1.2 Hz, 1H), 2.22 (d, *J* = 1.2 Hz, 3H), 1.77 (d, *J* = 1.8 Hz, 3H); ^{13}C NMR ($CDCl_3$, 75 MHz) δ 170.8 (4°), 160.2 (4°), 144.1 (4°), 131.3 (CH), 128.4 (CH), 127.4 (CH), 127.0 (CH), 125.1 (CH), 124.2 (4°), 121.2 (CH), 110.2 (CH), 91.1 (4°), 80.5 (CH), 23.1 (CH_3), 21.0 (CH_3); HRMS (ESI+) calcd for $C_{17}H_{16}O_3Na$ $[M+Na]^+$: *m/z* 291.0992, found: *m/z* 291.0982. IR (neat): 2360, 2342, 1736, 1600, 1478, 1371, 1230, 1017, 977, 923, 752, 700 (cm^{-1}).

*2-Butyl-2-phenyl-2,3-dihydrobenzofuran-3-yl acetate (**4baa**)*

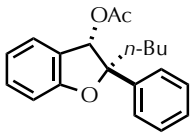

According to the general procedure with 2-butylbenzofuran (35 mg, 0.2 mmol) and phenylboronic acid (37 mg, 0.30 mmol). FC (pentane/Et_2O 200:1 to 10:1) gave **4baa** as a colorless solid (55 mg, 0.18 mmol, 89%, dr 89:11). The crystal suitable for X-ray analysis was obtained from hexane.

^{1}H NMR ($CDCl_3$, 300 MHz) δ 7.54 (dd, *J* = 7.2, 1.5 Hz, 2H), 7.37–7.26 (m, 5H), 7.06 (d, *J* = 8.1 Hz, 1H), 6.95–6.90 (m, 1H), 6.40 (s, 1H), 2.25–2.14 (m, 1H), 2.21 (s, 3H), 2.03–1.93 (m, 1H), 1.53–1.29 (m, 3H), 1.04–0.93 (m, 1H), 0.87 (t, *J* = 7.5 Hz, 3H); ^{13}C NMR ($CDCl_3$, 75 MHz) δ 170.7 (4°), 160.1 (4°), 142.3 (4°), 131.1 (CH), 128.2 (CH), 127.2 (CH), 126.8 (CH), 125.6 (CH), 124.2 (4°), 121.0 (CH), 110.1 (CH), 93.4

(4°), 80.9 (CH), 34.8 (CH_2), 25.6 (CH_2), 22.9 (CH_2), 20.9 (CH_3), 13.8 (CH_3); mp: 73–74 °C; HRMS (ESI+) calcd for $C_{20}H_{22}O_3$ $[M+Na]^+$: *m/z* 333.1461, found: *m/z* 333.1454; IR (neat): 2930, 2871, 2360, 2342, 1737, 1479, 1229, 1025, 963, 750, 702 (cm^{-1}).

*2-Methyl-2-phenyl-2,3-dihydrobenzofuran-3-yl propionate (**4aab**)*

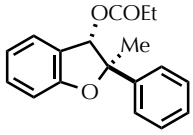

According to the general procedure with 2-methylbenzofuran (26 mg, 0.20 mmol), phenylboronic acid (37 mg, 0.30 mmol) and propionic acid (0.40 mL) instead of acetic acid. FC (pentane/Et_2O 200:1 to 10:1) gave **4aab** as a colorless oil (35 mg, 0.12 mmol, 62%, dr 85:15). The diastereomers were additionally separated with FC to give nearly pure major isomer (20 mg, 0.071 mmol, 35%, dr 97:3).

^{1}H NMR ($CDCl_3$, 300 MHz) δ 7.57 (dd, *J* = 7.2, 1.5 Hz, 2H), 7.37–7.27 (m, 5H), 7.04 (d, *J* = 8.1 Hz, 1H), 6.95–6.90 (m, 1H), 6.37 (s, 1H), 2.48 (q, *J* = 7.5 Hz, 2H), 1.75 (s, 3H), 1.25 (t, *J* = 7.5 Hz, 3H); ^{13}C NMR ($CDCl_3$, 75 MHz) δ 174.4 (4°), 160.2 (4°), 144.2 (4°), 131.3 (CH), 128.4 (CH), 127.5 (CH), 127.0 (CH), 125.1 (CH), 124.3 (4°), 121.3 (CH), 110.2 (CH), 91.2 (4°), 80.4 (CH), 27.7 (CH_2), 23.1 (CH_3), 9.1 (CH_3); HRMS (ESI+) calcd for $C_{18}H_{18}O_3Na$ $[M+Na]^+$: *m/z* 305.1148, found: *m/z* 305.1140; IR (neat): 2983, 2941, 2361, 2342, 1734, 1600, 1478, 1254, 1169, 1063, 922, 750, 700 (cm^{-1}).

*4-Methoxy-2-methyl-2-phenyl-2,3-dihydrobenzofuran-3-yl acetate (**4caa**)*

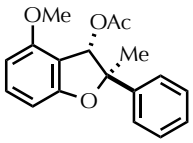

According to the general procedure with 4-methoxy-2-methylbenzofuran (32 mg, 0.20 mmol) and phenylboronic acid (37 mg, 0.30 mmol). FC (pentane/Et_2O 200:1 to 10:1) gave **4caa** as a colorless oil (52 mg, 0.17 mmol, 87%, dr 85:15).

^{1}H NMR ($CDCl_3$, 300 MHz) δ 7.70 (d, *J* = 7.2 Hz, 2H), 7.43–7.31 (m, 4H), 6.75 (d, *J* = 7.8 Hz, 1H), 6.60 (s, 1H), 6.50 (d, *J* = 8.4 Hz, 1H), 3.84 (s, 3H), 2.29 (s, 3H), 1.79 (s, 3H); ^{13}C NMR ($CDCl_3$, 75 MHz) δ 169.2 (4°), 160.0 (4°), 156.0 (4°), 142.5 (4°), 130.9 (CH), 126.7 (CH), 127.5 (CH), 123.4 (CH), 109.3 (4°), 101.7 (CH), 101.4 (CH), 90.2 (4°), 76.8 (CH), 53.78 (CH_3), 21.5 (CH_3), 19.3 (CH_3); HRMS (ESI+) calcd for $C_{18}H_{18}O_4Na$ $[M+Na]^+$: *m/z* 321.1097, found: *m/z* 321.1099; IR (neat): 2360, 2342, 1736, 1611, 1495, 1465, 1372, 1334, 1221, 1082, 1060, 1017, 974, 920, 763, 722, 701 (cm^{-1}).

*5-Methoxy-2-methyl-2-phenyl-2,3-dihydrobenzofuran-3-yl acetate (**4daa**)*

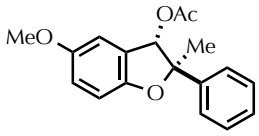

According to the general procedure with 5-methoxy-2-methylbenzofuran (32 mg, 0.20 mmol) and phenylboronic acid (37 mg, 0.30 mmol). FC (pentane/Et_2O 200:1 to 10:1) gave **4daa** as a colorless oil (57 mg, 0.19 mmol, 96%, dr 89:11).

^{1}H NMR ($CDCl_3$, 300 MHz) δ 7.41 (d, *J* = 7.5 Hz, 2H), 7.20 (t, *J* = 7.5 Hz, 2H), 7.13 (t, *J* = 6.0 Hz, 1H), 6.80 (s, 1H), 6.78–6.70 (m 2H), 6.17 (s, 1H), 3.60 (s, 3H), 2.07 (s, 3H), 1.60 (s, 3H); ^{13}C NMR ($CDCl_3$, 75 MHz) δ 170.7 (4°), 154.4 (4°), 154.3 (4°), 144.1 (4°), 128.3 (CH), 127.3 (CH), 125.0 (CH), 124.6 (4°), 117.7 (CH), 111.50 (CH), 110.40 (CH), 91.7 (4°), 80.8 (CH), 55.9 (CH_3), 23.0 (CH_3), 20.9 (CH_3); HRMS (ESI+) calcd for $C_{18}H_{18}O_4Na$ $[M+Na]^+$: *m/z* 321.1097, found: *m/z* 321.1097; IR (neat): 2361, 2342, 1737, 1371, 1227, 1018, 933, 801, 761, 701 (cm^{-1}).

*7-Methoxy-2-methyl-2-phenyl-2,3-dihydrobenzofuran-3-yl acetate (**4eaa**)*

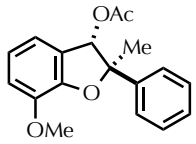

According to the general procedure with 7-methoxy-2-methylbenzofuran (32 mg, 0.20 mmol) and phenylboronic acid (37 mg, 0.30 mmol). FC (pentane/Et_2O 200:1 to 10:1) gave **4eaa** as a colorless oil (53 mg, 0.18 mmol, 89%, dr 91:9).

^{1}H NMR ($CDCl_3$, 300 MHz) δ 7.61 (d, *J* = 7.5 Hz, 2H), 7.38 (t, *J* = 7.5 Hz, 2H), 7.29 (t, *J* = 7.5 Hz, 1H), 6.98–6.10 (m, 3H), 6.41 (s, 1H), 4.03 (s, 3H), 2.23 (s, 3H), 1.83 (s, 3H); ^{13}C NMR ($CDCl_3$, 75 MHz) δ 170.3 (4°), 148.6 (4°), 144.2 (4°), 143.4 (4°), 128.0 (CH), 127.0 (CH), 124.7 (4°), 124.5 (CH), 121.4 (CH), 118.1 (CH), 113.0 (CH), 91.5 (4°), 80.4 (CH), 55.6 (CH_3), 22.7 (CH_3), 20.6 (CH_3); HRMS (ESI+) calcd for $C_{18}H_{18}O_4Na$ $[M+Na]^+$: *m/z* 321.1097, found: *m/z* 321.1096; IR (neat): 2361, 2342, 1733, 1602, 1478, 1371, 1230, 1013, 921, 828, 752 (cm^{-1}).

*2,7-Dimethyl-2-phenyl-2,3-dihydrobenzofuran-3-yl acetate (**4faa**)*

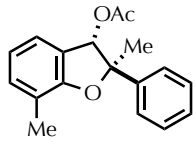

According to the general procedure with 2,7-dimethylbenzofuran (29 mg, 0.20 mmol) and phenylboronic acid (37 mg, 0.30 mmol). FC (pentane/Et_2O 200:1 to 10:1) gave

4faa as a colorless oil (51 mg, 0.18 mmol, 90%, dr 94:6).

^{1}H NMR ($CDCl_3$, 300 MHz) δ 7.61 (d, *J* = 7.2 Hz, 2H), 7.39 (t, *J* = 7.2 Hz, 2H), 7.33–7.28 (m, 1H), 7.19 (t, *J* = 7.5 Hz, 2H), 6.89 (t, *J* = 7.5 Hz, 1H), 6.41 (s, 1H), 2.48 (s, 3H), 2.25 (s, 3H), 1.82 (s, 3H); ^{13}C NMR ($CDCl_3$, 75 MHz) δ 170.1 (4°), 158.0 (4°), 143.6 (4°), 131.5 (CH), 127.7 (CH), 126.7 (CH), 124.2 (CH), 123.5 (CH), 122.6 (4°), 120.5 (CH), 119.6 (4°), 90.1 (4°), 80.2 (CH), 22.5 (CH_3), 20.4 (CH_3), 14.5 (CH_3); HRMS (ESI+) calcd for $C_{18}H_{18}O_3Na$ [M+Na]$^+$: *m/z* 305.1148, found: *m/z* 305.1149, IR (neat): 2361, 2342, 1734, 1370, 1220, 1016, 924, 753, 699 (cm^{-1}).

*2,4,6-Trimethyl-2-phenyl-2,3-dihydrobenzofuran-3-yl acetate (**4gaa**)*

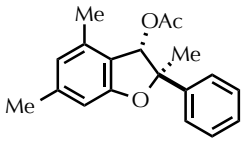

According to the general procedure with 2,4,6-trimethylbenzofuran (32 mg, 0.20 mmol) and phenylboronic acid (37 mg, 0.30 mmol). FC (pentane/Et_2O 200:1 to 10:1) gave **4gaa** as a colorless oil (51 mg, 0.17 mmol, 86%, dr 90:10).

^{1}H NMR ($CDCl_3$, 300 MHz) δ 7.61 (dd, *J* = 7.2, 1.2 Hz, 2H), 7.34 (t, *J* = 7.2 Hz, 2H), 7.25 (m, 1H), 6.70 (s, 1H), 6.57 (s, 1H), 6.42 (s, 1H), 2.34 (s, 3H), 2.21 (s, 3H), 2.14 (s, 3H), 1.70 (s, 3H); ^{13}C NMR ($CDCl_3$, 75 MHz) δ 170.8 (4°), 160.3 (4°), 144.2 (4°), 141.6 (4°), 136.3 (4°), 128.2 (CH), 127.1 (CH), 125.0 (CH), 123.2 (CH), 119.4 (4°), 107.9 (CH), 91.1 (4°), 79.5 (CH), 23.0 (CH_3), 21.5 (CH_3), 20.6 (CH_3), 17.6 (CH_3); HRMS (ESI+) calcd for $C_{19}H_{20}O_3Na$ [M+Na]$^+$: *m/z* 319.1305, found: *m/z* 319.1304; IR (neat): 2381, 2343, 1736, 1692, 1445, 1371, 1232, 1214, 1015, 971, 834, 762, 701 (cm^{-1}).

*7-Chloro-2,4,-dimethyl-2-phenyl-2,3-dihydrobenzofuran-3-yl acetate (**4haa**)*

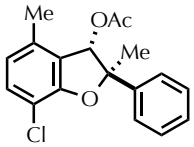

According to the general procedure with 7-chloro-2,4-dimethylbenzofuran (29 mg, 0.16 mmol) and phenylboronic acid (37 mg, 0.30 mmol). FC (pentane/Et_2O 200:1 to 10:1) gave **4haa** as a colorless oil (36 mg, 0.11 mmol, 66%, dr 76:24).

^{1}H NMR ($CDCl_3$, 300 MHz) δ 7.59 (dd, *J* = 6.9, 1.5 Hz, 2H), 7.38–7.34 (m, 3H), 7.22 (d, *J* = 8.1 Hz, 1H), 6.67 (d, *J* = 8.1 Hz, 1H), 6.47 (s, 1H), 2.22 (s, 3H), 2.14 (s, 3H), 1.74 (s, 3H); ^{13}C NMR ($CDCl_3$, 75 MHz) δ 170.6 (4°), 155.8 (4°), 143.4 (4°), 135.4 (4°), 130.9 (CH), 128.5 (CH), 127.5 (CH), 124.9 (CH), 124.1 (4°), 123.2 (CH),

112.7 (4°), 92.2 (4°), 79.9 (CH), 23.0 (CH_3), 20.5 (CH_3), 17.4 (CH_3); HRMS (ESI+) calcd for $C_{18}H_{17}ClO_3Na$ $[M+Na]^+$: *m/z* 339.0758, found: *m/z* 339.0759; IR (neat): 2360, 2342, 1740, 1227, 1019, 911, 679 (cm^{-1}).

*2-Methyl-2-phenyl-1,2-dihydronaphtho[2,1-b]furan-1-yl acetate (**4iaa**)*

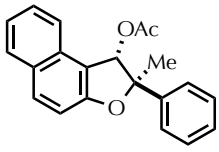

According to the general procedure with 2-methylnaphtho[2,1-*b*]furan (29 mg, 0.20 mmol) and phenylboronic acid (37 mg, 0.30 mmol). FC (pentane/Et_2O 200:1 to 10:1) gave **4iaa** as a colorless oil (56 mg, 0.18 mmol, 88%, dr 78:22).

^1H NMR ($CDCl_3$, 300 MHz) δ 7.73 (d, *J* = 8.7 Hz, 1H), 7.67 (d, *J* = 7.8 Hz, 1H), 7.51 (d, *J* = 7.5 Hz, 2H), 7.45–7.08 (m, 7H), 6.76 (s, 1H), 2.08 (s, 3H), 1.58 (s, 3H); ^{13}C NMR ($CDCl_3$, 75 MHz) δ 168.6 (4°), 156.3 (4°), 141.6 (4°), 130.2 (CH), 128.3 (4°), 127.1 (4°), 126.4 (4°), 126.0 (CH), 125.1 (CH), 125.0 (CH), 122.5 (CH), 121.0 (CH), 119.5 (CH), 112.6 (CH), 109.7 (CH), 89.8 (4°), 77.4 (CH), 20.6 (CH_3), 18.5 (CH_3); HRMS (ESI+) calcd for $C_{21}H_{18}O_3Na$ $[M+Na]^+$: *m/z* 341.1148, found: *m/z* 341.1148; IR (neat): 2361, 2342, 1734, 1636, 1370, 1218, 1016, 970, 809, 700 (cm^{-1}).

*(4-Fluorophenyl)-2-methyl-2,3-dihydrobenzofuran-3-yl acetate (**4aba**)*

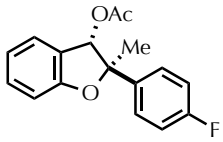

According to the general procedure with 2-methylbenzofuran (26 mg, 0.20 mmol) and *p*-fluorophenylboronic acid (42 mg, 0.30 mmol). FC (pentane/Et_2O 200:1 to 10:1) gave **4aba** as a colorless oil (48 mg, 0.17 mmol, 84%, dr 91:9).

^1H NMR ($CDCl_3$, 300 MHz) δ 7.54–7.50 (m, 2H), 7.33–7.28 (m, 2H), 7.03–6.97 (m, 3H), 6.97–6.91 (m, 1H), 6.29 (s, 1H), 2.19 (s, 3H), 1.72 (s, 1H); ^{13}C NMR ($CDCl_3$, 75 MHz) δ 170.8 (4°) 163.6 (C, J_{C-F} = 245 Hz) 160.4 (C, J_{C-F} = 245 Hz), 160.0 (4°), 139.8 (4°), 131.3 (CH), 126.9 (CH), 123.9 (4°), 121.3 (CH), 115.3 (CH) 115.1 (CH), 110.1 (CH), 90.8 (4°), 80.4 (CH), 23.1 (CH_3), 20.9 (CH_3); HRMS (ESI+) calcd for $C_{17}H_{15}FO_3Na$ $[M+Na]^+$: *m/z* 309.0897, found: *m/z* 309.0902. IR (neat): 2361, 2342, 1734, 1603, 1509, 1480, 1372, 1227, 1070, 1015, 836, 751 (cm^{-1}).

*(4-Chlorophenyl)-2-methyl-2,3-dihydrobenzofuran-3-yl acetate (**4aca**)*

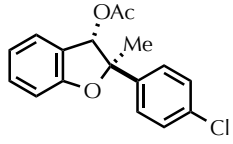

According to the general procedure with 2-methylbenzofuran (26 mg, 0.20 mmol) and *p*-chlorophenylboronic acid (47 mg, 0.30 mmol). FC (pentane/Et_2O 200:1 to 10:1) gave **4aca** as a colorless oil (29 mg, 0.095 mmol, 48%, dr 89:11).

^{1}H NMR ($CDCl_3$, 300 MHz) δ 7.50 (dd, *J* = 6.6, 2.1 Hz, 2H), 7.41–7.26 (m, 4H), 7.01 (d, *J* = 7.8 Hz, 1H), 6.95–6.90 (m, 1H), 6.30 (s, 1H), 2.19 (s, 3H), 1.71 (s, 3H); ^{13}C NMR ($CDCl_3$, 75 MHz) δ 170.8 (4°), 159.9 (4°), 142.6 (4°), 133.3 (4°), 131.3 (CH), 128.5 (CH), 126.9 (CH), 126.5 (CH), 123.8 (4°), 121.4 (CH), 110.1 (CH), 90.7 (4°), 80.2 (CH), 22.9 (CH_3), 20.9 (CH_3); HRMS (ESI+) calcd for $C_{17}H_{15}ClO_3Na$ $[M+Na]^+$: *m/z* 325.0602, found: *m/z* 325.0601. IR (neat): 2361, 2342, 1734, 1481, 1231, 1013, 753 (cm^{-1}).

*(4-Bromophenyl)-2-methyl-2,3-dihydrobenzofuran-3-yl acetate (**4ada**)*

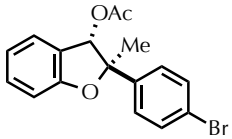

According to the general procedure with 2-methylbenzofuran (26 mg, 0.20 mmol) and *p*-bromophenylboronic acid (60 mg, 0.30 mmol). FC (pentane/Et_2O 200:1 to 10:1) gave **4ada** as a colorless oil (38 mg, 0.11 mmol, 55%, dr 89:11).

^{1}H NMR ($CDCl_3$, 300 MHz) δ 7.54–7.44 (m, 4H), 7.38–7.30 (m, 2H), 7.05 (d, *J* = 8.1 Hz, 1H), 6.97 (t, *J* = 7.2 Hz, 1H), 6.30 (s, 1H), 2.22 (s, 3H), 1.73 (s, 3H); ^{13}C NMR ($CDCl_3$, 75 MHz) δ 170.2 (4°), 159.3 (4°), 142.6 (4°), 130.9 (CH), 130.8 (CH), 130.2 (4°), 127.4 (CH), 126.3 (CH), 123.1 (4°), 120.8 (CH), 109.5 (CH), 90.1 (4°), 79.6 (CH), 22.3 (CH_3), 20.3 (CH_3); HRMS (ESI+) calcd for $C_{17}H_{15}BrO_3Na$ $[M+Na]^+$: *m/z* 369.0097, found: *m/z* 325.0101. IR (neat): 2361, 2342, 1738, 1481, 1230, 1009, 753 (cm^{-1}).

*2-Methyl-(p-tolyl)-2,3-dihydrobenzofuran-3-yl acetate (**4aea**)*

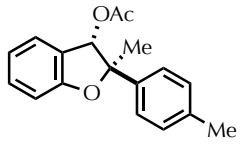

According to the general procedure with 2-methylbenzofuran (26 mg, 0.20 mmol) and *p*-tolylboronic acid (41 mg, 0.30 mmol). FC (pentane/Et_2O 200:1 to 10:1) gave **4aea** as a colorless oil (33 mg, 0.12 mmol, 58%, dr 88:12).

^{1}H NMR ($CDCl_3$, 300 MHz) δ 7.43 (d, *J* = 8.1 Hz, 2H), 7.26–7.16 (m, 2H), 7.04 (d, *J* = 8.0 Hz, 2H), 7.02 (d, *J* = 8.0 Hz, 1H), 6.93–6.88 (m, 1H), 6.32 (s, 1H), 2.31 (s, 3H), 2.18 (s, 3H), 1.73 (s, 3H); ^{13}C NMR ($CDCl_3$, 75 MHz) δ 170.7 (4°), 160.2 (4°), 141.1

(4°), 137.1 (4°), 131.2 (CH), 129.0 (CH), 126.9 (CH), 124.9 (CH), 124.3 (4°), 121.3 (CH), 110.1 (CH), 91.1 (4°), 80.5 (CH), 23.1 (CH_3), 21.0 (CH_3), 20.9 (CH_3); HRMS (ESI+) calcd for $C_{18}H_{18}O_3$ $[M+Na]^+$: *m/z* 305.1148, found: *m/z* 305.1151. IR (neat): 1734, 1601, 1479, 1230, 1016, 919, 817, 751 (cm^{-1}).

*2-Methyl-(m-tolyl)-2,3-dihydrobenzofuran-3-yl acetate (**4afa**)*

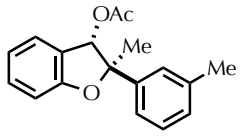

According to the general procedure with 2-methylbenzofuran (26 mg, 0.20 mmol) and *m*-tolylboronic acid (41 mg, 0.30 mmol). FC (pentane/Et_2O 200:1 to 10:1) gave **4afa** as a colorless oil (29 mg, 0.10 mmol, 51%, dr 86:14).

^1H NMR ($CDCl_3$, 300 MHz) δ 7.25–7.18 (m, 5H), 7.15–7.10 (m, 1H), 7.05 (d, *J* = 7.8 Hz, 2H), 7.02 (d, *J* = 8.4 Hz, 1H), 6.93–6.88 (m, 1H), 6.33 (s, 1H), 2.33 (s, 3H), 2.17 (s, 3H), 1.72 (s, 3H); ^{13}C NMR ($CDCl_3$, 75 MHz) δ 170.8 (4°), 160.3 (4°), 144.1 (4°), 138.1 (4°), 131.3 (CH), 128.4 (CH), 128.3 (CH), 127.0 (CH), 125.7 (CH), 124.4 (4°), 122.2 (CH), 121.1 (CH), 110.2 (CH), 91.2 (4°), 80.5 (CH), 23.2 (CH_3), 21.6 (CH_3), 21.0 (CH_3); HRMS (ESI+) calcd for $C_{18}H_{18}O_3Na$ $[M+Na]^+$: *m/z* 305.1148, found: *m/z* 305.1149; IR (neat): 2361, 2342, 1736, 1479, 1219, 1017, 751, 706 (cm^{-1}).

*2-(4-Methoxyphenyl)-methyl-2,3-dihydrobenzofuran-3-yl acetate (**4aga**)*

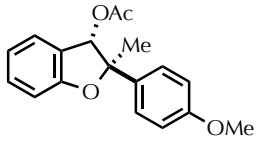

According to the general procedure with 2-methylbenzofuran (26 mg, 0.20 mmol) and 4-methoxyphenylboronic acid (46 mg, 0.30 mmol). FC (pentane/Et_2O 200:1 to 10:1) gave **4aga** as a colorless oil (17 mg, 0.057 mmol, 28%, dr 83:17).

^1H NMR ($CDCl_3$, 300 MHz) δ 7.46 (dd, *J* = 5.1, 3.0 Hz, 2H), 7.39–7.27 (m, 2H), 7.02–6.89 (m, 2H), 6.85 (dd, *J* = 5.1, 3.0 Hz, 2H), 6.30 (s, 1H), 3.77 (s, 3H), 2.18 (s, 3H), 1.72 (s, 3H); ^{13}C NMR ($CDCl_3$, 75 MHz) δ 170.7 (4°), 160.1 (4°), 158.8 (4°), 136.0 (4°), 131.1 (CH), 126.9 (CH), 126.1 (CH), 124.2 (4°), 121.1 (CH), 113.7 (CH), 110.0 (CH), 90.9 (4°), 80.4 (CH), 55.1 (CH_3), 23.0 (CH_3), 20.9 (CH_3); HRMS (ESI+) calcd for $C_{18}H_{18}O_4Na$ $[M+Na]^+$: *m/z* 321.1097, found: *m/z* 321.1097; IR (neat): 2361, 2342, 1734, 1812, 1512, 1372, 1231, 1019, 753 (cm^{-1}).

Hydrolysis of 4aaa

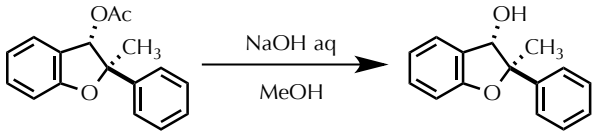

4aaa
dr (90:10)

5aa
90%, dr (90:10)

*2-Methyl-2-phenyl-2,3-dihydrobenzofuran-3-ol (**5aa**)*

4aaa (127 mg, 0.47 mmol, dr 90:10), MeOH (15 mL) and 1M NaOH solution (3.7 mL) were added to a reaction tube and stirred overnight at room temperature. The mixture was extracted with CH_2Cl_2 (3 x 5.0 mL). The combined organic layers were dried over $MgSO_4$ and filtered. The volatiles were removed under reduced pressure to afford **5aa** as a colorless solid (96 mg, 0.42 mmol, 90%, dr 90:10). The solid was recrystallized from hexane solution to give diastereomerically pure alcohol as colorless crystals (45 mg, 0.20 mmol, 42%).

^{1}H NMR ($CDCl_3$, 300 MHz) δ 7.43 (m, 2H), 7.35–7.21 (m, 5H), 6.99 (d, J = 8.1 Hz, 1H), 6.94–6.89 (m, 1H), 5.14 (d, J = 8.7 Hz, 1H), 2.04 (d, J = 8.7 Hz, 1H), 1.70 (s, 3H); ^{13}C NMR ($CDCl_3$, 75 MHz) δ 159.3(4°), 145.1 (4°), 130.8 (CH), 128.4 (CH), 128.0 (4°), 127.2 (CH), 126.1 (CH), 124.7 (CH), 121.2 (CH), 110.4 (CH), 92.3 (4°), 80.4 (CH), 22.5 (CH_3); HRMS (ESI+) calcd for $C_{15}H_{14}O_2Na$ $[M+Na]^+$: m/z 249.0886, found: m/z 249.0889; mp: 102–103 °C; IR (neat): 3328, 2361, 2342, 1599, 1477, 1252, 1022, 919, 752, 700 (cm^{-1}).

X-ray Crystallography

X-ray data set was collected with a Nonius KappaCCD diffractometer. Programs used: data collection COLLECT (Nonius B.V., 1998), data reduction Denzo-SMN (Z. Otwinowski and W. Minor, *Methods in Enzymology*, 1997, **276**, 307), absorption correction Denzo (Z. Otwinowski, D. Borek, W. Majewski & W. Minor, *Acta Cryst*. 2003, **A59**, 228), structure solution SHELXS-97 (G. M. Sheldrick, *Acta Cryst*. 1990, **A46**, 467), structure refinement SHELXL-97 (G. M. Sheldrick, *Acta Cryst*. 2008, **A64**, 112), graphics XP (BrukerAXS, 2000). R_1 values are given for the observed reflections, wR_2 values for all reflections.

X-ray crystal structure analysis for **4baa**: formula $C_{20}H_{22}O_3$, M = 310.38, colorless crystal, 0.30 × 0.23 × 0.10 mm, a = 12.9968(1), b = 13.4352(1), c = 10.0076(1) Å, β = 101.394(1)°, V = 1713.03(3) Å^3, ϱ_{calc} = 1.203 gcm^{-3}, μ = 0.636 mm^{-1}, empirical absorption correction (0.832 ≤ T ≤ 0.939), Z = 4, monoclinic, space group $P2_1/c$ (No. 14), λ = 1.54178 Å, T = 223(2) K, ω and ϕ scans, 13135 reflections collected ($\pm h$, $\pm k$, $\pm l$), [(sinθ)/λ] = 0.60 Å^{-1}, 2981 independent (R_{int} = 0.040) and 2678 observed reflections [I>2σ(I)], 210 refined parameters, R_1 = 0.045, wR_2 = 0.122, max. (min.) residual electron density 0.20 (–0.19) e.Å^{-3}, hydrogen atoms calculated and refined as riding atoms.

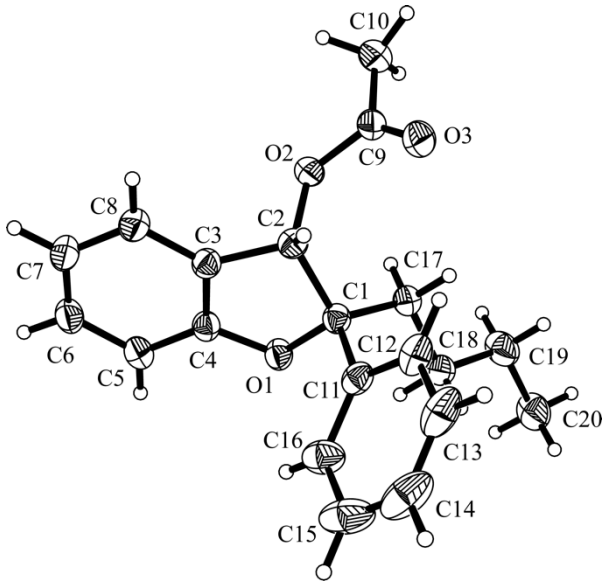

Figure S1. X-ray structure of **4baa** (thermals ellipsoids are shown with 30% probability).

X-ray crystal structure analysis for **5aa**: formula $C_{15}H_{14}O_2$, M = 293.26, colorless crystal, 0.62 × 0.12 × 0.10 mm, a = 25.2302(7), b = 25.2302(7), c = 10.3026(6) Å, α = 90, β = 90, γ = 120°, V = 5679.6(4) Å^3, ϱ_{calc} = 1.191 gcm^{-3}, μ = 0.623 mm^{-1}, empirical absorption correction (0.698 ≤ T ≤ 0.940), Z = 18, trigonal, space group R-3 (No. 148), λ = 1.54178 Å, T = 223(2) K, ω and φ scans, 16174 reflections collected (±h, ±k, ±l), [(sinθ)/λ] = 0.60 Å^{-1}, 2209 independent (R_{int} = 0.054) and 1829 observed reflections [I>2σ(I)], 159 refined parameters, R_1 = 0.041, wR_2 = 0.103, max. (min.) residual electron density 0.11 (–0.15) e.Å^{-3}, the hydrogen at O2 atom was refined freely; others were calculated and refined as riding atoms.

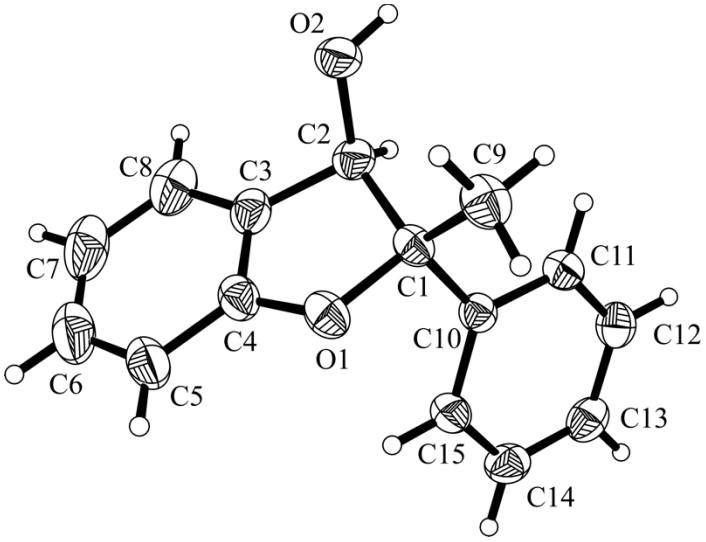

Figure S2. X-ray structure of **5aa** (thermals ellipsoids are shown with 30% probability).

CCDC 963178 (**4baa**) and 963177 (**5aa**) contains the supplementary crystallographic data for this paper. These data can be obtained free of charge at www.ccdc.cam.ac.uk/conts/retrieving.html [or from the Cambridge Crystallographic Data Centre, 12 Union Road, Cambridge CB2 1EZ, UK; fax: (internat.) +44(1223)336-033, E-mail: deposit@ccdc.cam.ac.uk].

5. References

[1] Hydrogenation: (a) Y. G. Zhou, *Acc. Chem. Res.*, 2007, **40**, 1357; (b) N. Ortega, S. Urban, B. Beiring and F. Glorius, *Angew. Chem., Int. Ed.*, 2012, **51**, 1710; (c) N. Ortega, B. Beiring, S. Urban and F. Glorius, *Tetrahedron,* 2012, **68**, 5185.

[2] For reviews on total synthesis by dearomatization strategies, see: (a) S. P. Roche and J. A. Porco Jr. *Angew. Chem., Int. Ed.*, 2011, **50**, 4068; (b) C.-X. Zhuo, W. Zhang and S.-L. You, *Angew. Chem., Int. Ed.*, 2012, **51**, 12662.

[3] Reviews on the use of TEMPO in synthesis: (a) T. Vogler and A. Studer, *Synthesis*, 2008, 1979; (b) L. Tebben and A. Studer, *Angew. Chem., Int. Ed.*, 2011, **50**, 5034; (c) S. Wertz and A. Studer, *Green Chem.*, 2013, **15**, 3116.

[4] Transition metal-catalyzed oxidative multi-component coupling of heteroarenes involving dearomatization: (a) S. Kirchberg, R. Fröhlich and A. Studer, *Angew. Chem., Int. Ed.*, 2009, **48**, 4235; (b) S. Kirchberg, R. Fröhlich and A. Studer, *Angew. Chem., Int. Ed.*, 2010, **49**, 6877.

[5] R. F. Heck, *J. Am. Chem. Soc.*, 1968, **90**, 5542.

[6] Acyloxyarylation of terminal olefins: (a) K. K. Mayer, S. Prior and W. Wiegrebe, *Monatsh. Chem.*, 1986, **117**, 511; (b) R. C. Larock and H. Song, *Synth. Commun.*, 1989, **19**, 1463; (c) R. C. Larock and L. Guo, *Synlett*, 1995, 465; (d) F. Ek, L.-G. Wistrand and T. Frejd, *J. Org. Chem.*, 2003, **68**, 1911; (e) S. Protti, M. Fagnoni and A. Albini, *J. Am. Chem. Soc.*, 2006, **128**, 10670; (f) M. D. Obushak, V. S. Matiychuk and V. V. Turytsya, *Tetrahedron Lett.*, 2009, **50**, 6112; (g) V. Dichiarante, M. Fagnoni and A. Albini, *J. Org. Chem.*, 2010, **75**, 1271; (h) G. Zhang, L. Cui, Y. Wang and L. Zhang, *J. Am. Chem. Soc.*, 2010, **132**, 1474; (i) A. D. Melhado, W. E. Brenzovich Jr, A. D. Lackner and F. D. Toste, *J. Am. Chem. Soc.*, 2010, **132**, 8885; (j) L. T. Ball, M. Green, G. C. Lloyd-Jones and C. A. Russell, *Org. Lett.*, 2010, **12**, 4724; (k) W. E. Brenzovich Jr, J.-F. Brazeau and F. D. Toste, *Org. Lett.*, 2010, **12**, 4728; (l) A. D. Satterfield, A. Kubota and M. S. Sanford, *Org. Lett.*, 2011, **13**, 1076; (m) E. T. da Penha, J. A. Forni, A. F. P. Biajoli and C. R. D. Correia, *Tetrahedron Lett.*, 2011, **48**, 6342; (n) L. T. Ball, G. C. Lloyd-Jones and C. A. Russell, *Chem.– Eur. J.*, 2012, **18**, 2931. (o) C. Raviola, S. Protti, D. Ravelli, M. Mella, A. Albini and M. Fagnoni, *J. Org. Chem.*, 2012, **77**, 9094.

[7] Acyloxyarylation of internal olefins; (a) J. F. Jamie and R. W. Rickards, *J. Chem.*

Soc., Perkin Trans. 1, 1997, 3613; (b) K. Saito, K. Ono, M. Sano, S. Kiso and T. Takeda, *Heterocycles*, 2002, **57**, 1781.

[8] Selected examples on oxidative C–H arylation with arylboronic acids (a) S.-D. Yang, C.-L. Sun, Z. Fang, B.-J. Li, Y.-Z. Li and Z.-J. Shi, *Angew. Chem., Int. Ed.*, 2008, **47**, 1473; (b) S. K. Guchhait, M. Kashyap and S. Saraf, *Synthesis*, 2010, 1166.

[9] C–H arylations with arylboronic acids using TEMPO as an oxidant: (a) T. Vogler and A. Studer, *Org. Lett.*, 2008, **10**, 129; (b) S. Kirchberg, T. Vogler and A. Studer, *Synlett*, 2008, 2841; (c) S. Kirchberg, S. Tani, K. Ueda, J. Yamaguchi, A. Studer and K. Itami, *Angew. Chem., Int. Ed.*, 2011, **50**, 2387; (d) M. Steinmetz, K. Ueda, S. Grimme, J. Yamaguchi, S. Kirchberg, K. Itami and A. Studer, *Chem.– Asian. J.*, 2012, **7**, 1256; (e) K. Yamaguchi, J. Yamaguchi, A. Studer and K. Itami, *Chem. Sci.*, 2012, **3**, 2165; (f) Z. He, S. Kirchberg, R. Fröhlich and A. Studer, *Angew. Chem., Int. Ed.*, 2012, **51**, 3699.

[10] Natural products having 2-aryl-3-oxy-2,3-dihydrobenzofuran structure; (a) G. Brader, S. Vajrodaya, H. Greger, M. Bacher, H. Kalchhauser and O. Hofer, *J. Nat. Prod.*, 1998, **61**, 1482; (b) H.-L. Liu, X.-F. Huang, X. Wan and L.-Y. Kong, *Helv. Chim. Acta*, 2007, **90**, 1117; (c) C.-C. Huang, Y.-T. Tung, K.-C. Cheng and J.-H. Wu, *Food Chem.*, 2011, **125**, 726; (d) J. M. Chambers, L. M. Lindqvist, A. Webb, D. C. S. Huang, G. P. Savage and M. A. Rizzacasa, *Org. Lett.*, 2013, **15**, 1406; (e) Y.-C. Tsai, S.-Y. Chiang, M.-E. Shazly, C.-C. Wu, L. Beerhues, W.-C. Lai, S.-F. Wu, M.-H. Yen, Y.-C. Wu and F. R. Chang, *Food Chem.*, 2013, **140**, 305; (f) L. Pan, U. M. Acuña, J. Li, N. Jena, T. N. Ninh, C. M. Pannell, H. Chai, J. R. Fuchs, E. J. C. de Blanco, D. D. Soejarto and A. D. Kinghorn, *J. Nat. Prod.*, 2013, **76**, 394.

[11] A. I. Roshchin, S. M. Kel'chevski, N. A. Bumagin, *J. Organomet. Chem.*, 1998, **560**, 163.

[12] M. E. Meza-Aviñez, M. Ordoñez, Ma. Fernández-Zertuche, L. Rodríguez-Fragoso, J. Reyes-Esparza and J. Reyes-Esparza, 2005, *Bioorg. Med. Chem.*, 2005, **13**, 6521.

[13] S. W. Youn and J. I. Eom, *Org. Lett.*, 2005, **7**, 3355.

Chapter 2

1,3,5-Triaryl-2-Pyridylidene: Base-Promoted Generation and Complexation

Abstract

A base-promoted generation of sterically hindered 1,3,5-triaryl-2-pyridylidene from the corresponding pyridinium salt is described. The thus-generated 2-pyridylidene was trapped by S_8 and Me_2SAuCl to form 2-pyridinethione and a 2-pyridylidene–gold(I) complex, respectively. Rearrangement of pyridylidene to pyrido[1,2-*a*]indole indicates high reactivity of the carbene center of 2-pyridylidene.

1. Introduction

N-Heterocyclic carbenes (NHCs) have a great role in synthetic organic chemistry. NHCs are recognized as useful ligands for transition metal catalysts and as a new class of nucleophilic organic catalysts (Figure 1).[1] Recently, stable singlet carbenes bearing one bound heteroatom rather than two have attracted attention because of their high HOMO energy levels.[2] Representative compounds, cyclic amino alkyl carbenes (CAAC), showed unusual properties such as strong σ-donation to transition metals and cleavage of unreactive H–H or N–H bonds.[3a–i] Recently, aminoylide carbenes (AYC) were also reported as strong donating ligands.[3j–l] In this chapter, the generation and trapping reactions of 1,3,5-triaryl-2-pyridylidene are described.

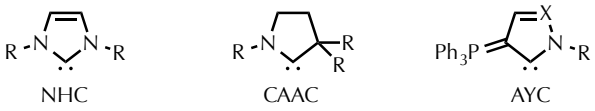

Figure 1. *N*-heterocyclic carbene (NHC), cyclic amino alkyl carbene (CAAC) and aminoylide carbene (AYC).

Pyridylidene is a pyridine-based carbene species bearing one heteroatom. In Figure 2, pyridine (**A**) and the isomeric 2-, 3-, and 4-pyridylidenes (**B**, **C**, and **D**) are depicted. According to theoretical studies, 2- and 4-pyridylidene are stable singlet carbenes with higher HOMO energies than those of other NHCs and even CAAC. High nucleophilicity and basicity of free pyridylidene and strong σ-donation of a pyridylidene ligand were predicted.[4] Since its first indication of generating 2-pyridylidene (**B**) in 1937 by Hammick *et al.*,[5a] there have been a number of theoretical and experimental studies on the free carbene and transition metal complexes of pyridylidenes.[4–7] However, the isolation of pyridylidenes has not been achieved yet.[7,8] Reaction of pyridinium salt with strong bases and ruthenium to form bridged pyridylidene complexes reported by Cabeza *et al.* is the only example describing the generation and reactivity of pyridylidenes.[7] Thus, the stability and reactivity of pyridylidene toward electrophilic reagents remain unclear.

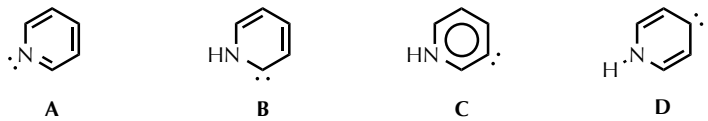

Figure 2. Pyridine (**A**) and pyridylidenes (**B**, **C**, **D**) as isomers of pyridine.

The strategy for generating reasonably stable 2-pyridylidene is shown in Figure 3. It was envisaged that (i) three bulky aryl groups introduced at the 1,3,5-positions would

help stabilize otherwise reactive 2-pyridylidene, and (ii) the target carbene could be generated by the deprotonation of the corresponding pyridinium salt by a strong base. The formation of pyridylidene should then be confirmed by trapping experiments with S_8 or a gold(I) complex, which are well known as reactive reagents toward free NHCs.

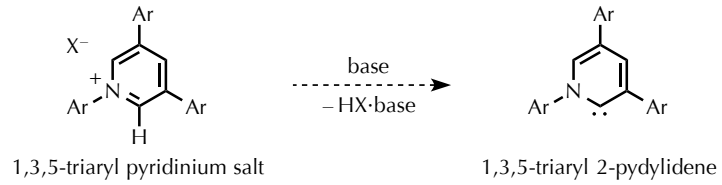

Figure 3. Synthetic strategy for 2-pyridylidene.

2. Results and Discussion

Pyridinium salt bearing sterically demanding substituents at 1,3,5-positions was first synthesized (Scheme 1). Aryl groups with methyl substituents at *ortho*-positions were chosen for effective kinetic stabilization of reactive carbene centers. The Suzuki–Miyaura cross-coupling[9] of 3,5-dibromopyridine and 2,6-dimethylphenylboronic acid (Xyl-$B(OH)_2$) in the presence of a $Pd(PPh_3)_4$ catalyst and $Ba(OH)_2$ produced 3,5-Xyl_2pyridine (**1**) in 80% yield. A Zincke salt[10] was then produced by the reaction of **1** with 1-chloro-2,4-dinitrobenzene. The chloride anion was then exchanged with triflate using silver triflate to afford pyridinium **2·OTf**. As Zincke salt **2·OTf** was slowly decomposed to starting material **1**, the following reaction was performed without isolation. Finally 2,4-dinitrophenyl group was replaced by a mesityl (1,3,5-trimethylphenyl) group by treating **2·OTf** with $MesNH_2$ at 150 °C. The desired sterically hindered 1,3,5-triaryl 2-pyridinium **3** was obtained in 34% yield over three steps from **1**. The structures of **3** and synthetic intermediate **1** were confirmed by ^1H, ^{13}C NMR, elemental analysis, and X-ray crystallography.[11]

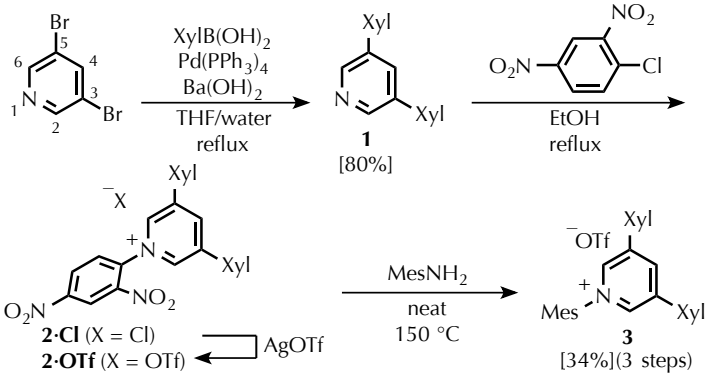

Scheme 1. Synthesis of pyridinium **3**. Xyl = 2,6-$Me_2C_6H_3$, Mes =2,4,6-$Me_3C_6H_2$, Tf = CF_3SO_2.

With the requisite pyridinium **3** in hand, its reaction with a base was next examined. After many attempts the author found that lithium hexamethyldisilazide (LiHMDS) produced 2-pyridylidene **4** in THF at room temperature (Scheme 2). The generation of **4** was confirmed by trapping it with S_8 and Me_2SAuCl to yield the corresponding pyridinethione **5** (82% yield) and 2-pyridylidene–gold(I) complex **6** (27% yield), respectively. Other strong bases such as NaH or KH were also able to generate pyridylidene species **4** from **3**.

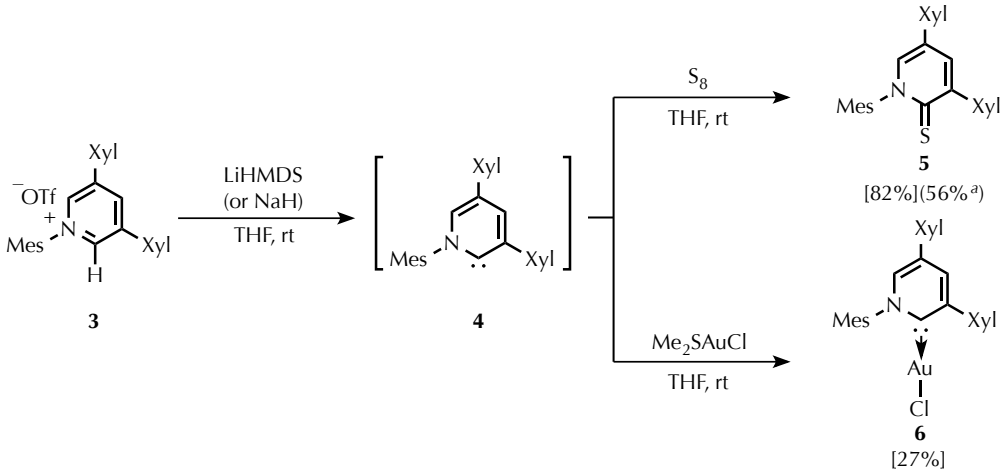

Scheme 2. Generation of 2-pyridylidene **4** and its reactions. Yields are isolated yields. [a]NaH was used instead of LiHMDS. HMDS = $N(SiMe_3)_2$

It should be noted that no 4-pyridylidene product was observed in these reactions. Preferential deprotonation at the 2-position of pyridylidene might be due to the higher acidity of the hydrogen atoms at the 2-position. To estimate the acidity of the hydrogen atoms at the 2- and 4-position, DFT calculation was performed by using B3LYP/6-31+G(d) level of theory.[12] It was found that 2-pyridylidene is 13.3 kcal mol^{-1} (ΔH) more stable than 4-pyridylidene, which is consistent with the experimental results.

On the other hand, treatment of **3** with *tert*-butyllithium caused nucleophilic attack of the *tert*-butyl group at the 4-position of **3** to form 1,4-dihydropyridine derivative **7** in 39% yield (Scheme 3). Treatment of **3** with $NaBH_4$ led to the formation of dihydropyridine derivatives **8a** and **8b** (83% yield, **8a**/**8b** = 1:0.6). As the mixture of **8a** and **8b** did not undergo any reaction with S_8 to form **5**, a possibility that 1,2-dihydropyridine **8a** is involved in the reaction of **3** with NaH can be excluded. However, a possible involvement of the $N(SiMe_3)_2$ adduct in the LiHMDS-mediated generation of **4** cannot be completely excluded.[8b]

The formation of **6** represents the first example of the synthesis of the pyridylidene–gold(I) complex from the reaction of a pyridinium and a base. This

method does not require any substituents such as chloro or carboxyl groups on the pyridinium precursor. This is the most direct way to produce transition metal pyridylidene complexes among previously reported methods.[6]

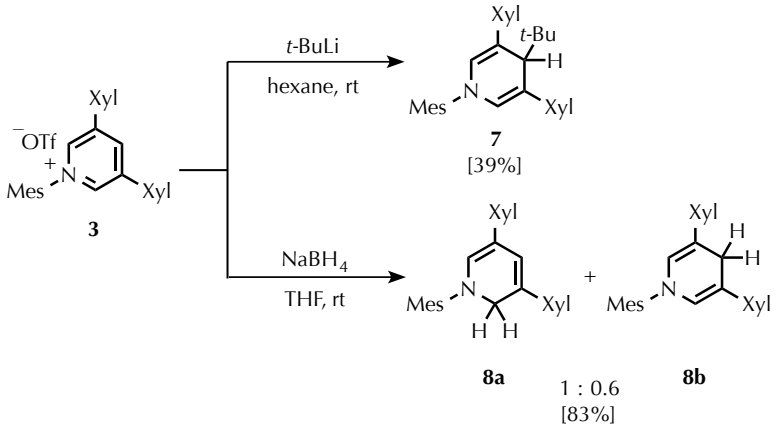

Scheme 3. Reactions of **3** with *t*-BuLi and $NaBH_4$.

The X-ray crystal structures of **3**·toluene and **6**·toluene are shown in Figure 4. In both structures, Xyl and Mes groups are at about right angles to the pyridine ring to minimize steric hindrance of the methyl groups. Due to the carbene character of **6**, the N(1)–C(1)–C(2) angle of **6** (116.0(5)°) is smaller than that of **3** (121.38(13)° and 120.79(15)°). However, there is no other significant structural difference of the pyridine rings between **3** and **6**. It should be noted that the Au–Cl bond length of **6** (2.2845(16) Å) indicates the strong *trans* influence of the 2-pyridylidene ligand.[13]

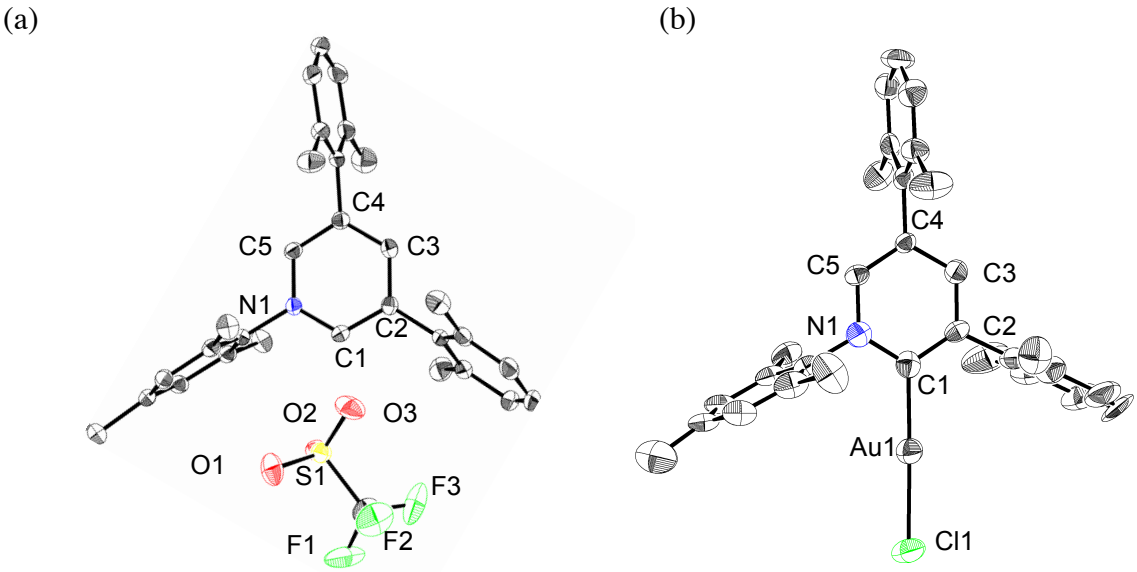

Figure 4. ORTEP drawings of **3**·toluene (a) and **6**·toluene (b) with 50% thermal ellipsoids. Hydrogen atoms and toluene are omitted for clarity.

During the attempt to isolate 2-pyridylidene **4**, the author identified 7,9-Xyl_2-2,4-Me_2-pyrido[1,2-*a*]indole (**9**), a decomposed product, by NMR spectroscopy and X-ray crystallography.[14] Shown in Scheme 4 is a plausible mechanism for the generation of **9**. Proton transfer from the benzylic position of the mesityl group to the carbene carbon affords zwitterionic compound **10**. Nucleophilic attack of the benzylic anion at the 2-position of pyridinium results in the formation of 9*a*,10-dihydropyrido-[1,2-*a*]indole **11**, which is oxidized and aromatized to **9**. Similar rearrangement reactions of NHCs were reported.[15] These results clearly indicate the high reactivity (nucleophilicity and basicity) of the carbene center of 2-pyridylidene.

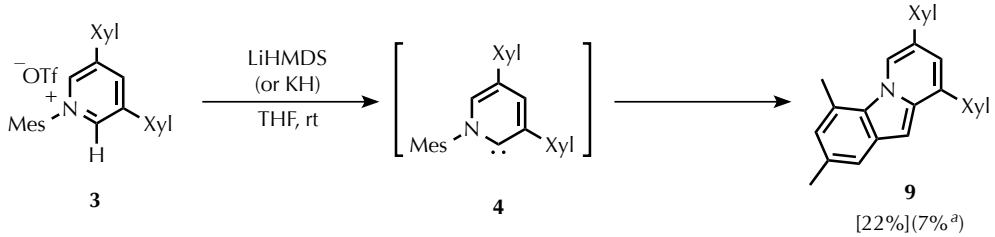

3 **4** **9**

[22%](7%[a])

Plausible Mechanism

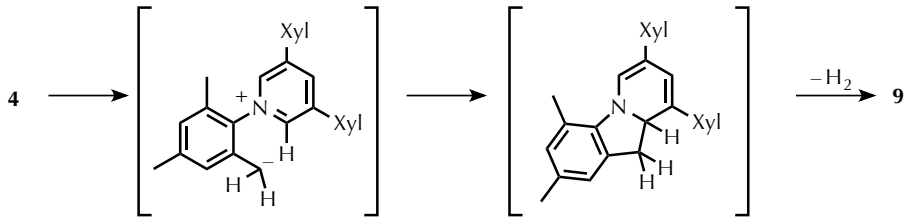

10 **11**

Scheme 4. Rearrangement of **4** to pyrido[1,2-*a*]indole **9** and its plausible mechanism. [a]KH was used instead of LiHMDS.

3. Conclusion

The author has established that a sterically hindered 1,3,5-triaryl-2-pyridylidene could be generated by the reaction of the corresponding pyridinium salt with a strong base such as LiHMDS, NaH and KH. The thus-generated 2-pyridylidene was trapped by S_8 and Me_2SAuCl to form 2-pyridinethione and a 2-pyridylidene–gold(I) complex, respectively. Rearrangement of pyridylidene to pyrido[1,2-*a*]indole indicates a high reactivity of the carbene center of 2-pyridylidene. As 2-pyridylidenes are among the most electron-donating and nucleophilic *N*-heterocyclic carbenes, the present findings should provide tremendous opportunity for using 2-pyridylidenes for various purposes.

4. Experimental

General

Unless otherwise noted, all materials including dry solvents were obtained from commercial suppliers and used without further purification. Tetrahydrofuran (THF) and diethyl ether were purified by passing through a solvent purification system (Glass Contour). All reactions were performed using standard vacuum-line and Schlenk techniques. Work-up and purification procedures were carried out with reagent-grade solvents under air.

Analytical thin-layer chromatography (TLC) was performed using E. Merck silica gel 60 F_{254} precoated plates (0.25 mm). The developed chromatogram was analyzed by UV lamp (254 nm and 365 nm). Flash column chromatography was performed with E. Merck silica gel 60 (230–400 mesh). Preparative thin-layer chromatography (PTLC) was performed using Wako-gel® B5-F silica coated plates (0.75 mm) prepared in our laboratory. High-resolution mass spectra (HRMS) were obtained from a JEOL JMS700 (fast atom bombardment mass spectrometry, FAB MS) and a JEOL JMST100TD instrument (DART). Melting points were measured on a MPA100 Optimelt automated melting point system. Nuclear magnetic resonance (NMR) spectra were recorded on JEOL JNM-ECA-600 (^{1}H 600 MHz, ^{13}C 150 MHz) spectrometer and JEOL JNM-ECS-400 (^{1}H 400 MHz, ^{13}C 100 MHz) spectrometer. Chemical shifts for ^{1}H NMR are expressed in parts per million (ppm) relative to $CHCl_3$ (δ 7.26 ppm) and benzene-d_6 (δ 7.15 ppm). Chemical shifts for ^{13}C NMR are expressed in ppm relative to $CDCl_3$ (δ 77.0 ppm) and benzene-d_6 (δ 128.1 ppm). Data are reported as follows: chemical shift, multiplicity (s = singlet, d = doublet, dd = doublet of doublets, t = triplet, m = multiplet), coupling constant (Hz), and integration.

Compound data

*3,5-Bis(2,6-dimethylphenyl)pyridine (**1**)*

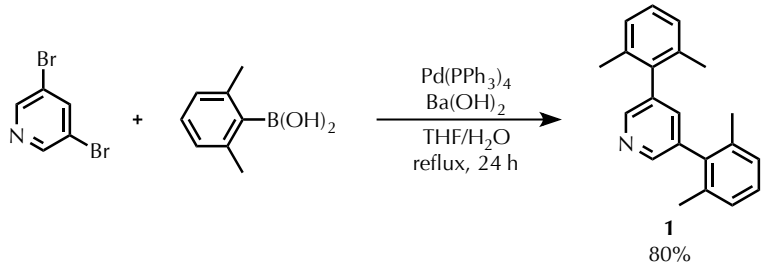

1
80%

A two-necked 300 mL flask equipped a reflux tube and containing a magnetic stirring bar was dried under vacuum and filled with argon after cooling to room temperature. 3,5-dibromopyridine (1.9 g, 8.0 mmol), 2,6-dimethylphenylboronic acid (2.5 g, 17 mmol), $Ba(OH)_2$ (5.5 g, 32 mmol), and $Pd(PPh_3)_4$ (462 mg, 0.40 mmol) are added in dry THF (100 mL) and H_2O (10 mL) under argon atmosphere. The mixture was stirred at reflux for 24 h. After the reaction mixture was cooled to room temperature, the reaction mixture was quenched with 50 mL of water, extracted with EtOAc (50 mL × 4), dried over Na_2SO_4, and concentrated under reduced pressure. The crude product was purified by silica gel column chromatography (EtOAc/hexane = 1:10) to obtain **1** (1.8 g, 80%) as a white solid. Suitable single crystal for X-ray analysis was obtained from MeOH solution at –30 °C.

^{1}H NMR ($CDCl_3$, 600 MHz) δ 8.43 (d, J = 2 Hz, 2H), 7.33 (t, J = 2 Hz, 1H), 7.21 (t, J = 8 Hz, 2H), 7.14 (d, J = 8 Hz, 4H), 2.09 (s, 12H); ^{13}C NMR ($CDCl_3$, 150 MHz) δ 148.4 (CH), 137.7 (4°), 137.5 (CH), 136.3 (4°), 136.2 (4°), 127.8 (CH), 127.5 (CH), 21.0 (CH_3); mp: 132.9–134.9 °C; Anal. calcd. for $C_{21}H_{21}N$: C 87.76, H 7.36, N 4.87. found: C 87.65, H 7.31, N 4.62.

*3,5-Bis(2,6-dimethylphenyl)-1-mesitylpyridinium triflate (**3**)*

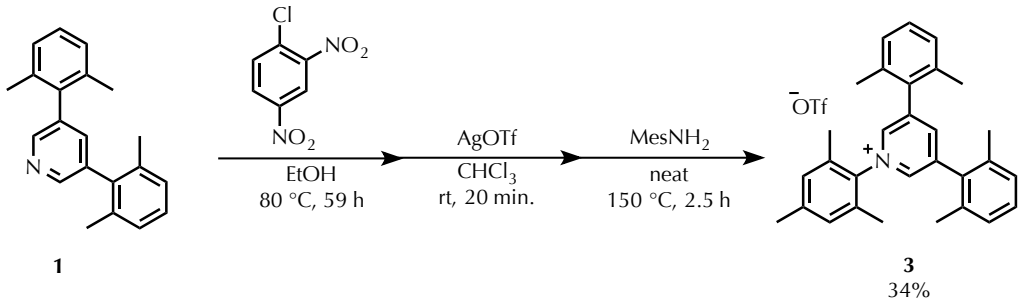

1 **3** 34%

A mixture of diarylpyridine **1** (574 mg, 2.0 mmol), 1-chloro-2,4-dinitrobenzene (405 mg, 2.0 mmol), and EtOH (3.0 mL) in a 10-mL Schlenk tube equipped a reflux tube and a magnetic stirring bar was stirred at 80 °C for 59 h under air. After the reaction mixture was cooled to room temperature, the reaction mixture was reprecipitated with acetone. The insoluble material was separated with filtration and dried under reduced pressure to obtain as a white solid. The solid was dissolved in $CHCl_3$ (20 mL), and AgOTf (513 mg, 2.0 mmol) was added to the solution. The mixture was stirred at room temperature for 20 min. The residue was filtered off with $CHCl_3$, and the solution was concentrated under reduced pressure. 2,4,6-Trimethylaniline (12 mL) was added to the mixture under air. The mixture was stirred at 150 °C for 2.5 h. After the reaction mixture was cooled to room temperature, the mixture was reprecipitated with toluene. The insoluble material was collected with filtration. The product was purified by recrystallization with $CHCl_3$/toluene at room temperature to obtain pyridinium triflate **3**·toluene (446 mg, 34% 3 steps) as a colorless crystal.

^{1}H NMR ($CDCl_3$, 600 MHz) δ 8.70 (d, J = 2 Hz, 2H), 8.27 (s, 1H), 7.32 (t, J = 8 Hz, 2H), 7.24–7.21 (m, 6H), 7.16–7.13 (m, 5H), 2.38 (s, 3H), 2.34 (s, 3H), 2.17 (s, 12H), 2.14 (s, 6H); ^{13}C NMR ($CDCl_3$, 150 MHz) δ 148.9 (CH), 144.5 (CH), 143.1 (4°), 142.3 (4°), 138.7 (4°), 137.8 (4°), 135.3 (4°), 132.0 (4°), 131.7 (4°), 130.33 (CH), 130.28 (CH), 129.0 (CH), 128.5 (CH), 128.2 (CH), 125.2 (CH), 120.6 (q, $J_{C–F}$ = 320 Hz, CF_3), 21.4 (CH_3), 21.1 (CH_3), 21.0 (CH_3), 17.3 (CH_3); mp: 206.2–208.2 °C; Anal. calcd. for $C_{38}H_{40}NO_3F_3S$: C 70.46, H 6.22, N 2.16. found: C 70.40, H, 6.29, N 1.88.

*3,5-Bis(2,6-dimethylphenyl)-1-mesitylpyridine-2-thione (**5**)*

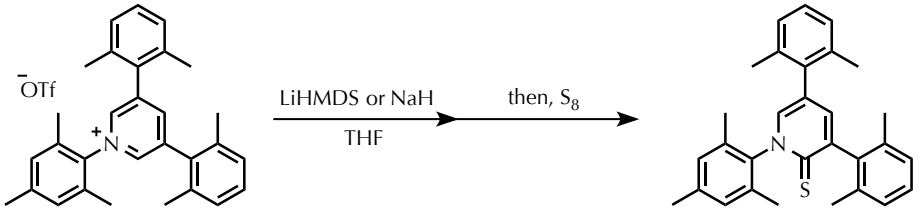

3 **5**
82% (LiHMDS)
56% (NaH)

Method A

A 10-mL Schlenk tube equipped reflux tube and containing stirring bar was dried under vacuum and filled with argon after cooling to room temperature. A mixture of pyridinium triflate **3** (32 mg, 50 μmol) and LiHMDS (1.0 M, 50 μL, 50 μmol) in dry THF (1.0 mL) was stirred at room temperature for 20 min. After the reaction, the solution of S_8 in toluene (0.10 M, 1.0 mL) was added to the reaction mixture at room temperature. The reaction mixture was filtered and the solution was concentrated under reduced pressure. The crude product was purified by silica gel column chromatography (EtOAc/hexane = 1:5) and recrystallized with THF/pentane at room temperature to obtain **5** (18 mg, 82%) as a yellow crystal.

Method B

A 10-mL Schlenk tube equipped reflux tube and containing stirring bar was dried under vacuum and filled with argon after cooling to room temperature. A mixture of pyridinium triflate **3·OTf** (11 mg, 18 μmol) and NaH (4.3 mg, 180 μmol) in dry THF (1.0 mL) was stirred at 50 °C for 1.5 h. After the reaction, the solution of S_8 in toluene (0.1 M, 0.5 mL) was added to the reaction mixture at room temperature. The reaction mixture was filtered and the solution was concentrated under reduced pressure. The crude product was purified by PTLC (EtOAc/hexane = 1:5) to obtain **5** (4.9 mg, 56%) as a yellow solid.

^{1}H NMR ($CDCl_3$, 400 MHz) δ 7.34 (d, *J* = 2 Hz, 1H), 7.16 (m, 2H), 7.12–7.10 (m, 5H), 7.01 (s, 2H), 2.34 (s, 3H), 2.24 (s, 6H), 2.23 (s, 6H), 2.16 (s, 6H); ^{13}C NMR ($CDCl_3$, 100 MHz) δ 178.4 (4° C=S), 146.5 (4°), 141.3 (4°), 139.4 (4°), 138.8 (CH), 138.6 (4°), 137.1 (CH), 136.2 (4°), 135.4 (4°), 135.3 (4°), 133.0 (4°), 129.6 (CH), 128.3 (CH), 127.8 (CH), 127.6 (CH), 127.4 (CH), 125.1 (4°), 21.2 (CH_3), 20.9 (CH_3), 19.8 (CH_3), 17.8 (CH_3); HRMS (FAB+) calcd. for $C_{30}H_{31}NSNa$ $[M+Na]^+$: *m/z* 460.2075, found: *m/z* 460.2069; mp: 260.3–262.3 °C (dec.).

*3,5-Bis(2,6-dimethylphenyl)-1-mesitylpyridylidenegold(I) chloride (**6**)*

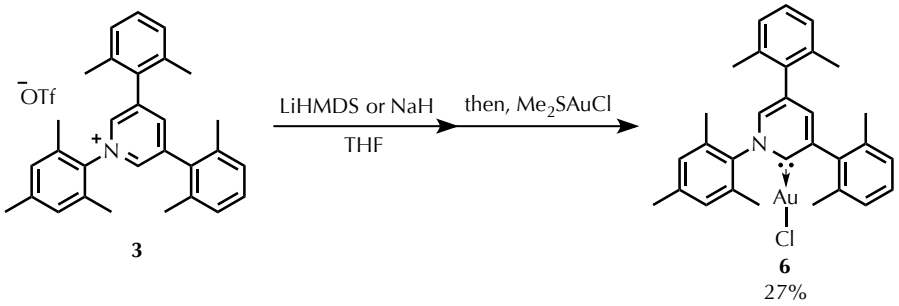

3 **6** 27%

A 10 mL Schlenk tube containing stirring bar was dried under vacuum and filled with argon after cooling to room temperature. LiHMDS in THF solution (1.0 M, 115 μL, 115 μmol) was added to the solution of pyridinium triflate **3** (25 mg, 38 μmol) in dry THF (2.0 mL). The mixture was stirred at room temperature for 20 min. MeS_2AuCl (12 mg, 38 μmol) was added to the reaction mixture. The reaction solution was filtered and concentrated under reduced pressure. The crude product was purified by silica gel column chromatography ($MeOH/CHCl_3$ = 1:20) and recrystallized with $CHCl_3$/toluene at room temperature to obtain **6**·toluene (6.8 mg, 27%) as a pale yellow crystal.

^{1}H NMR ($CDCl_3$, 400 MHz) δ 7.97 (d, *J* = 2 Hz, 1H), 7.71 (d, *J* = 2 Hz, 1H), 7.27–7.21 (m, 4H), 7.18–7.12 (m, 7H), 7.03 (s, 2H), 2.36 (s, 3H), 2.35 (s, 3H), 2.13 (brs, 12H), 2.09 (s, 6H); ^{13}C NMR ($CDCl_3$, 100 MHz) δ 189.3 (4°, $C_{carbene}$), 151.7 (4°), 144.9 (4°), 140.4 (4°), 140.3 (CH), 139.8 (4°), 139.4 (4°), 137.8 (4°), 135.6 (4°), 135.5 (4°), 135.1 (4°), 134.1 (4°), 131.6 (4°), 129.8 (CH), 129.2 (CH), 129.0 (4°), 128.5 (CH), 128.2 (CH), 128.1 (CH), 127.8 (CH), 125.2 (CH), 21.2 (CH_3), 21.1 (CH_3), 20.8 (CH_3), 17.6 (CH_3); mp: 253.4–263.4 °C (dec.); Anal. calcd. for $C_{37}H_{39}NAuCl$: C 60.87, H 5.38, N 1.92. found: C 60.67, H 5.25, N 1.90.

*4-(tert-Butyl)-3,5-bis(2,6-dimethylphenyl)-1-mesityl-1,4-dihydropyridine (**7**)*

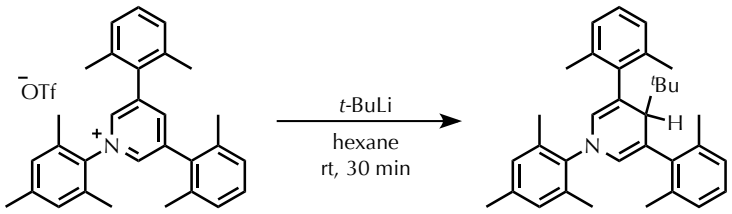

3 **7**
39%

A 10-mL Schlenk tube containing stirring bar was dried under vacuum and filled with argon after cooling to room temperature. A pentane solution of *t*-BuLi (1.6 M, 190 μL, 304 μmol) was added dropwise to the solution of pyridinium triflate **3·OTf** (65 mg, 100 μmol) in dry hexane (1.0 mL). The mixture was stirred at room temperature for 30 min. The reaction mixture was concentrated under reduced pressure. The crude product was purified by recrystallization with hexane at –25 °C to obtain **7** (18 mg, 39%) as a colorless crystal.

^{1}H NMR ($CDCl_3$, 600 MHz) δ 7.06–6.99 (m, 6H), 6.93 (s, 1H), 6.83 (s, 1H), 6.00 (s, 2H), 3.73 (s, 1H), 2.63 (s, 6H), 2.57 (s, 6H), 2.44 (s, 3H), 2.27 (s, 3H), 2.08 (s, 3H); ^{13}C NMR ($CDCl_3$, 150 MHz) δ 144.2 (4°), 140.7 (4°), 137.2 (4°), 136.9 (4°), 136.4 (4°), 136.6 (4°), 135.7 (4°), 133.9 (CH), 129.4 (CH), 128.8 (CH), 127.8 (CH), 125.0 (CH), 109.9 (4°), 50.1 (CH), 40.5 (4°), 29.2 (CH_3), 22.4 (CH_3), 22.1 (CH_3), 20.1 (CH_3), 18.5 (CH_3), 17.5 (CH_3); HRMS (DART+) calcd. for $C_{34}H_{42}N$ $[M+H]^+$: *m/z* 464.3317, found: *m/z* 464.3319; mp: 214.5–216.5 °C (dec.).

*Synthesis of 3,5-bis(2,6-dimethylphenyl)-1-mesityl-1,2-dihydropyridine (**8a**) and 3,5-bis(2,6-dimethylphenyl)-1-mesityl-1,4-dihydropyridine (**8b**)*

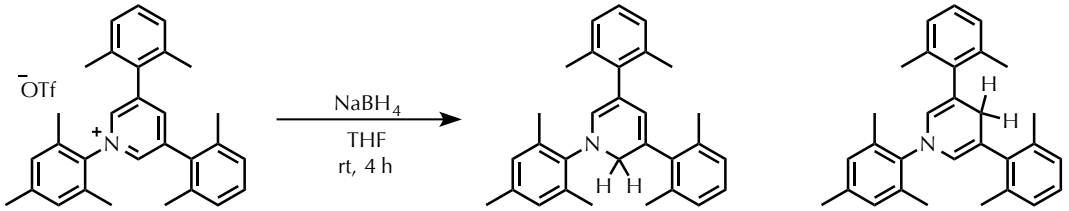

3 **8a** 1 : **8b** 0.6, 83%

A 30-mL screw-capped vial containing stirring bar was dried and filled with argon after cooling to room temperature. $NaBH_4$ (8.0 mg, 0.21 mmol) was added to the solution of pyridinium triflate **3** (33 mg, 52 μmol) in dry THF (0.5 mL). The mixture was stirred at room temperature for 4 h. The reaction mixture was treated in glove box filled with argon and was concentrated under reduced pressure. The crude product was filtered with hexane and recrystallized with dry hexane at –30 °C to obtain a mixture of **8a** and **8b** (17 mg, 83%, **8a**/**8b** = 1:0.6) as a colorless crystal.

^{1}H NMR (benzene-d_6, 600 MHz) δ **8a**: 7.15–6.98 (m, 8H), 6.71 (d, *J* = 1 Hz, 2H), 5.44 (dt, *J* = 1, 1 Hz, 1H), 5.42 (d, *J* = 1 Hz, 1H), 4.10 (d, *J* = 1 Hz, 2H), 2.41 (s, 6H), 2.35 (s, 6H), 2.25 (s, 6H), 2.11 (s, 3H); **8b**: 7.15–6.98 (m, 8H), 6.69 (d, *J* = 1 Hz, 2H), 5.19 (t, *J* = 1 Hz, 2H), 3.14 (t, *J* = 1 Hz, 2H), 2.42 (s, 12H), 2.21 (s, 6H), 2.11 (s, 3H); ^{13}C NMR (benzene-d_6, 150 MHz) δ 142.5 (4°), 141.1 (4°), 141.0 (4°), 140.8 (4°), 140.2 (4°), 137.9 (4°), 137.2 (4°), 136.9 (4°), 136.8 (4°), 136.6 (4°), 136.5 (4°), 136.3 (4°), 133.5 (CH), 129.7 (CH), 129.3 (CH), 128.5 (4°), 128.3 (4°), 128.1 (4°), 128.0 (4°), 127.8 (CH), 127.8 (CH), 127.7 (CH), 127.1 (CH), 126.8 (CH), 126.6 (CH), 126.4 (CH), 123.0 (4°), 107.9 (4°), 107.2 (4°), 52.5 (CH_2), 31.9 (CH_2), 21.3 (CH_3), 21.0 (CH_3), 21.0 (CH_3), 20.3 (CH_3), 20.0 (CH_3), 18.6 (CH_3), 18.1 (CH_3); HRMS (FAB+) calcd. for $C_{30}H_{32}N$ $[M–H]^+$: *m*/*z* 406.2535, found: *m*/*z* 406.2527.

*7,9-Bis(2,6-dimethylphenyl)-2,4-dimethylpyrido[1,2-a]indole (**9**)*

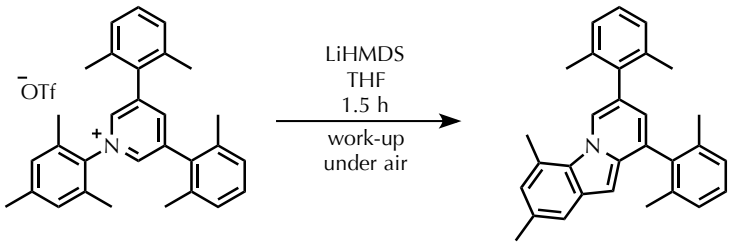

3 **9** 22%

A 10-mL Schlenk tube containing stirring bar was dried under vacuum and filled with argon after cooling to room temperature. LiHMDS (8.3 mg, 50 μmol) was added to the solution of pyridinium triflate **3** (32 mg, 50 μmol) in dry THF (1.0 mL). The mixture was stirred at room temperature for 1.5 h. The reaction mixture was concentrated under reduced pressure. The crude product was purified by silica gel column chromatography (EtOAc/hexane = 1:5) and recrystallized with EtOH (slow evapolation) to obtain pyrido[1,2-*a*]indole **9** (4.5 mg, 22%) as a yellow crystal.

^{1}H NMR ($CDCl_3$, 600 MHz) δ 8.51 (d, *J* = 2 Hz, 1H), 7.34 (s, 1H), 7.25–7.20 (m, 2H), 7.17–7.16 (m, 4H), 6.85 (s, 1H), 6.51 (d, *J* = 2 Hz, 1H), 6.15 (s, 1H), 2.87 (s, 3H), 2.46 (s, 3H), 2.25 (s, 6H), 2.15 (s, 6H); ^{13}C NMR ($CDCl_3$, 150 MHz) δ 138.4 (4°), 137.6 (4°), 137.3 (4°), 136.7 (4°), 135.7 (4°), 132.0 (4°), 131.5 (4°), 130.4 (4°), 127.7 (4°), 127.61 (CH), 127.57 (CH), 127.49 (CH), 127.41 (CH), 124.5 (CH), 124.4 (CH), 123.7 (CH), 122.9 (4°), 120.0 (4°), 117.7 (CH), 92.0 (CH), 21.5 (CH_3), 21.4 (CH_3), 20.1 (CH_3), 19.8 (CH_3); HRMS (FAB+) calcd. for $C_{30}H_{29}N$ $[M]^+$: *m/z* 403.2300, found: *m/z* 403.2322; mp: 254.4–256.4 °C (dec.).

The NMR yield of **9** by the reaction of **3** with KH was determined as follows. A 10-mL Schlenk tube equipped reflux tube and containing stirring bar was dried under vacuum and filled with argon after cooling to room temperature. A mixture of **3** (50 mg, 77 μmol) and KH (34 mg, 771 μmol) in dry THF (0.77 mL) was stirred at room temperature for 12 h. The reaction mixture was concentrated under reduced pressure to afford **9** (7% ^{1}H NMR yield). The NMR yield was determined by using CH_2Cl_4 (4.2 mg, 25 μmol) as an internal standard.

X-ray Crystallography

Details of the crystal data and a summary of the intensity data collection parameters for **1**, **3**·toluene, **5**, **6**·toluene, **7** and **9** are listed in Table S1. In each case, a suitable crystal was mounted with mineral oil on a glass fiber and transferred to the goniometer of a Rigaku Saturn CCD diffractometer. Graphite-monochromated Mo Kα radiation (λ = 0.71070 Å) was used. The structures were solved by direct methods with (SIR-97)[16] and refined by full-matrix least-squares techniques against F^2 (SHELXL-97).[17] The intensities were corrected for Lorentz and polarization effects. Non-hydrogen atoms were refined anisotropically. Hydrogen atoms were placed using AFIX instructions.

Table S1. Crystallographic data and refinement details for **1**, **3**·toluene, **5**, **6**·toluene, **7** and **9**.

	1	**3**·toluene	**5**	**6**·toluene	**7**	**9**
formula	$C_{21}H_{21}N$	$C_{38}H_{40}F_3NO_3S$	$C_{30}H_{31}NS$	$C_{37}H_{39}AuClN$	$C_{34}H_{41}N$	$C_{30}H_{29}N$
fw	287.39	647.77	437.62	730.11	463.68	403.54
T (K)	123(2)	123(2)	123(2)	103(2)	123(2)	123(2)
λ (Å)	0.71070	0.71070	0.71070	0.71070	0.71070	0.71070
cryst syst	Monoclinic	Monoclinic	Monoclinic	Monoclinic	Triclinic	Triclinic
space group	$P2_1/c$	$P2_1/n$	$P2_1/c$	$P2_1/n$	P-1	P-1
a, (Å)	13.283(3)	14.1166(19)	11.751(4)	13.600(2)	9.355(4)	11.727(3)
b, (Å)	8.3330(14)	17.674(2)	19.429(6)	16.635(3)	13.050(5)	12.934(3)
c, (Å)	15.160(3)	14.3488(19)	22.402(7)	14.925(3)	13.097(4)	15.910(4)
α, (deg)	90	90	90	90	62.601(11)	98.919(2)
β, (deg)	101.272(2)	107.5846(18)	97.269(6)	111.5120(18)	79.653(16)	105.428(5)
γ, (deg)	90	90	90	90	89.316(18)	93.867
V, (Å^3)	1645.6(5)	3412.8(8)	5074(3)	3141.3(9)	1391.9(9)	2283.2(9)
Z	4	4	8	4	2	4
D_{calc}, (g / cm^3)	1.160	1.261	1.146	1.544	1.106	1.174
μ (mm^{-1})	0.067	0.148	0.144	4.794	0.063	0.067
F(000)	616	1368	1872	1456	1504	864
cryst size (mm)	0.15 × 0.15 × 0.10	0.20 × 0.15 × 0.15	0.10 × 0.10 × 0.02	0.05 × 0.05 × 0.05	0.20 × 0.10 × 0.10	0.15 × 0.03 × 0.01
2θ range, (deg)	3.08-25.00	3.03-25.00	3.16-25.00	3.00-25.00	3.04-25.00	3.08-25.00
reflns collected	10602	22492	33370	40677	9281	15506
indep reflns/R_{int}	2878/0.0288	5977/0.0338	8903/0.0760	5529/0.0441	4791/0.0392	7886/0.0618
params	203	423	591	370	326	571
GOF on F^2	1.045	1.067	1.088	1.139	0.968	1.062
R_1, wR_2 [I>2σ(I)]	0.0414, 0.0988	0.0435, 0.1028	0.1084, 0.2705	0.0421, 0.0882	0.0489, 0.1227	0.0770, 0.1595
R_1, wR_2 (all data)	0.0495, 0.1040	0.0503, 0.1081	0.1590, 0.3154	0.0477, 0.0913	0.0706, 0.1361	0.1384, 0.1913

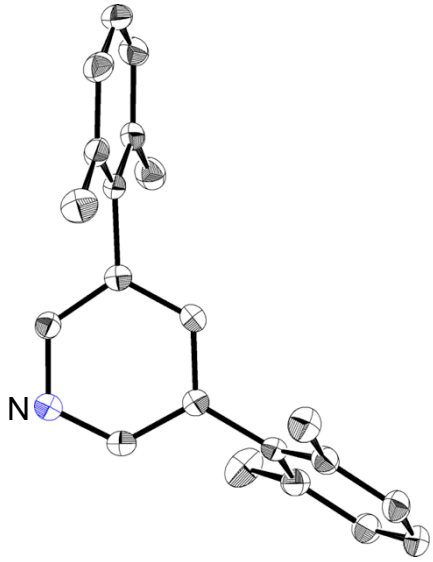

Figure S1. ORTEP drawing of **1** with 50% thermal ellipsoid. All hydrogen atoms are omitted for clarity.

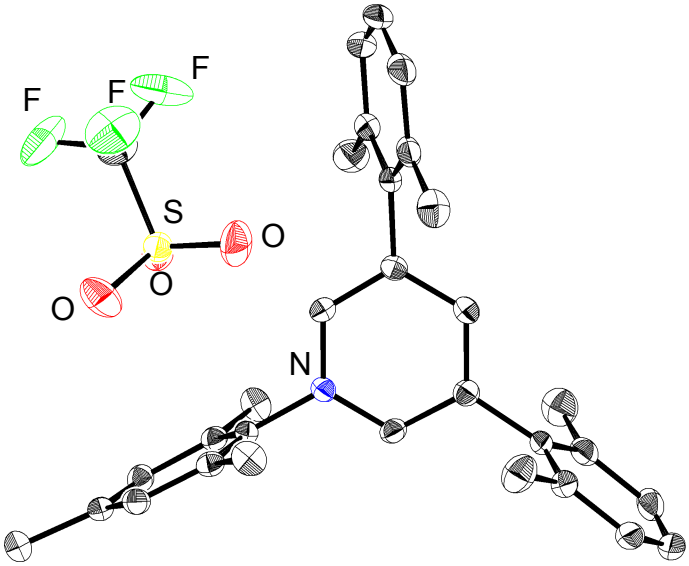

Figure S2. ORTEP drawing of **3**·toluene with 50% thermal ellipsoid. All hydrogen atoms and toluene molecule are omitted for clarity.

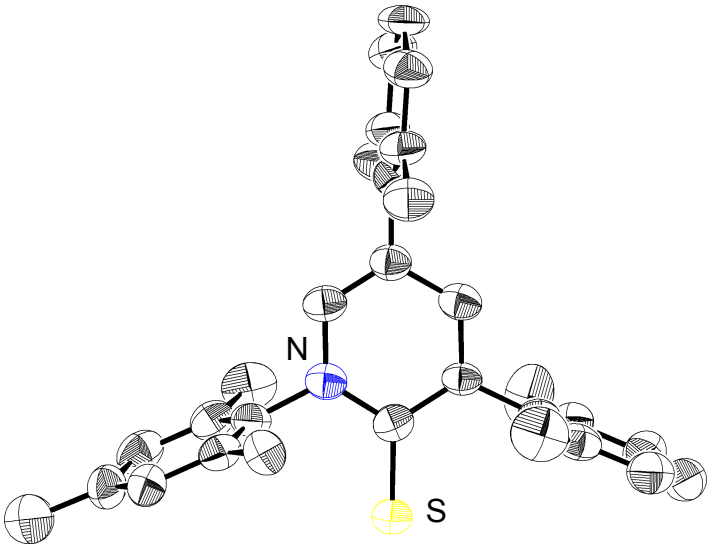

Figure S3. ORTEP drawing of **5** with 50% thermal ellipsoid. All hydrogen atoms are omitted for clarity.

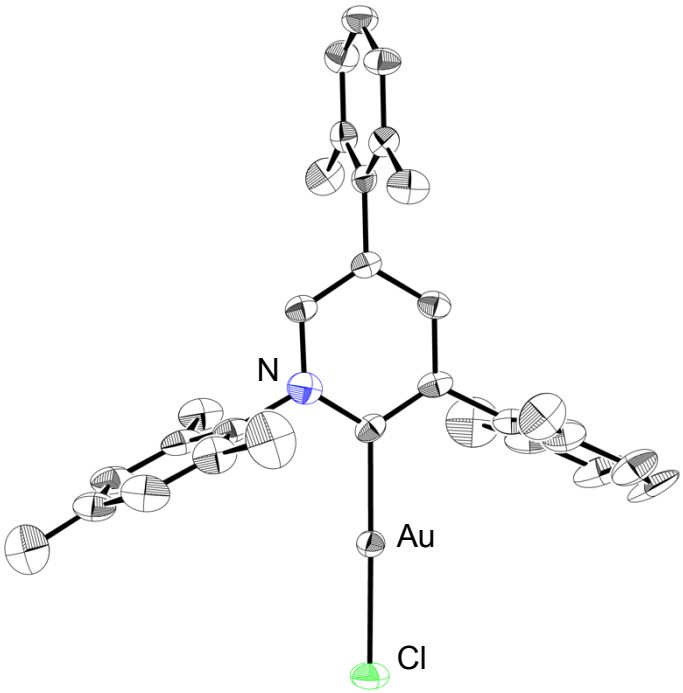

Figure S4. ORTEP drawing of **6**·toluene with 50% thermal ellipsoid. All hydrogen atoms and toluene molecule are omitted for clarity.

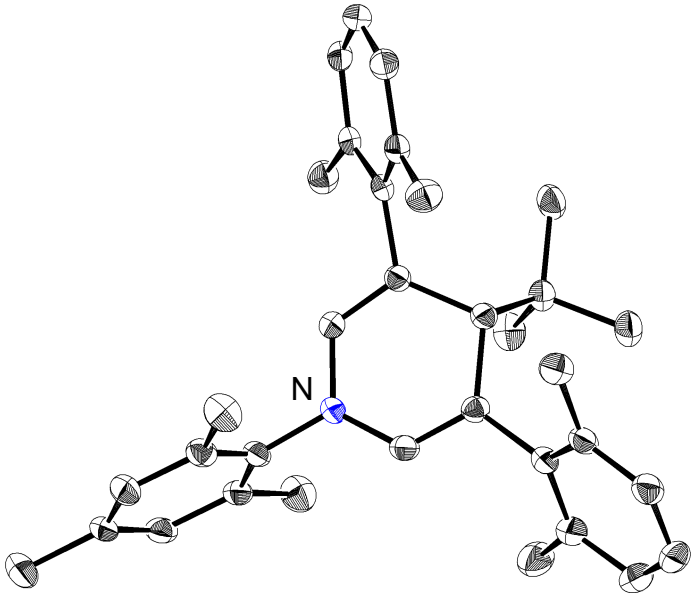

Figure S5. ORTEP drawing of **7** with 50% thermal ellipsoid. All hydrogen atoms are omitted for clarity.

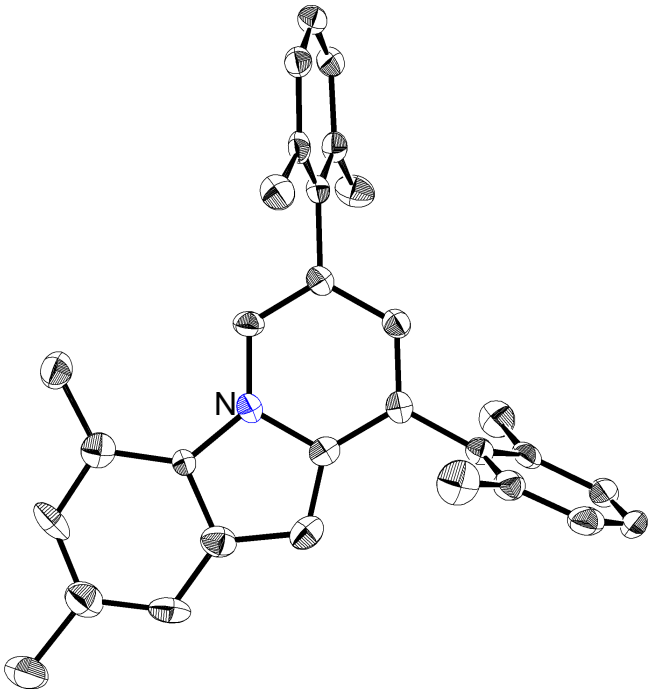

Figure S6. ORTEP drawing of **9** with 50% thermal ellipsoid. All hydrogen atoms are omitted for clarity.

Computational Study

The Gaussian 09 program[18] running on a SGI Altix4700 system was used for optimization (B3LYP/6-31+G(d)). All structures were optimized without any symmetry assumptions. Zero-point energy, enthalpy, and Gibbs free energy at 298.15 K and 1 atm were estimated from the gas-phase studies. Harmonic vibration frequency calculation at the same level was performed to verify all stationary points as local minima (with no imaginary frequency). Visualization of the results was performed by use of GaussView 5.0.

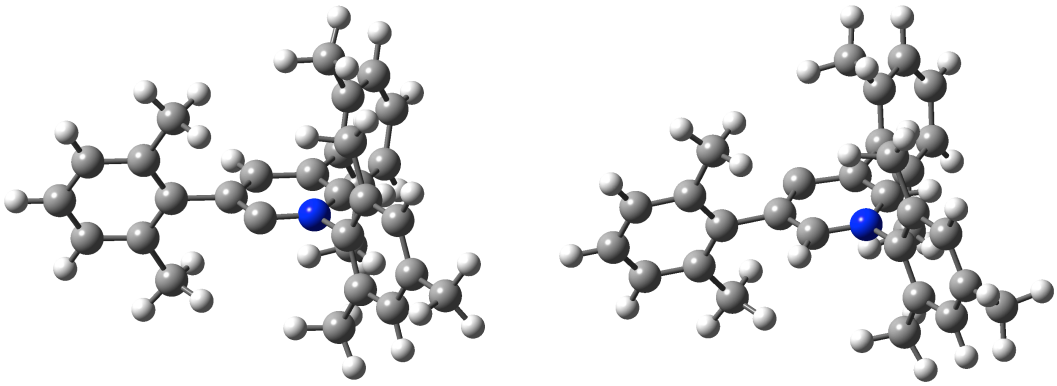

Figure S7. Optimized structures of 2-pyridylidene **4** (left) and 4-pyridylidene **4'** (right).

Table S2. Uncorrected and thermal-corrected energies of stationary points (Hartree).[a]

compound	*E*	*E* + *ZPE*	*H*	*G*
4	-1216.61973919	-1216.096649	-1216.064916	-1216.161509
4'	-1216.59836160	-1216.075584	-1216.043714	-1216.141343

a) *E*: electronic energy; *ZPE*: zero-point energy; *H* (= $E + ZPE + E_{vib} + E_{rot} + E_{trans} + RT$): sum of electronic and thermal enthalpies; *G* (= $H - TS$): sum of electronic and thermal free energies.

Table S3. Cartesian coordinates for optimized compounds.

Optimized structure of **4**

C	0.441010	-1.328289	-0.013784	H	-3.658206	-4.374201	-2.147240	C	-1.313562	-2.772127	2.451275
C	-0.985989	-1.191178	-0.005421	H	-2.888849	-4.934366	2.041663	H	-0.222255	-2.762165	2.344157
C	-1.619355	0.045846	0.014964	H	-3.973441	-5.684349	-0.062279	H	-1.614819	-1.760916	2.753019
C	-0.875807	1.249517	0.025656	C	-1.535478	2.594346	0.055241	H	-1.573185	-3.457013	3.265516
C	0.495145	1.124285	0.011892	C	-1.973307	3.131016	1.287022	C	-2.232771	-2.108171	-2.519538
H	-2.707593	0.107178	0.022628	C	-1.730092	3.309886	-1.147299	H	-2.702969	-1.116947	-2.488408
H	1.164328	1.979304	0.017737	C	-2.598409	4.385020	1.296480	H	-1.169923	-1.950407	-2.737997
C	2.541362	-0.143858	-0.021616	C	-2.359964	4.560855	-1.097491	H	-2.673881	-2.655665	-3.359118
C	3.233275	-0.098115	1.196995	C	-2.791786	5.098384	0.114177	C	-1.277346	2.751903	-2.479855
C	3.206261	-0.222726	-1.254866	H	-2.935394	4.802759	2.242493	H	-0.184758	2.669118	-2.537456
C	4.633271	-0.120158	1.155608	H	-2.514204	5.114372	-2.021018	H	-1.679559	1.747970	-2.659127
C	4.605481	-0.241312	-1.242473	H	-3.279463	6.069839	0.136867	H	-1.604140	3.397947	-3.300948
C	5.338048	-0.191905	-0.050420	N	1.082756	-0.115827	-0.007688	C	-1.775135	2.382407	2.587645
H	5.184041	-0.085794	2.093877	C	2.444635	-0.317917	-2.555067	H	-2.292200	1.415346	2.585465
H	5.135122	-0.302379	-2.191699	H	1.827267	-1.223997	-2.574417	H	-0.715642	2.172122	2.778085
C	-1.814553	-2.444271	-0.024574	H	1.769344	0.534105	-2.701725	H	-2.158515	2.964433	3.431738
C	-2.422264	-2.871196	-1.225348	H	3.133495	-0.350289	-3.404902	C	6.849096	-0.247583	-0.067933
C	-1.977283	-3.195583	1.159913	C	2.502675	-0.055980	2.518345	H	7.205056	-1.282403	-0.162887
C	-3.195440	-4.040311	-1.220810	H	1.883755	0.844319	2.620329	H	7.261866	0.316307	-0.912338
C	-2.760871	-4.356355	1.128762	H	1.834278	-0.918693	2.623056	H	7.275879	0.162378	0.853817
C	-3.370285	-4.779573	-0.051945	H	3.211909	-0.068262	3.351721				

Optimized structure of **4'**

C	1.009078	1.196419	-0.016774	H	3.450303	6.009898	-0.108589	H	1.680042	1.763437	2.679139
C	1.798574	0.003184	-0.000479	C	1.689715	-2.536755	0.037793	H	1.581798	3.424668	3.294477
C	1.013159	-1.192712	0.017252	C	2.226008	-3.028842	1.247656	C	2.127033	2.228945	-2.525347
C	-0.372459	-1.179525	0.016495	C	1.810378	-3.288587	-1.150668	H	2.622585	1.258458	-2.403694
H	-0.993103	-2.072049	0.026962	C	2.859064	-4.278439	1.254043	H	1.087032	2.022991	-2.810968
C	-2.511659	-0.004045	0.002562	C	2.453579	-4.533414	-1.108618	H	2.602909	2.760439	-3.356364
C	-3.188043	-0.091960	1.229484	C	2.972058	-5.031767	0.085662	C	1.288753	-2.761835	-2.471138
C	-3.189248	0.077224	-1.226307	H	3.272410	-4.658541	2.186009	H	0.192979	-2.690162	-2.485867
C	-4.588627	-0.094945	1.200252	H	2.553708	-5.110816	-2.025463	H	1.677698	-1.758309	-2.679889
C	-4.587924	0.069205	-1.197765	H	3.469640	-5.998533	0.104234	H	1.584868	-3.419998	-3.294829
C	-5.305829	-0.013225	0.002113	N	-1.059358	-0.001613	0.001982	C	2.141972	-2.220379	2.522965
H	-5.129874	-0.164095	2.141572	C	-2.445741	0.168840	-2.539095	H	2.635580	-1.249099	2.399691
H	-5.129594	0.127134	-2.139951	H	-1.868061	1.097979	-2.614586	H	1.102261	-2.016022	2.810719
C	1.681172	2.542677	-0.038670	H	-1.736039	-0.656807	-2.664770	H	2.620614	-2.750638	3.353183
C	2.212430	3.036979	-1.249847	H	-3.146206	0.142526	-3.378934	C	-0.376483	1.178623	-0.013679
C	1.802860	3.294349	1.149776	C	-2.445893	-0.186042	2.542866	H	-1.000171	2.069033	-0.023179
C	2.841702	4.288481	-1.257450	H	-1.872686	-1.117916	2.619632	C	-6.817213	0.006988	-0.001684
C	2.442105	4.541169	1.106468	H	-1.732522	0.636382	2.668322	H	-7.225272	-0.357318	0.946699
C	2.955722	5.041611	-0.089044	H	-3.146805	-0.155822	3.382203	H	-7.196585	1.026005	-0.155167
H	3.251260	4.670259	-2.190405	C	1.286471	2.765377	2.471405	H	-7.223615	-0.615028	-0.807331
H	2.543025	5.118483	2.023280	H	0.191046	2.689150	2.488634				

5. References

[1] (a) G. Bertrand, *J. Organomet. Chem.*, 2005, **690**, 5541; (b) R. H. Crabtree, *Coord. Chem. Rev.*, 2007, **251**, 595; (c) F. Glorius, *Top. Organomet. Chem.*, 2007, 21; (d) S. P. Nolan, *N-Heterocycic Carbenes in Synthesis*, Wiley-VCH, Weinheim, 2006; (e) F. E. Hahn and M. C. Jahnke, *Angew. Chem., Int. Ed.*, 2008, **47**, 3122; (f) M. Melaimi, M. Soleilhavoup and G. Bertrand, *Angew. Chem., Int. Ed.*, 2010, **49**, 8810.

[2] (a) A. A. Tukov, A. T. Normand and M. S. Nechaev, *Dalton Trans.*, 2009, 7015; (b) O. Schuster, L. Yang, H. G. Raubenheimer and M. Albrecht, *Chem. Rev.*, 2009, **109**, 3445; (c) ref. *1e*.

[3] (a) G. D. Frey, V. Lavallo, B. Donnadieu, W. W. Schoeller and G. Bertrand, *Science*, 2007, **316**, 439; (b) D. R. Anderson, V. Lavallo, D. J. O'Leary, G. Bertrand and R. H. Grubbs, *Angew. Chem., Int. Ed.*, 2007, **46**, 7262; (c) D. R. Anderson, T. Ung, G. Mkrtumyan, G. Bertrand, R. H. Grubbs and Y. Schrodi, *Organometallics*, 2008, **27**, 563; (d) V. Lavallo, G. D. Frey, B. Donnadieu, M. Soleilhavoup and G. Bertrand, *Angew. Chem., Int. Ed.*, 2008, **47**, 5224; (e) X. Zeng, G. D. Frey, R. Kinjo, B. Donnadieu and G. Bertrand, *J. Am. Chem. Soc.*, 2009, **131**, 8690; (f) X. Zeng, G. D. Frey, S. Kousar and G. Bertrand, *Chem.– Eur. J.*, 2009, **15**, 3056; (g) X. Zeng, M. Soleilhavoup and G. Bertrand, *Org. Lett.*, 2009, **11**, 3166; (h) X. Zeng, R. Kinjo, B. Donnadieu and G. Bertrand, *Angew. Chem., Int. Ed.*, 2010, **49**, 942; (i) R. Kinjo, B. Donnadieu and G. Bertrand, *Angew. Chem., Int. Ed.*, 2011, **50**, 5560; (j) M. Alcarazo, K. Radkowski, R. Goddard and A. Fürstner, *Chem. Commun.*, 2011, **47**, 776; (k) A. Fürstner, M. Alcarazo, K. Radkowski and C. W. Lehmann, *Angew. Chem., Int. Ed.*, 2008, **47**, 8302; (l) S.-y. Nakafuji, J. Kobayashi and T. Kawashima, *Angew. Chem., Int. Ed.*, 2008, **47**, 1141.

[4] Theoretical studies on pyridylidenes: (a) O. Hollóczki and L. Nyulászi, *J. Org. Chem.*, 2008, **73**, 4794; (b) M. Z. Kassaee, F. A. Shakib, M. R. Momeni, M. Ghambarian and S. M. Musavi, *Tetrahedron*, 2009, **65**, 10093; (c) ref. *2a*.

[5] (a) M. R. F. Ashworth, R. P. Daffern and D. Ll. Hammick, *J. Chem. Soc.*, 1939, 809; (b) P. Dyson and D. Ll. Hammick, *J. Chem. Soc.*, 1937, 1724; (c) D. Lavorato, J. K. Terlouw, T. K. Dargel, W. Koch, G. A. McGibbon and H. Schwarz, *J. Am. Chem. Soc.*, 1996, **118**, 11898.

[6] Pyridylidene–metal complexes: (a) ref. **2b** and references therein; (b) E. T. J. Strong, J. T. Price and N. D. Jones, *Dalton Trans*., 2009, 9123; (c) E. Stander-Grobler, O. Schuster, G. Heydenrych, S. Cronje, E. Tosh, M. Albrecht, G. Frenking and H. G. Raubenheimer, *Organometallics*, 2010, **29**, 5821; (d) M. Roselló-Merino, J. Díez and S. Conejero, *Chem. Commun*., 2010, **46**, 9247; (e) B. Crociani, F. di Bianca, A. Giovenco and A. Scrivanti, *J. Organomet. Chem*., 1983, **251**, 393; (f) J. S. Owen, J. A. Labinger and J. E. Bercaw, *J. Am. Chem. Soc*., 2004, **126**, 8247; (g) N. A. Piro, J. S. Owen and J. E. Bercaw, *Polyhedron*, 2004, **23**, 2797.

[7] Pyridylidene–ruthenium complexes: (a) J. A. Cabeza and P. García-Álvarez, *Chem. Soc. Rev*., 2011, **40**, 5389; (b) J. A. Cabeza, I. del Río, E. Pérez-Carreño, M. G. Sánchez-Vega and D. Vázquez-García, *Angew. Chem., Int. Ed*., 2009, **48**, 555; (c) J. A. Cabeza, I. del Río, E. Pérez-Carreño, M. G. Sánchez-Vega and D. Vázquez-García, *Organometallics*, 2010, **29**, 4464; (d) J. A. Cabeza, I. del Río, E. Pérez-Carreño and V. Pruneda, *Organometallics*, 2011, **30**, 1148.

[8] Attempt to isolate pyridylidene derivatives: (a) X. Cattoën, D. Bourissou and G. Bertrand, *Tetrahedron Lett*., 2006, **47**, 531; (b) S. Gómez-Bujedo, M. Alcarazo, C. Pichon, E. Álvarez, R. Fernández and J. M. Lassaletta, *Chem. Commun*., 2007, 1180.

[9] (a) N. Miyaura, K. Yamada and A. Suzuki, *Tetrahedron Lett*., 1979, **20**, 3437; (b) N. Miyaura and A. Suzuki, *J. Chem. Soc., Chem. Commun*., 1979, 866; (c) N. Miyaura and A. Suzuki, *Chem. Rev*., 1995, **95**, 2457.

[10] (a) T. Zincke, Justus *Liebigs Ann. Chem*., 1904, **330**, 361; (b) T. Zincke, G. Heuser and W. Möller, *Justus Liebigs Ann. Chem*., 1904, **333**, 296.

[11] Electronic supplementary information (ESI) available: Experimental procedures, spectra of new compounds, and details of computational study. CCDC 879859 (**1**), 879860 (**3**·toluene), 879861 (**5**), 879862 (**6**·toluene), 879863 (**7**) and 879864 (**9**).

[12] (a) ref. *S3*; (b) A. D. Becke, *J. Chem. Phys*., 1993, **98**, 5648; (c) C. Lee, W. Yang and R. G. Parr, *Phys. Rev. B*, 1988, **37**, 785.

[13] 2-Pyridylidene–AuCl complex(Au–Cl 2.2989(16) Å): (a); ref. *6d*; 4-Pyridylidene–AuCl complex (Au–Cl 2.304(2) and 2.314(2) Å): (b) C. E. Strasser, E. Stander-Grobler, O. Schuster, S. Cronje and H. G. Raubenheimer, *Eur. J. Inorg. Chem*., 2009, 1905; representative NHC–AuCl complexes (Au–Cl 2.2761(6) Å):

(c) P. de Frémont, N. M. Scott, E. D. Stevens and S. P. Nolan, *Organometallics*, 2005, **24**, 2411; (Au–Cl 2.305(2), 2.295(3) Å): (d) *8b*; (Au–Cl 2.2713(18) Å): (e); ref. *19d*.

[14] Synthesis of pyrido[1,2-*a*]indole from *N*-arylpyridinium: F. D. Saeva and H. R. Luss, *J. Org. Chem.*, 1988, **53**, 1804.

[15] Intramolecular benzylic C–H cleavage of NHCs: (a) Y. Canac, S. Conejero, M. Soleilhavoup, B. Donnadieu and G. Bertrand, *J. Am. Chem. Soc.*, 2006, **128**, 459; (b) T. W. Hudnall and C. W. Bielawski, *J. Am. Chem. Soc.*, 2009, **131**, 16039; (c) R. S. Holdroyd, M. J. Page, M. R. Warren and M. K. Whittlesey, *Tetrahedron Lett.*, 2010, **51**, 557; (d) E. Aldeco-Perez, A. J. Rosenthal, B. Donnadieu, P. Parameswaran, G. Frenking and G. Bertrand, *Science*, 2009, **326**, 556; (e) R. S. Holdroyd, M. J. Page, M. R. Warren and M. K. Whittlesey, *Tetrahedron Lett.*, 2010, **51**, 557.

[16] A. Altomare, M. C. Burla, M. Camalli, G. L. Cascarano, C. Giacovazzo, A. Guagliardi, A. G. G. Moliterni, G. Polidori, R. Spagna, *J. Appl. Crystallogr.,* 1999, **32**, 115–119.

[17] G. M. Sheldrick, University of Göttingen: Göttingen, Germany, 1997.

[18] M. J. Frisch, G. W. Trucks, H. B. Schlegel, G. E. Scuseria, M. A. Robb, J. R. Cheeseman, G. Scalmani, V. Barone, B. Mennucci, G. A. Petersson, H. Nakatsuji, M. Caricato, X. Li, H. P. Hratchian, A. F. Izmaylov, J. Bloino, G. Zheng, J. L. Sonnenberg, M. Hada, M. Ehara, K. Toyota, R. Fukuda, J. Hasegawa, M. Ishida, T. Nakajima, Y. Honda, O. Kitao, H. Nakai, T. Vreven, J. A. Montgomery, Jr., J. E. Peralta, F. Ogliaro, M. Bearpark, J. J. Heyd, E. Brothers, K. N. Kudin, V. N. Staroverov, R. Kobayashi, J. Normand, K. Raghavachari, A. Rendell, J. C. Burant, S. S. Iyengar, J. Tomasi, M. Cossi, N. Rega, J. M. Millam, M. Klene, J. E. Knox, J. B. Cross, V. Bakken, C. Adamo, J. Jaramillo, R. Gomperts, R. E. Stratmann, O. Yazyev, A. J. Austin, R. Cammi, C. Pomelli, J. W. Ochterski, R. L. Martin, K. Morokuma, V. G. Zakrzewski, G. A. Voth, P. Salvador, J. J. Dannenberg, S. Dapprich, A. D. Daniels, O. Farkas, J. B. Foresman, J. V. Ortiz, J. Cioslowski, and D. J. Fox, *Gaussian 09, Revision A.02*, Gaussian, Inc., Wallingford CT, 2009

Chapter 3

Pyridylidene Ligand Facilitates Gold-Catalyzed Oxidative C–H Arylation of Heterocycles

Abstract

2-Pyridylidene effectively facilitates the gold-catalyzed oxidative C–H arylation of heteroarenes with arylsilanes as a unique electron-donating ligand on gold. Employment of pyridylidene ligand, which is one of the strongest electron-donating nonclassical *N*-heterocyclic carbenes, resulted in the rate acceleration of heterocycle C–H arylation reaction over conventional ligands such as triphenylphosphine and classical *N*-heterocyclic carbene. *In situ* observation and isolation of 2-pyridylidene-gold(III) species as well as DFT study indicated unusual stability of gold(III) species stabilized by strong electron donation from 2-pyridylidene ligand. Thus, gold(I)-to-gold(III) oxidation process is thought to be facilitated by highly electron-donating 2-pyridylidene ligand.

1. Introduction

Over the past decade, gold salts and complexes have emerged as a unique catalyst for the transformation of alkynes, alkenes and allenes.[1,2] In most of gold-catalyzed reactions, phosphines, *N*-heterocyclic carbenes, pyridines and salen ligands have been applied as ligands for controlling activity and stability of catalysts, and chemo-, regio- and enantioselectivities of the reactions.[3] Recent advances in the gold-catalyzed reactions are represented by oxidative coupling that is expected to proceed through gold(I)/gold(III) catalytic cycle.[4–8] In particular, Lloyd-Jones and Russell's elegant works on gold-catalyzed oxidative C–H arylation of simple arenes with arylsilanes have opened the way to novel gold-catalyzed reactions that could not be achieved with other transition metals (Scheme 1).[7a,b] In these reactions, oxidation of gold(I) to gold(III) is thought to be a key step in the catalytic cycle consisting of transmetalation with arylsilane, C–H activation and reductive elimination steps.[7b] While gold(I) complexes bearing various ligands are used as gold(III) precursors, it remains unclear whether ligands can still coordinate to the gold center or not under such oxidative reaction conditions. For example, triphenylphosphine is easily oxidized to triphenylphosphine oxide by hypervalent iodine reagent, which has been used as an oxidant for gold-catalyzed C–H arylation.[7b] Appropriate ligands that are tolerant to the oxidative conditions would offer numerous benefits such as high activity and stability of gold catalyst, thereby achieving otherwise-difficult oxidative transformations.[4]

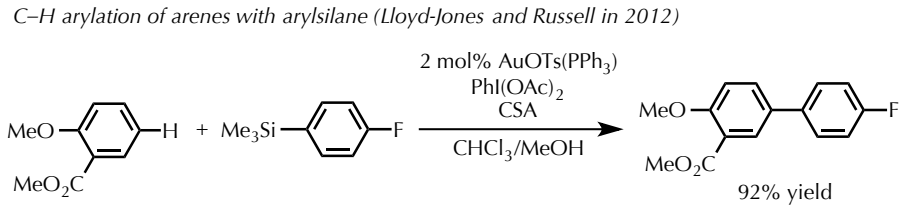

Scheme 1. Gold-catalyzed oxidative C–H arylation of arenes with arylsilanes.

In Chapter 2, the author has introduced highly electron-donating triaryl-2-pyridylidene[9,10] (PyC: pyridine-based carbene) as a new type of nonclassical *N*-heterocyclic carbene,[11,12] and demonstrated that it worked as one of the strongest electron-donating carbene ligand when it is coordinated to a gold(I) (Figure 1).[10a] AuCl(PyC) complex is very stable even in air and moisture, and is isolable by column chromatography on silica gel. Thus it was envisioned that gold complex with strongly

electron-donating PyC would promote the gold(I)-to-gold(III) oxidation process, facilitating oxidative coupling reactions. In this chapter, the author report that PyC ligand accelerates gold-catalyzed oxidative C–H arylation of heteroarenes that has been know to be very sluggish with typical ligand system.[7] The C–H arylation reactions of isoxazole, indole, and benzothiophene are presented. In addition, direct observation and isolation of PyC-gold(III) complexes are described.

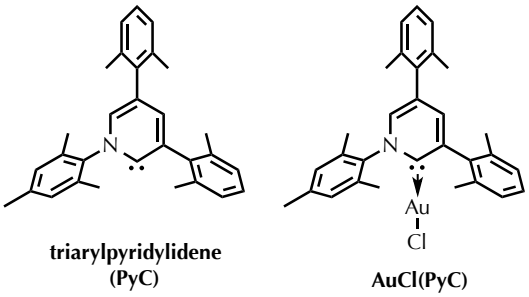

Figure 1. Triaryl-2-pyridylidene (PyC) and PyC-gold(I) complex [AuCl(PyC)].

2. Results and Discussion

Ligand effect of PyC in gold-catalyzed aromatic C–H arylation

In this study, the author selected gold-catalyzed oxidative C–H arylation of arenes with arylsilanes[7a,b] reported by Lloyd-Jones and Russell to test the ligand effect of PyC (Table 1). Likely due to the low stability of electron-rich heteroarene substrates toward oxidative conditions,[13] their original conditions usually do not work well for these substrates. For example, when isoxazole (**1a**: 1 equiv)[14] was treated with 1-bromo-4-(trimethylsilyl)benzene (**2a**: 1 equiv) in chloroform/methanol solution at 65 °C in the presence of $AuCl(PPh_3)$ (5 mol%), iodosobenzoic acid (IBA: 1 equiv) and (+)-10-camphorsulfonic acid (CSA: 1 equiv), the corresponding C–H arylation product **3aa** was obtained only in 10% yield (Table 1, entry 1). Although the application of IPr, a conventional NHC ligand, to the reaction did not afford **3aa** at all (entry 2), PyC promoted the reaction with higher yield of 4-arylisoxazole **3aa** under these conditions (30%, entry 3). In the AuCl(PyC)-catalyzed reaction, **1a** was fully consumed, and 4,4'-dibromobiphenyl (**4a**) derived from the homo-coupling of arylsilane **2a** was also detected. Furthermore, significant amount of methyl 2-iodobenzoate (**5**) was generated through the esterification of co-product (2-iodobenzoic acid) with methanol. Other iodine(III) reagents such as $PhI(OAc)_2$, $PhI(OCOCF_3)_2$ and PhI(OH)(OTs) were also

tested, but they all resulted in lower yields than IBA mainly due to the formation of diaryliodonium ($PhI(4\text{-}BrC_6H_4)^+$) produced by the reaction with arylsilane **2a** (entries 4–6).[7b] The reaction conditions with *p*-toluenesulfonic acid (TsOH) instead of CSA was less effective (entry 7). It was clearly seen that both CSA and methanol had significant effect for the reaction progress (entries 8 and 9). Nevertheless, the highest yield by the use of AuCl(PyC) may be attributed to the positive effect of highly electron-donating PyC ligand.

Table 1. Effect of ligands and oxidants in gold-catalyzed oxidative C–H arylation of isoxazole **1a**.[a]

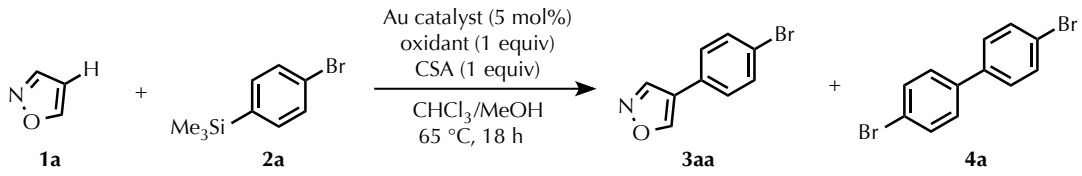

1a **2a** **3aa** **4a**

Entry	Au catalyst	Oxidant	Yield[%][b]	
			3aa	**4a**
1	$AuCl(PPh_3)$	IBA	10	7
2	AuCl(IPr)	IBA	0	0
3	AuCl(PyC)	IBA	30	12
4	AuCl(PyC)	$PhI(OAc)_2$	4	5
5	AuCl(PyC)	$PhI(OCOCF_3)_2$	3	4
6[c]	AuCl(PyC)	PhI(OH)(OTs)	9	5
7[d]	AuCl(PyC)	IBA	13	5
8[c]	AuCl(PyC)	IBA	0	9
9[e]	AuCl(PyC)	IBA	3	36

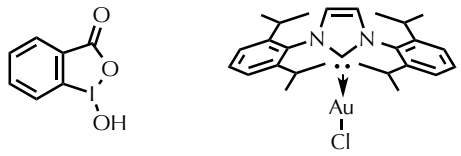

IBA AuCl(IPr)

[a]Reaction conditions: **1a** (0.20 mmol), **2a** (0.20 mmol), Au catalyst (5 mol %), oxidant (0.20 mmol), (+)-10-camphorsulfonic acid (CSA) (0.20 mmol), $CHCl_3$/MeOH (10:1, 1.1 mL), 65 °C. [b]Determined by GC analysis with *n*-nonane as an internal standard. [c]Without CSA.[d]$TsOH{\cdot}H_2O$ was used instead of CSA. [e]$CHCl_3$ (1.0 mL) was used as solvent.

Oxidative C–H arylation of heteroarenes with arylsilanes catalyzed by AuCl(PyC)

Having discovered the positive effect of using PyC as a ligand in gold-catalyzed C–H arylation, we further examined the C–H arylation of various heteroarenes with arylsilanes (Table 2). It should be noted that all of the examined heteroarenes were not successfully applied in the previous gold-catalyzed C–H arylation. The reactions of **1a** with halogenated aryltrimethylsilanes **2a** and **2b** afforded coupling products **3aa** and **3ab** in 14% and 15% isolated yields, respectively (entries 1 and 2).[15] 5-Methylisoxazole (**1b**) was arylated with bromo-, fluoro- and trifluoromethyl-substituted aryltrimethylsilanes **2a**, **2b** and **2c** to give the corresponding 4-aryl-5-methylisoxazoles **3ba**, **3bb** and **3bc**, respectively, in higher efficiency compared with **1a** (entries 3–5). These may be due to the higher tolerability of **1b** than **1a** toward undesired decomposition. The introduction of 3,5-dibromophenyl groups onto methylisoxazole **1b** resulted in the lower yields of heterobiaryl **3bd** (entry 6). In the reaction of 5-phenylisoxazole (**1c**), the selective arylation at C4-position occurred without any arylation on the phenyl group (entry 7). 3,5-Dimethylisoxazole (**1d**) showed low reactivity probably due to the steric hindrance, but the reaction gave sterically congested heterobiaryl **3da** in 17% yield (entry 8). In the case of the reaction of indole **1e**, only 3-arylindole **3ea** was exclusively obtained in 44% yield (entry 9). On the other hand, arylation of benzo[*b*]thiophene (**1f**) mainly afforded 2-arylbenzothiophene **3fa** along with the small amount of 3-arylbenzothiophene **3fa'** (entry 10).

Table 2. AuCl(PyC)-catalyzed oxidative C–H arylation of heteroarenes with arylsilanes.[a]

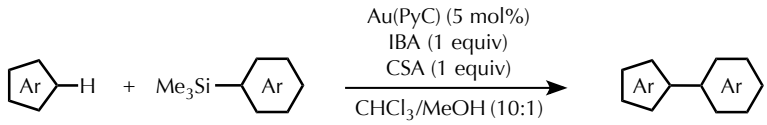

Entry	1	2	3	Yield[b]
1	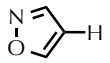 **1a**	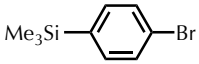 **2a**	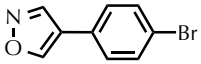 **3aa**	14%
2	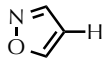 **1a**	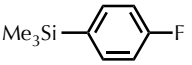 **2b**	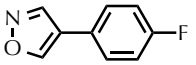 **3ab**	15%
3	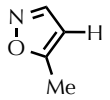 **1b**	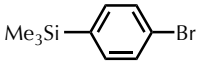 **2a**	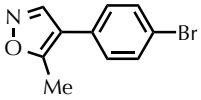 **3ba**	55%
4	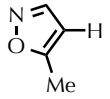 **1b**	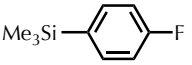 **2b**	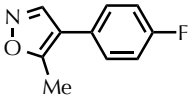 **3bb**	54%
5	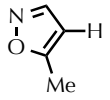 **1b**	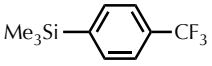 **2c**	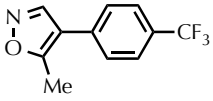 **3bc**	33%
6	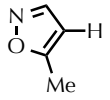 **1b**	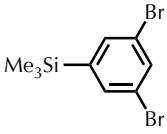 **2d**	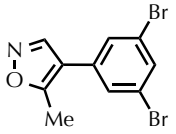 **3bd**	13%
7	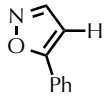 **1c**	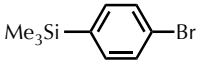 **2a**	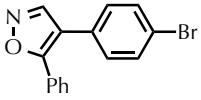 **3ca**	28%
8	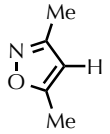 **1d**	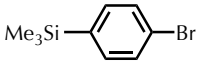 **2a**	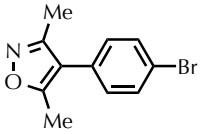 **3da**	17%
9	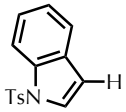 **1e**	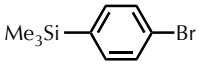 **2a**	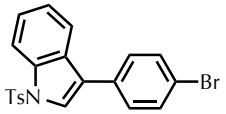 **3ea**	44%
10	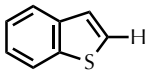 **1f**	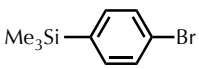 **2a**	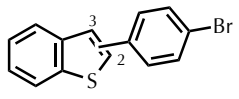 **3fa** (C2) : **3fa'** (C3) = 83 : 17	22%

[a]Reaction conditions: **1** (0.20 mmol), **2** (0.20 mmol), AuCl(PyC) (5 mol %), IBA (0.20 mmol), CSA (0.20 mmol), $CHCl_3$/MeOH (10:1, 1.1 mL), 65 °C, 18–48 h. [b]Isolated yield.

Reaction progress analysis

To unveil the detail ligand effect of PyC, time-production profiles of coupling product **3ba** were investigated for the reaction of **1b** and **2a** with AuCl(PyC), $AuCl(PPh_3)$ and AuCl(IPr). The yields of **3ba** were determined directly by GC analysis, whereas the consumption of IBA (oxidant) was estimated by the production of methyl 2-iodobenzoate **5**. The reaction plots with AuCl(PyC), $AuCl(PPh_3)$ and AuCl(IPr) are depicted in Figure 2. Noteworthy observations are as follows; (i) the reaction with AuCl(PyC) was fastest among those with three catalysts (Figures 2a), (ii) the induction periods with regard to the formation of **3ba** were found in the reactions using AuCl(PyC) and $AuCl(PPh_3)$ (Figures 2a and 2b), and (iii) the oxidant started consuming at the initiation of reactions with all catalysts (Figure 2c). In the reaction using AuCl(PyC), the coupling product **3ba** was generated after shorter induction period about 3 h to reach to 60% yield after 50 h (Figures 2a). On the other hand, the reaction using $AuCl(PPh_3)$ initiated after longer induction period (ca. 5 h), and the yield of **3ba** did not exceed the yield with AuCl(PyC) even after 100 hours (see experimental section for details). No coupling product was produced with AuCl(IPr) despite the consumption of about 10% of IBA was observed.

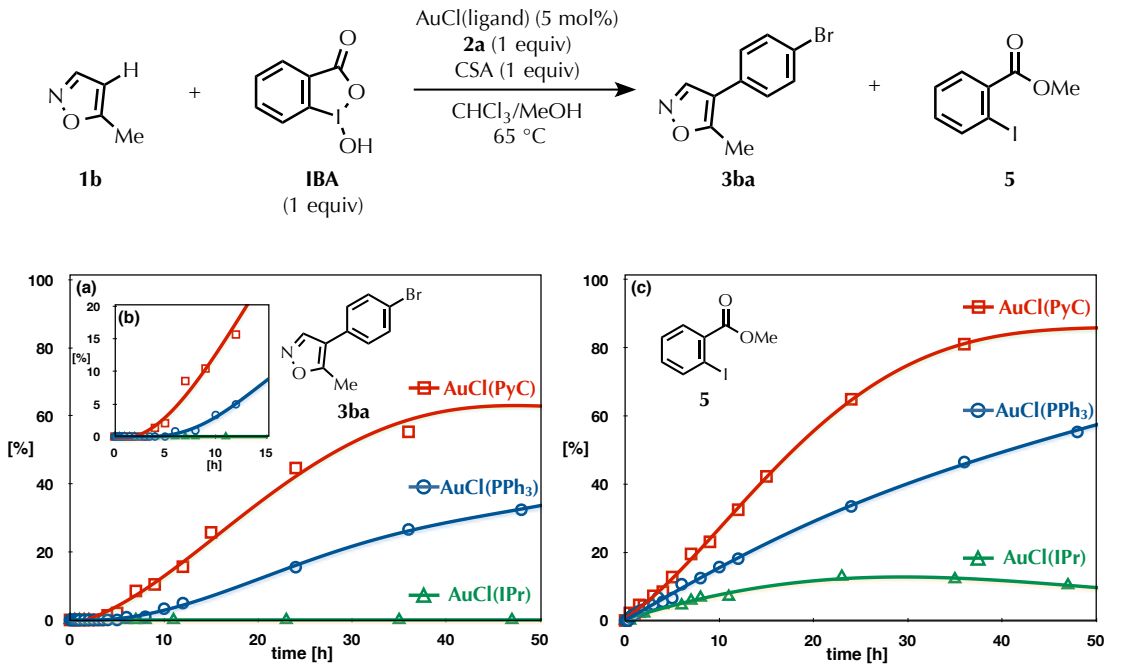

Figure 2. Time-yield profiles of 4-(4-bromophenyl)-5-methylisoxazole (**3ba**) and methyl 2-iodobenzoate (**5**) with AuCl(PyC), $AuCl(PPh_3)$ and AuCl(IPr). (a) Yields of **3ba**. (b) Magnified figure of (a). (c) Yields of **5**. All yields were determined by GC analysis with *n*-nonane as an internal standard.

Mechanistic considerations

Based on the above results and the literatures,[7,8] the author proposes the reaction mechanism of the current gold-catalyzed C–H arylation of heteroarenes with arylsilanes as shown in Figure 3. A gold(I) complex **A** is first oxidized to gold(III) species **B** by the iodine(III) reagent **E** derived from IBA by the exchange of a hydroxy group with existing acid such as CSA, HCl and MeOH. It was independently confirmed that the esterification of 2-iodobenzoic acid takes place to give **5** under the reaction conditions; 2-iodobenzoic acid was smoothly converted to **5** in chloroform/methanol solution at 65 °C. Transmetalation of gold(III) complex **B** with arylsilane **2** affords monoarylated gold(III) intermediate **C**. Electrophilic metalation of heteroarene **1** with **C** with concurrent generation of acid (HX) produces diarylated gold(III) species **D**. Finally, the reductive elimination from **D** releases the coupling product **3** along with the regeneration of gold(I) species **A**. The side reaction leading to the homo-coupling of arylsilane likely occurs *via* over transmetalation of monoarylated gold(III) species **C** with arylsilane **2** or disproportionation of **C** to give **4**.[8]

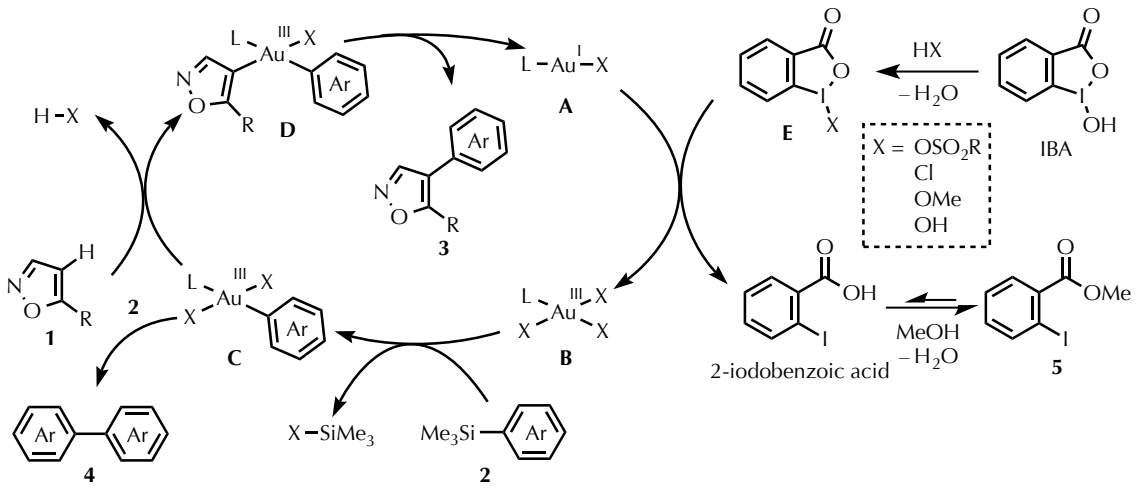

Figure 3. Plausible reaction mechanism of gold-catalyzed oxidative C–H arylation of heteroarenes with arylsilanes.

Direct observation and isolation of PyC-gold(III) complex

To verify the hypothesis that PyC accelerates the gold(I)-to-gold(III) oxidation, the direct observation and the isolation of PyC-gold(III) complex were attempted. First of all, gold(III) complex $AuCl_3$(PyC) was newly synthesized by treating AuCl(PyC) with $PhICl_2$ (see experimental section).[16] The X-ray crystallographic analysis was

successfully accomplished with a colorless single crystal of $AuCl_3$(PyC) which was recrystallized from nitrobenzene and pentane (Figure 4).[17] The X-ray crystal structure shows that four bonds on gold are in a planar surface, and pyridylidene face and the added two chlorine atoms are in vertical positions. The ligand arrangement is quite similar to a series of reported NHC-$AuCl_3$ complexes.[16]

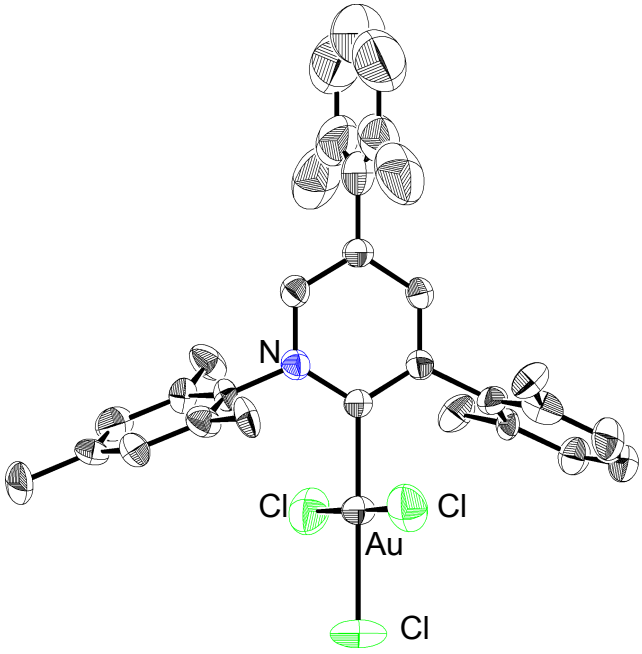

Figure 4. ORTEP drawing of $AuCl_3$(PyC) with 50% probability. Hydrogen atoms and solvent are omitted for clarity.

With the authentic $AuCl_3$(PyC) in hand, the direct observation of PyC-gold(III) complex under the C–H arylation conditions was carried out. Treatment of AuCl(PyC) with 5-fluoroiodosobenzoic acid (5F-IBA) and CSA in $CDCl_3/CD_3OD$ at 65 °C resulted in the full consumption of 5F-IBA within 30 min (monitored by ^{19}F NMR) (Scheme 2). While the resulting mixture seemed to contain several catalytically active PyC-gold(III) complexes, the formation of various gold(III) species bearing hydroxyl, methoxy, sulfoxy and chloro groups made the analysis and isolation difficult. However, the subsequent addition of excess amount of LiCl enabled detecting the gold(III) species as $AuCl_3$(PyC) by ^1H and ^{13}C NMR analyses. The ^1H NMR analysis revealed that about 90% of AuCl(PyC) was consumed and $AuCl_3$(PyC) was produced in 50% NMR yield. Fortunately, the isolation from the messy crude mixtures was accomplished to give $AuCl_3$(PyC) in 24% isolated yield. The same experiment with AuCl(IPr) complex was

also conducted. From the ^{19}F and ^{1}H NMR analyses, approximately a half of AuCl(IPr) and oxidant 5F-IBA remained unreacted after heating for 30 min, and $AuCl_3$(IPr) was observed only in 34% ^{1}H NMR yield.[16]

These observations on gold(III) species support the hypothesis that highly electron-donating PyC ligand strongly coordinates to a gold center and promotes the gold(I)-to-gold(III) oxidation by stabilizing a gold(III) species without dissociation. An IPr-gold(III) complex is known to be stable, but the lower electron-donation of IPr than PyC seems to result in the inefficient oxidation of AuCl(IPr). DFT calculation on oxidation process of AuCl(ligand) to $AuCl_3$(ligand) also clarified the advantage of PyC ligand over IPr by 3.6 kcal mol^{-1} (see experimental section). While it still remains unclear how PyC ligand affects transmetalation, C–H metalation and reductive elimination steps, the acceleration of oxidation and the stabilization effect of both gold(I) and gold(III) species might prevent the ligand dissociation and formation of inactive gold nanoparticles, and prolong the catalyst life-time, resulting in the facilitation of reaction.

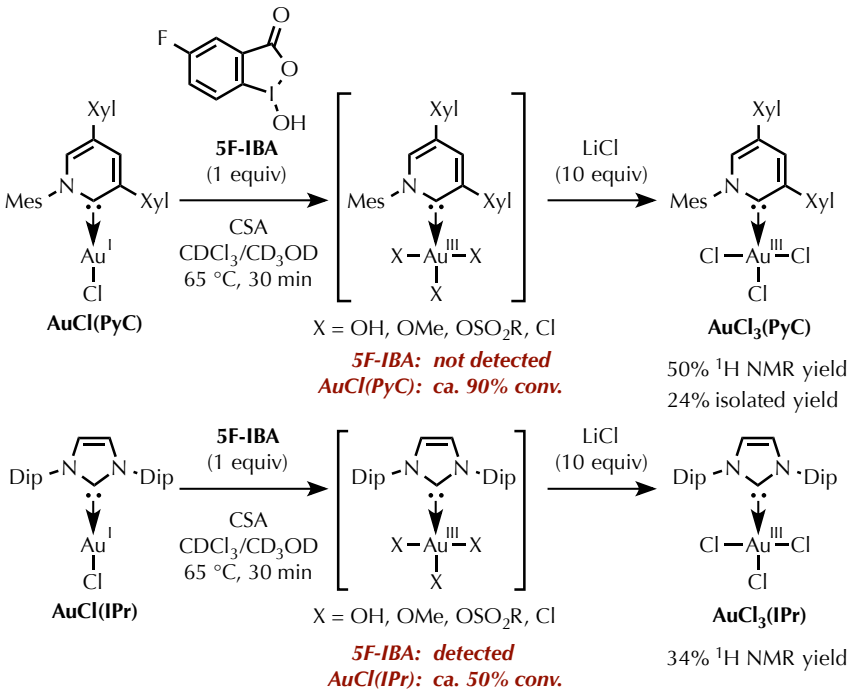

Scheme 2. Direct observation and isolation of carbene-gold(III) complex. Mes = 2,4,6-$Me_3C_6H_2$, Xyl = $Me_2C_6H_3$, Dip = 2,6-*i*-$Pr_2C_6H_3$.

3. Conclusions

In summary, the author has developed the oxidative C–H arylation of various heteroarenes with arylsilanes catalyzed by PyC-gold complex, and revealed the advantageous features of using PyC ligand. Through the reaction progress experiments and stoichiometric oxidation of gold(I) complexes, it was suggested that the highly electron-donating PyC ligand promotes the gold(I)-to-gold(III) oxidation and stabilizes the gold(III) species, thereby facilitating the oxidative coupling reactions.

4. Experimental

General

Unless otherwise noted, all materials including dry solvents were obtained from commercial suppliers and used without further purification. All reactions were performed using standard vacuum-line, Schlenk techniques, and screw cap tube. Work-up and purification procedures were carried out with reagent-grade solvents under air.

Analytical thin-layer chromatography (TLC) was carried out on *Merck* silica gel 60 F_{254} plates; detection by UV or dipping into a solution of $Ce(SO_4)_2 \cdot H_2O$ (10 g), phosphomolybdic acid hydrate (25 g), conc. H_2SO_4 (60 mL) and H_2O (0.94 L) or $NaHCO_3$ (5.0 g), $KMnO_4$ (1.5 g) and H_2O (0.20 L) followed by heating. Flash chromatography (FC) was carried out on *Merck* or *KANTO* silica gel 60 (40–100 μm) with an air pressure of about 1.1–1.5 bar. Preparative thin-layer chromatography (PTLC) was performed using Wako-gel® B5-F silica coated plates (0.75 mm) prepared in our laboratory. High-resolution mass spectra (HRMS) were obtained from *Thermo Fisher* Exactive Plus (ESI) and (APCI). Nuclear magnetic resonance (NMR) spectra were recorded on *JEOL* JNM-ECA-600 (^{1}H: 600 MHz, ^{13}C: 150 MHz). Chemical shifts for ^{1}H NMR are expressed in parts per million (ppm) relative to $CHCl_3$ (δ 7.26ppm). Chemical shifts for ^{13}C NMR are expressed in ppm relative to $CHCl_3$ (δ 77.0ppm). Data are reported as follows: chemical shift, multiplicity (s = singlet, d = doublet, dd = doublet of doublets, dt = doublet of triplets, t = triplet, m = multiplet), coupling constant (Hz), and integration.

Preparation of (triarylpyridylidene)gold chloride [AuCl(PyC)]

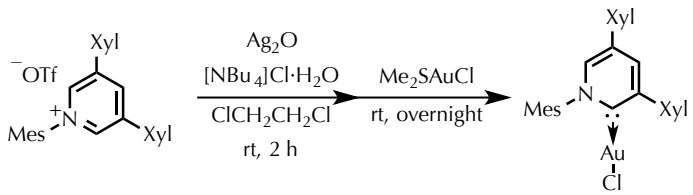

40%

Silver(I) oxide (232 mg, 1.0 mmol) was added into a reaction vessel filled with 1,2-dichloroethane (5.0 mL) solution of 3,5-bis(2,6-dimethylphenyl)-1-mesityl-pyridinium triflate·toluene[10a] (648 mg, 1.0 mmol) and tetrabutylammonium chloride hydrate (1.4 g, 5.0 mmol) under N_2 atmosphere. The reaction mixture was stirred until

silver(I) oxide powder disappeared (1–2 h) at room temperature in dark before chloro(dimethylsulfide)gold(I) was added. Further overnight stirring afforded yellow solution and black solid. Addition of chloroform (10 mL) gave insoluble white precipitation, and these solids were removed by Celite® filtration and the filtrate was concentrated under reduced pressure. The crude oily mixture was purified by column chromatography on silica gel with chloroform/methanol (20:1) as the eluents and the fractions were concentrated under reduced pressure. Reprecipitation from chloroform/toluene gave colorless microcrystal. Further purification was conducted by recrystallization from chloroform/toluene to produce Au(PyC)·toluene as a white crystal (281 mg, 0.40 mmol, 40% yield). Toluene in the crystal was removed by evaporation of chloroform solution. The characterization data for compound Au(PyC) corresponded to the reported values.[10a]

Oxidation of (triarylpyridylidene)gold chloride

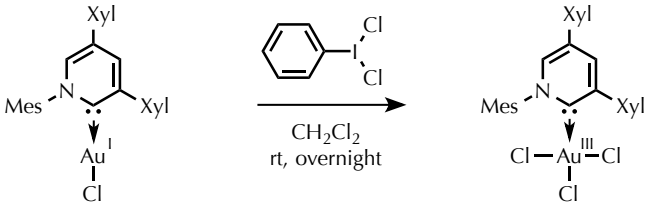

Oxidation of AuCl(PyC) was performed according to the literature.[16] dichloro(phenyl)-λ^3-iodane (55 mg, 0.20 mmol) was added into the solution of AuCl(PyC) (128 mg, 0.200 mmol) in dichloromethane (2.0 mL) under N_2 atmosphere. The reaction mixture was stirred at room temperature for 19 h and was filtered with a pad of Celite®. The filtrate was poured into hexane and the resulting precipitation was collected by filtration to obtain pure $AuCl_3$(PyC) as a white solid (140 mg, 99%). The colorless single crystal for X-ray diffraction analysis was obtained by recrystallization from nitrobenzene and pentane.

In situ observation and isolation of (triarylpyridylidene)gold trichloride

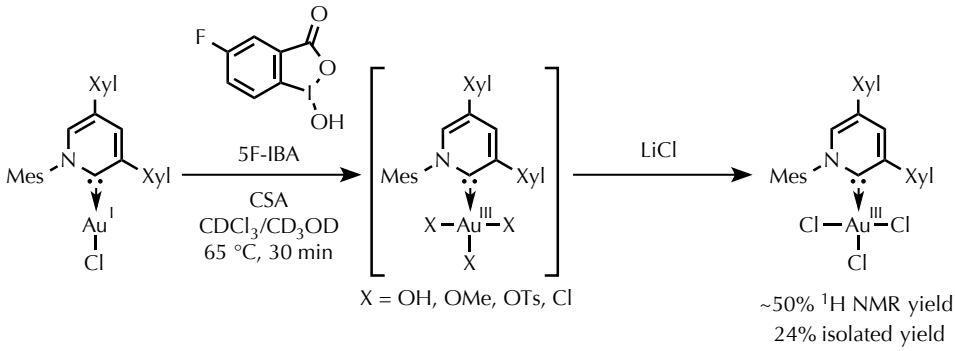

AuCl(PyC) (13 mg, 20 μmol), 5-fluoro-2-iodosobenzoic acids (5F-IBA) (5.6 mg, 20 μmol) and (+)-10-camphorsulfonic acid (CSA) (4.6 mg, 20 μmol) were placed in a screw NMR tube, and $CDCl_3/CD_3OD$ (10:1, 0.60 mL) was added under N_2 atmosphere. The tube was sealed with a cap equipped with a Teflon®-coated silicon rubber septum, and heated at 65 °C for 30 min. After cooling to room temperature, lithium chloride (8.4 mg, 0.20 mmol) was added. Then 1,1,2,2-tetrachloroethane (as an internal standard) was added and NMR yield of $AuCl_3(PyC)$ was estimated by ^1H NMR. The solvent was removed *in vacuo*, and the residue was dissolved in ethyl acetate, organic layer was washed with saturated $NaHCO_3$ aq., and brine, dried over Na_2SO_4, filtrated and concentrated *in vacuo* to afford crude mixture. The crude mixture was further washed with Et_2O to give pure $AuCl_3(PyC)$ as white powder (3.4 mg, 24%).

General procedure for triarylpyridylidene-gold-catalyzed oxidative C–H arylation of heteroarenes with arylsilanes

Triarylpyridylidene-gold complex AuCl(PyC) (6.4 mg, 10 μmol, 5 mol%), heteroarene (0.20 mmol), and aryl(trimethyl)silane (0.20 mmol), 2-iodosobenzoic acids (IBA) (53 mg, 0.20 mmol), (+)-10-camphorsulfonic acid (CSA) (47 mg, 0.20 mmol) and a stirring bar were placed in a screw test tube, and dry chloroform/methanol (1.0 mL/0.10 mL) was added under N_2 atmosphere. The tube was sealed with a cap equipped with a Teflon®-coated silicon rubber septum, and the mixture was stirred at 65 °C for 18–48 h. The reaction was quenched by addition of excess saturated $NaHCO_3$ aq., the aqueous layer was extracted with dichloromethane and the combined organic layers were dried over Na_2SO_4, filtrated, and concentrated under reduced pressure. The residue was purified by flash chromatography (FC) to afford the coupling product.

General procedure for GC analysis of reaction profiles of each reaction component

A gold complex [AuCl(ligand)] (25 μmol, 5 mol%), 5-methylisozxazole (**1b**) (42 mg, 0.50 mmol), and (4-bromophenyl)(trimethyl)silane (**2a**) (115 mg, 0.50 mmol), 2-iodosobenzoic acids (IBA) (132 mg, 0.50 mmol), (+)-10-camphorsulfonic acid (CSA) (116 mg, 0.50 mmol), the internal standard (nonane, 50 μL) and a stirring bar were placed in a Schlenk tube, and dry chloroform/methanol (5.0 mL/0.50 mL) solution was added under N_2 atmosphere. The tube was sealed with a glass stopper, and the mixture was stirred at 65 °C. A tiny portion of reaction mixture was taken with a capillary under N_2 atmosphere, and its diluted solution was analyzed by GC.

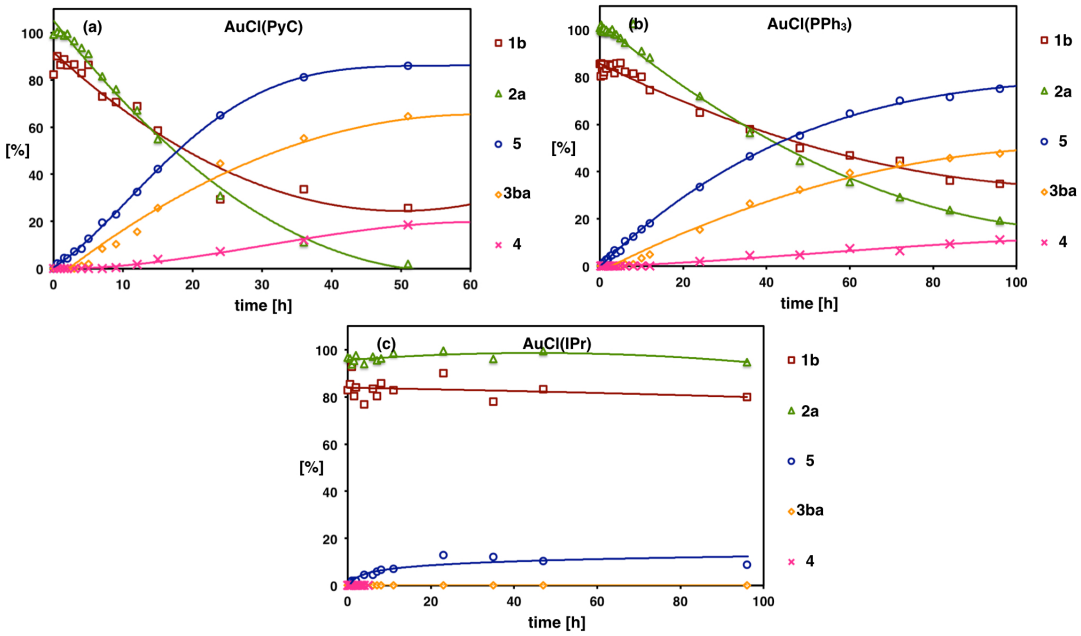

Figure S1. Time-yield profiles of 4-(4-bromophenyl)-5-methylisoxazole (**3ba**) and methyl 2-iodobenzoate (**5**) with (a) AuCl(PyC), (b) AuCl(PPh_3) and (c) AuCl(IPr). All yields were determined by GC analysis with *n*-nonane as an internal standard

Characterization of new compounds

[3,5-bis(2,6-dimethylphenyl)-1-mesityl-pyridylidene]gold trichloride [$AuCl_3$(PyC)]

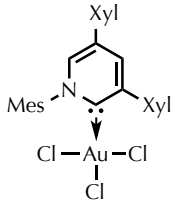

^{1}H NMR ($CDCl_3$, 600 MHz) δ 8.17 (d, *J* = 2.1 Hz, 1H), 7.90 (d, *J* = 2.1 Hz, 1H), 7.29 (td, *J* = 7.6, 2.7 Hz, 2H), 7.19 (d, *J* = 7.6 Hz, 2H), 7.16 (d, *J* = 7.6 Hz, 2H), 7.07 (s,

2H), 2.36 (s, 3H), 2.28 (s, 12H), 2.15 (s, 6H); ^{13}C NMR ($CDCl_3$, 150 MHz) δ 162.5 (CH), 149.6 (4°), 146.6 (CH), 144.7 (CH), 141.9 (4°), 141.5 (4°), 138.5 (4°), 136.4 (4°), 135.62 (4°), 135.58 (4°), 133.2 (4°), 132.2 (4°), 130.4 (CH), 129.9 (CH), 129.7 (CH), 128.32 (4°), 128.29 (CH), 22.1 (CH_3), 21.1 (CH_3), 20.9 (CH_3), 19.3 (CH_3); HRMS (ESI+) calcd for $C_{31}H_{35}AuCl_2NO$ $[M–Cl+MeOH]^+$: *m/z* 704.1756, found: 704.1722.

*4-(4-Bromophenyl)-isoxazole (**3aa**)*

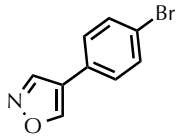

3aa was prepared according to the general procedure, employing isoxazole (**1a**) (14 mg, 0.20 mmol) and (4-bromophenyl)(trimethyl)silane (**2a**) (46 mg, 0.20 mmol) for 18 h. FC (hexane/ethyl acetate = 20:1 to 10:1) gave **3aa** as a pale yellow solid (6.1 mg, 0.027 mmol, 14%).

^{1}H NMR ($CDCl_3$, 600 MHz) δ 8.67 (s, 1H), 8.53 (s, 1H), 7.56–7.53 (m, 2H), 7.36–7.33 (m, 2H); ^{13}C NMR ($CDCl_3$, 150 MHz) δ 153.5 (CH), 147.7 (CH), 132.3 (CH), 127.9 (CH), 127.5 (4°), 122.0 (4°), 120.4 (4°); HRMS (ESI+) calcd for C_9H_7BrNO $[M+H]^+$: *m/z* 223.9706, found: *m/z* 223.9695.

*4-(4-Fluorophenyl)-isoxazole (**3ab**)*

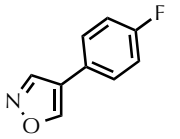

3ab was prepared according to the general procedure, employing isoxazole (**1a**) (14 mg, 0.20 mmol) and (4-fluorophenyl)(trimethyl)silane (**2b**) (37 mg, 0.20 mmol) for 24 h. FC (pentane/diethylether = 10:1) gave **3ab** as a pale yellow solid (4.9 mg, 0.030 mmol, 15%).

^{1}H NMR ($CDCl_3$, 600 MHz) δ 8.64 (s, 1H), 8.52 (s, 1H), 7.46–7.43 (m, 2H), 7.14–7.10 (m, 2H); ^{13}C NMR ($CDCl_3$, 150 MHz) δ 162.5 (4°, J = 247 Hz), 153.2 (CH), 147.9 (CH), 128.2 (CH, J = 8.6 Hz), 124.7 (4°, J = 2.9 Hz), 120.5 (4°), 116.3 (CH, J = 21 Hz); HRMS (ESI+) calcd for C_9H_7FNO $[M+H]^+$: *m/z* 164.0506, found: *m/z* 164.0500.

*4-(4-Bromophenyl)-5-methylisoxazole (**3ba**)*

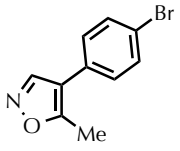

3ba was prepared according to the general procedure, employing 5-methylisoxazole (**1b**) (17 mg, 0.20 mmol) and (4-bromophenyl)(trimethyl)silane (**2a**) (46 mg, 0.20 mmol) for 24 h.

FC (pentane/diethylether = 10:1) gave **3ba** as a pale yellow oil (26 mg, 0.11 mmol, 55%).

^{1}H NMR ($CDCl_3$, 600 MHz) δ 8.32 (s, 1H), 7.57–7.54 (m, 2H), 7.26–7.23 (m, 2H), 2.55 (s, 3H); ^{13}C NMR ($CDCl_3$, 150 MHz) δ 164.5 (4°), 149.8 (CH), 132.1 (CH), 129.0 (4°), 128.9 (CH), 121.4 (4°), 115.5 (4°), 11.8 (CH_3); HRMS (ESI+) calcd for $C_{10}H_9BrNO$ $[M+H]^+$: *m/z* 237.9862, found: *m/z* 237.9855.

*4-(4-Fluorophenyl)-5-methylisoxazole (**3bb**)*

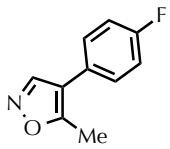

3bb was prepared according to the general procedure, employing 5-methylisoxazole (**1b**) (17 mg, 0.20 mmol) and (4-fluorophenyl)(trimethyl)silane (**2b**) (37 mg, 0.20 mmol) for 24 h. FC (pentane/diethylether = 10:1) gave **3bb** as a yellow oil (19 mg, 0.11 mmol, 54%).

^{1}H NMR ($CDCl_3$, 600 MHz) δ 8.31 (s, 1H), 7.35–7.31 (m, 2H), 7.15–7.10 (m, 2H), 2.54 (s, 3H); ^{13}C NMR ($CDCl_3$, 150 MHz) δ 164.2 (4°), 162.1 (4°, *J* = 247 Hz), 150.0 (CH), 129.1 (CH, *J* = 8.6 Hz), 126.1 (4°, *J* = 2.9 Hz), 116.0 (CH, *J* = 22 Hz), 115.6 (4°), 11.6 (CH_3); HRMS (ESI+) calcd for $C_{10}H_9FNO$ $[M+H]^+$: *m/z* 178.0663, found: *m/z* 178.0658.

*4-(4-Trifluoromethylphenyl)-5-methylisoxazole (**3bc**)*

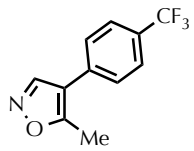

3bc was prepared according to the general procedure, employing 5-methylisoxazole (**1b**) (17 mg, 0.20 mmol) and (4-trifuoromethylphenyl)(trimethyl)silane (**2c**) (44 mg, 0.20 mmol) for 48 h. FC (hexane/ethyl acetate = 50:1 to 10:1) gave **3bc** as a colorless oil (15 mg, 0.066 mmol, 33%).

^{1}H NMR ($CDCl_3$, 600 MHz) δ 8.39 (s, 1H), 7.70 (d, *J* = 7.2 Hz, 2H), 7.50 (d, *J* = 8.4 Hz, 2H), 2.60 (s, 3H); ^{13}C NMR ($CDCl_3$, 150 MHz) δ 165.2 (4°), 149.8 (CH), 133.8 (4°), 129.6 (4°, *J* = 33 Hz), 127.6 (CH), 126.0 (CH, *J* = 4.4 Hz), 124.0 (4°, *J* = 270 Hz), 115.4 (4°), 11.9 (CH_3); HRMS (ESI+) calcd for $C_{11}H_9F_3NO$ $[M+H]^+$: *m/z* 228.0631, found: *m/z* 228.0622.

*4-(3,5-Dibromo)-5-methylisoxazole (**3bd**)*

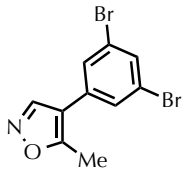

3bd was prepared according to the general procedure, employing 5-methylisoxazole (**1b**) (17 mg, 0.20 mmol) and (3,5-dibromophenyl)(trimethyl)silane (**2d**) (62 mg, 0.20 mmol) for 48 h. FC (hexane/ethylacetate = 50:1 to 10:1) gave **3bd** as a white solid (8.3 mg, 0.026 mmol, 13%).

^{1}H NMR ($CDCl_3$, 600 MHz) δ 8.33 (s, 1H), 7.64 (t, *J* = 1.8 Hz, 1H), 7.45 (d, *J* = 2.4 Hz, 2H), 2.58 (s, 3H); ^{13}C NMR ($CDCl_3$, 150 MHz) δ 165.3 (4°), 149.6 (CH), 133.6 (4°), 133.0 (CH), 129.1 (CH), 123.5 (4°), 114.2 (4°), 11.9 (CH_3); HRMS (ESI+) calcd for $C_{10}H_8Br_2NO$ $[M+H]^+$: *m/z* 317.8947, found: *m/z* 317.8935.

*4-(4-Bromophenyl)-5-phenylisoxazole (**3ca**)*

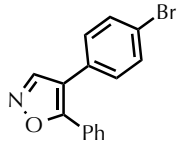

3ca was prepared according to the general procedure, employing 5-phenylisoxazole (**1c**) (29 mg, 0.20 mmol) and (4-bromophenyl)(trimethyl)silane (**2a**) (46 mg, 0.20 mmol) for 48 h. FC (hexane/ethyl acetate = 50:1 to 10:1) gave **3ca** as a white solid (17 mg, 0.057 mmol, 28%).

^{1}H NMR ($CDCl_3$, 600 MHz) δ 8.34 (s, 1H), 7.61 (dd, *J* = 8.1, 1.5 Hz, 2H), 7.54–7.51 (m, 2H), 7.45–7.38 (m, 3H), 7.27–7.24 (m, 2H); ^{13}C NMR ($CDCl_3$, 150 MHz) δ 164.3 (4°), 151.5 (CH), 132.2 (CH), 130.3 (CH), 130.2 (CH), 129.0 (4°), 128.9 (CH), 127.3 (4°), 127.3 (CH), 122.2 (4°), 115.1 (4°); HRMS (ESI+) calcd for $C_{15}H_{11}BrNO$ $[M+H]^+$: *m/z* 300.0019, found: *m/z* 300.0004.

*4-(4-Bromophenyl)-3,5-dimethylisoxazole (**3da**)*

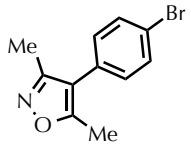

3da was prepared according to the general procedure, employing 3,5-dimethylisoxazole (**1d**) (19 mg, 0.20 mmol) and (4-bromophenyl)(trimethyl)silane (**2a**) (46 mg, 0.20 mmol) for 48 h. FC (pentane/dimethylether = 10:1) gave **3da** as a yellow solid (8.6 mg, 0.034 mmol, 17%).

^{1}H NMR ($CDCl_3$, 600 MHz) δ 7.57 (d, *J* = 8.4 Hz, 2H), 7.13 (d, *J* = 8.4 Hz, 2H), 2.39 (s, 3H), 2.25 (s, 3H); ^{13}C NMR ($CDCl_3$, 150 MHz) δ 165.3 (4°), 158.4 (4°), 132.0 (CH), 130.7 (CH), 129.4 (4°), 121.7 (4°), 115.7 (4°), 11.5 (CH_3) 10.7 (CH_3); HRMS (ESI+) calcd for $C_{11}H_{11}BrNO$ $[M+H]^+$: *m/z* 252.0019, found: *m/z* 252.0009.

*3-(4-Bromophenyl)-N-tosylindole (**3ea**)*

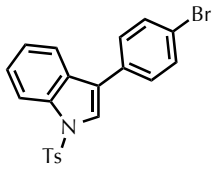

3ea was prepared according to the general procedure, employing *N-p*-toluenesulfonylindole (**1e**) (54 mg, 0.20 mmol) and (4-bromophenyl)(trimethyl)silane (**2a**) (46 mg, 0.20 mmol) for 48 h. FC (pentane/dimethylether = 10:1) gave **3ea** as a white solid (38 mg, 0.088 mmol, 44%).

^{1}H NMR ($CDCl_3$, 600 MHz) δ 8.07 (d, *J* = 8.4 Hz, 1H), 7.82 (d, *J* = 8.4 Hz, 2H), 7.72 (d, *J* = 8.4 Hz, 1H), 7.70 (s, 1H), 7.59 (d, *J* = 8.4 Hz, 2H), 7.47 (d, *J* = 8.4 Hz, 2H), 7.38 (t, *J* = 8.1 Hz, 1H), 7.30 (t, *J* = 7.5 Hz, 1H), 7.24 (d, *J* = 8.4 Hz, 2H), 2.34 (s, 3H); ^{13}C NMR ($CDCl_3$, 150 MHz) δ 145.1 (4°) 135.4 (4°), 135.1 (4°) 132.0 (CH), 130.0 (CH), 129.4 (CH), 128.9 (4°), 126.9 (CH), 125.0 (CH), 123.7 (CH), 123.0 (CH), 122.7 (4°), 121.4 (4°), 120.1 (CH), 113.9 (CH), 21.6 (CH_3), one 4° carbon peak should be overlapped; HRMS (ESI+) calcd for $C_{21}H_{17}BrNO_2S$ $[M+H]^+$: *m/z* 426.0158, found: *m/z* 426.0139.

*2-(4-Bromophenyl)-benzo[b]thiophene (**3fa**) and 3-(4-bromophenyl)-benzo[b]thiophene (**3fa'**)*

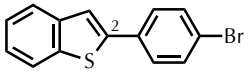

3fa

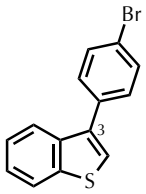

3fa'

3fa was prepared according to the general procedure, employing benzo[*b*]thiophene (**1f**) (27 mg, 0.20 mmol) and (4-bromophenyl)(trimethyl)silane (**2a**) (46 mg, 0.20 mmol) for 48 h. FC (pentane) gave **3fa** as mixture of **3fa'** (a white solid, 13 mg, 0.044 mmol, 22%, **3fa**:**3fa'** = 83:17). The characterization data for compound **3fa'** corresponded to the reported values.[18]

^{1}H NMR of **3fa** ($CDCl_3$, 600 MHz) δ 7.83 (d, *J* = 8.4 Hz, 1H), 7.78 (d, *J* = 7.2 Hz, 1H), 7.59–7.53 (m, 5H), 7.38–7.32 (m, 2H); ^{13}C NMR of **3fa** ($CDCl_3$, 150 MHz) δ 142.9 (4°), 140.6 (4°), 139.5 (4°), 133.3 (4°), 132.1 (CH), 127.9 (CH), 124.7 (CH), 124.6 (CH), 123.7 (CH), 122.3 (CH), 122.2 (4°), 119.9 (CH); HRMS (APCI+) calcd for $C_{14}H_9BrS$ $[M]^+$: *m/z* 287.9603, found: *m/z* 287.9596.

X-ray crystallography

Details of the crystal data and a summary of the intensity data collection parameters for $AuCl_3$(PyC) are listed in Table S1. In each case, a suitable crystal was mounted with mineral oil on a glass fiber and transferred to the goniometer of a Rigaku Saturn CCD diffractometer. Graphite-monochromated Mo Kα radiation (λ = 0.71075 Å) was used. The structures were solved by direct methods with (SIR-97)[19] and refined by full-matrix least-squares techniques against F^2(SHELXL-97).[20] The intensities were corrected for Lorentz and polarization effects. Non-hydrogen atoms were refined anisotropically. Hydrogen atoms were placed using AFIX instructions. The data can be obtained free of charge from The Cambridge Crystallographic Data Centre via www.ccdc.cam.ac.uk/data_request/cif (CCDC 1045812).

***Table S1**. Crystallographic data and structure refinement details for compound ([$AuCl_3$(PyC)]·$PhNO_2$).*

	$[AuCl_3(PyC)]\cdot PhNO_2$
formula	$C_{72}H_{70}Au_2Cl_6N_4O_4$
fw	1661.95
T (K)	103(2)
λ (Å)	0.71075
Cryst syst	Monoclinic
space group	*C*2/*c*
a, (Å)	8.332(5)
b, (Å)	25.831(13)
c, (Å)	16.488(9)
α, (deg)	90
β , (deg)	104.578(8)
γ , (deg)	90
V, (Å^3)	3434(3)
Z	2
D_{calc}, (g / cm^3)	1.607
μ (mm^{-1})	4.551
F(000)	1644
cryst size (mm)	0.10 × 0.10 × 0.05
2θ range, (deg)	3.00–25.00
reflns collected	11449
indep reflns/R_{int}	3024/0.0567
params	312
GOF on F^2	1.043
R_1, wR_2 [I>2σ(I)]	0.0522, 0.1235
R_1, wR_2 (all data)	0.0676, 0.1320

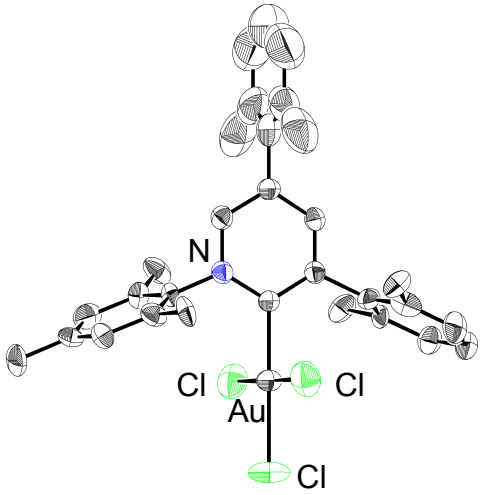

***Figure S1**. ORTEP drawing of $AuCl_3(PyC)$ with 50% probability. All hydrogen atoms and nitrobenzene molecule are omitted for clarity.*

Computational study

The Gaussian 09 program[21] running on a SGI Altix4700 system was used for optimization (B3LYP/SDD[22] for Au, 6-31G(d) for others). Structures were optimized without any symmetry assumptions. Zero-point energy, enthalpy, and Gibbs free energy at 298.15 K and 1 atm were estimated from the gas-phase studies. Harmonic vibration frequency calculation at the same level was performed to verify all stationary points as local minima (with no imaginary frequency). Visualization of the results was performed by use of GaussView 5.0.9 software.

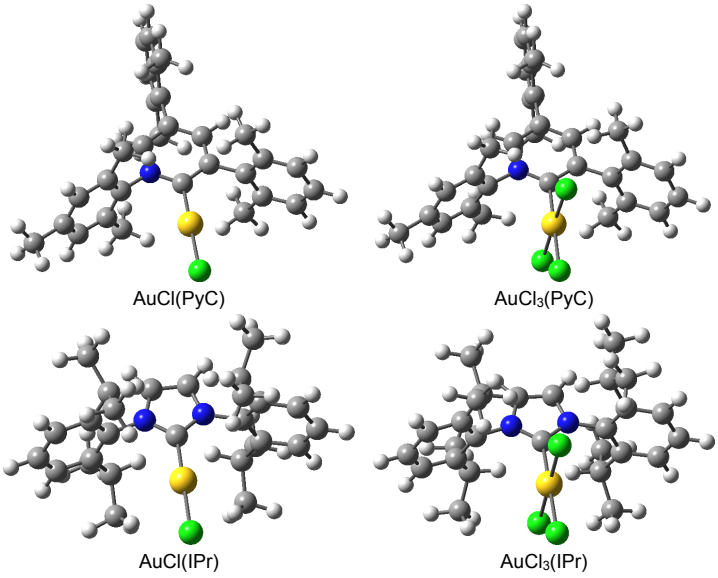

***Figure S2.** Optimized structures of gold complexes. C: gray, H: white, N: blue, Cl: green, Au: yellow.*

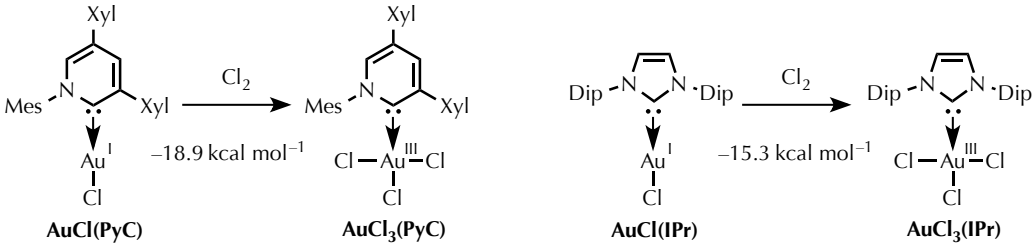

Scheme S1. *Hypothetical reactions for estimation of the stability of gold(III) complexes.*

Table S2. *Uncorrected and thermal-corrected (298 K) energies of stationary points (Hartree).*[a]

compound	*E*	*E* + *ZPE*	*H*	*G*
AuCl(PyC)	-1812.67004697	-1812.142233	-1812.106688	-1812.213402
$AuCl_3$(PyC)	-2733.05219302	-2732.520790	-2732.482012	-2732.594673
AuCl(IPr)	-1756.11982458	-1755.544370	-1755.509197	-1755.614045
$AuCl_3$(PyC)	-2676.49630661	-2675.917036	-2675.878847	-2675.988002
Cl_2	-920.349884457	-920.348706	-920.345190	-920.370557

a) *E*: electronic energy; *ZPE*: zero-point energy; *H* (= $E + ZPE + E_{vib} + E_{rot} + E_{trans} + RT$): sum of electronic and thermal enthalpies; *G* (= $H - TS$): sum of electronic and thermal free energies.

Table S3. *Cartesian coordinates for the gold complexes and chlorine.*

AuCl(PyC)

C	-0.686338	-1.334196	0.000074	H	1.223266	-6.365996	0.000263	H	-1.171639	-2.353408	2.657842
C	-2.063553	-1.144797	-0.000006	C	-4.120086	0.360864	0.000049	H	0.084655	-3.365845	3.384284
C	-2.638692	0.143335	0.000055	C	-4.811639	0.454251	1.226947	C	-0.134329	-2.693286	-2.549550
C	-1.760980	1.205133	0.000144	C	-4.811722	0.453554	-1.226855	H	-1.172417	-2.354162	-2.657585
H	-2.719914	-2.011902	-0.000100	C	-6.198247	0.645302	1.205664	H	0.507452	-1.810153	-2.656077
H	-2.089884	2.237721	0.000232	C	-6.198330	0.644602	-1.205588	H	0.084088	-3.366350	-3.383990
C	0.409028	2.230102	0.000026	C	-6.889334	0.740583	0.000034	C	-4.086105	0.353314	-2.550789
C	0.766753	2.800192	1.230823	H	-6.737181	0.717838	2.146908	H	-3.366363	1.170655	-2.684973
C	0.766391	2.800180	-1.230884	H	-6.737329	0.716591	-2.146838	H	-3.520644	-0.582125	-2.638817
C	1.518795	3.978262	1.200578	H	-7.965994	0.887549	0.000028	H	-4.792731	0.395463	-3.384743
C	1.518447	3.978246	-1.200873	N	-0.407771	1.016310	0.000114	C	-4.085965	0.354556	2.550894
C	1.911466	4.577842	-0.000209	C	0.389926	2.161686	-2.546114	H	-3.521128	-0.581212	2.639525
H	1.810675	4.433367	2.144205	H	0.893399	1.194853	-2.667121	H	-3.365665	1.171498	2.684440
H	1.810074	4.433329	-2.144589	H	-0.688816	1.980539	-2.627991	H	-4.792494	0.397757	3.384875
C	-0.137436	-2.730375	0.000118	H	0.685856	2.801438	-3.382015	C	2.761353	5.826604	-0.000327
C	0.105071	-3.384958	-1.226089	C	0.390723	2.161702	2.546177	H	3.828730	5.570546	-0.000019
C	0.105420	-3.384732	1.226380	H	-0.687881	1.979793	2.628101	H	2.573297	6.440327	-0.887504
C	0.594564	-4.695556	-1.204923	H	0.894884	1.195244	2.667343	H	2.572900	6.440763	0.886467
C	0.594924	-4.695324	1.205313	H	0.686215	2.801813	3.381960	C	0.200868	-0.217526	0.000078
C	0.840058	-5.349138	0.000220	C	-0.133652	-2.692825	2.549779	Au	2.211308	-0.383949	-0.000056
H	0.788817	-5.202537	-2.146734	H	0.508379	-1.809854	2.656137	Cl	4.532043	-0.589953	-0.000229
H	0.789469	-5.202121	2.147162								

$AuCl_3$(PyC)

C	-0.852015	-1.320809	0.075220	H	1.067140	-6.348485	0.230580	H	0.046875	-3.236463	3.520291
C	-2.238233	-1.150297	0.076545	C	-4.326226	0.303783	-0.003606	C	-0.782144	-2.952272	-2.380877
C	-2.841206	0.115626	0.007800	C	-5.028008	0.369038	1.219276	H	-1.876528	-2.850769	-2.364795
C	-1.985339	1.196166	-0.048046	C	-5.005699	0.400445	-1.236872	H	-0.356182	-1.976350	-2.625778
H	-2.871164	-2.032480	0.126879	C	-6.417094	0.537803	1.186756	H	-0.531979	-3.637401	-3.196176
H	-2.336620	2.219471	-0.098495	C	-6.395496	0.567326	-1.224948	C	-4.267130	0.326080	-2.555492
C	0.136077	2.301160	-0.060553	C	-7.098251	0.636636	-0.024329	H	-3.578727	1.170340	-2.688493
C	0.344343	2.971083	1.156642	H	-6.965650	0.590734	2.123590	H	-3.666113	-0.587136	-2.639377
C	0.524491	2.837636	-1.299853	H	-6.927453	0.641339	-2.169898	H	-4.969379	0.340863	-3.393852
C	1.087975	4.154182	1.114619	H	-8.177052	0.766030	-0.032440	C	-4.312004	0.262330	2.547952
C	1.261904	4.026001	-1.275357	N	-0.629499	1.045245	-0.038343	H	-3.792060	-0.697377	2.657842
C	1.581455	4.681292	-0.082386	C	0.123979	2.220088	-2.617541	H	-3.554720	1.046365	2.670265
H	1.281820	4.676784	2.048038	H	0.590440	1.242719	-2.771255	H	-5.019123	0.351807	3.377476
H	1.586915	4.451480	-2.221603	H	-0.963683	2.084743	-2.683420	C	2.432057	5.928644	-0.087696
C	-0.315614	-2.723528	0.126273	H	0.425893	2.869408	-3.443810	H	3.496452	5.670134	-0.017015
C	-0.259960	-3.483640	-1.064585	C	-0.261883	2.504697	2.459230	H	2.296604	6.503721	-1.009648
C	0.029981	-3.302000	1.368541	H	-1.336455	2.734279	2.495389	H	2.196780	6.579322	0.760879
C	0.250784	-4.784941	-1.004780	H	-0.132433	1.432325	2.616436	C	-0.015040	-0.177904	0.013574
C	0.532901	-4.608560	1.380718	H	0.209743	3.018151	3.301168	Au	2.061010	-0.308670	-0.024243
C	0.664760	-5.339447	0.203440	C	-0.182246	-2.576768	2.678069	Cl	2.014002	-0.782012	-2.337745
H	0.317519	-5.366349	-1.920528	H	0.454052	-1.691382	2.768319	Cl	2.201595	0.132851	2.290896
H	0.814870	-5.053809	2.331181	H	-1.224321	-2.248832	2.790435	Cl	4.417258	-0.475197	-0.085212

AuCl(IPr)

C	0.678108	0.000225	-2.656979	H	1.370313	2.383433	-1.187702	H	-1.370154	-2.383222	-1.187814
C	-0.678047	0.000267	-2.656990	C	2.411053	-2.578079	-0.911683	C	-3.044255	3.389541	-2.059311
H	1.392082	0.000311	-3.465262	H	1.369950	-2.383252	-1.187141	H	-3.024100	2.833497	-3.003849
H	-1.392006	0.000392	-3.465286	C	3.044760	3.389526	-2.059394	H	-4.089111	3.641219	-1.843818
C	2.465223	0.000054	-0.907902	H	4.089545	3.641236	-1.843596	H	-2.499657	4.329510	-2.206439
C	3.113445	-1.237086	-0.723446	H	3.024895	2.833521	-3.003962	C	-2.387480	3.389925	0.398843
C	3.113579	1.237126	-0.723516	H	2.500179	4.329485	-2.206642	H	-3.399796	3.652265	0.727671
C	4.461085	-1.206400	-0.344884	C	2.387319	3.389782	0.398585	H	-1.905887	2.825702	1.204116
C	4.461215	1.206314	-0.344948	H	1.905469	2.825532	1.203685	H	-1.832556	4.324434	0.253712
C	5.129930	-0.000073	-0.157312	H	3.399558	3.652040	0.727717	C	-3.044511	-3.389128	-2.059926
H	4.990671	-2.141817	-0.189795	H	1.832483	4.324330	0.253352	H	-4.089336	-3.640827	-1.844305
H	4.990901	2.141681	-0.189895	C	3.044055	-3.389102	-2.059824	H	-3.024510	-2.832951	-3.004391
H	6.175154	-0.000119	0.139814	H	3.023758	-2.832852	-3.004240	H	-2.499950	-4.329082	-2.207282
C	-2.465192	0.000127	-0.907944	H	4.088952	-3.640781	-1.844524	C	-2.387366	-3.389878	0.398126
C	-3.113471	1.237216	-0.723382	H	2.499471	-4.329056	-2.207089	H	-1.832502	-4.324389	0.252759
C	-3.113498	-1.236998	-0.723678	C	2.387587	-3.390065	0.398406	H	-1.905610	-2.825791	1.203398
C	-4.461114	1.206435	-0.344839	H	3.399933	-3.652521	0.727045	H	-3.399635	-3.652223	0.727087
C	-4.461141	-1.206278	-0.345131	H	1.906101	-2.826031	1.203876	Au	-0.000019	-0.000133	1.517572
C	-5.129911	0.000064	-0.157393	H	1.832621	-4.324525	0.253111	Cl	-0.000099	-0.000367	3.842650
H	-4.990743	2.141813	-0.189656	C	-2.411112	2.578253	-0.911437	N	1.079889	0.000124	-1.326043
H	-4.990790	-2.141684	-0.190181	H	-1.370049	2.383480	-1.187092	N	-1.079850	0.000166	-1.326062
H	-6.175140	0.000042	0.139716	C	-2.411180	-2.578013	-0.912037	C	0.000013	0.000052	-0.491192
C	2.411300	2.578181	-0.911739								

$AuCl_3(IPr)$

C	0.676288	-0.032413	-2.676852	H	1.546429	2.390487	-1.189370	C	-2.564123	3.236548	-2.353896
C	-0.676580	0.034421	-2.676754	C	2.313678	-2.686690	-0.934076	H	-2.257962	2.524276	-3.128668
H	1.388988	-0.069739	-3.484013	H	1.243889	-2.486153	-0.833621	H	-3.627297	3.457557	-2.506309
H	-1.389357	0.072437	-3.483817	C	2.963464	2.792192	-2.759804	H	-2.000678	4.164136	-2.508754
C	2.489332	-0.109616	-0.961815	H	4.047090	2.868167	-2.908741	C	-2.656353	3.754264	0.122723
C	3.070649	-1.375886	-0.735608	H	2.585945	2.034733	-3.455622	H	-3.684329	4.121087	0.019778
C	3.224490	1.094897	-0.912507	H	2.516747	3.754357	-3.036392	H	-2.520785	3.369791	1.137155
C	4.428314	-1.400993	-0.392531	C	3.101807	3.592973	-0.368029	H	-1.990499	4.615385	0.000318
C	4.578159	0.999849	-0.566920	H	2.928280	3.351574	0.683453	C	-2.964528	-2.789623	-2.761675
C	5.172085	-0.229204	-0.298546	H	4.165234	3.821037	-0.505474	H	-4.048189	-2.865154	-2.910608
H	4.908976	-2.354358	-0.201374	H	2.542705	4.505630	-0.602836	H	-2.586813	-2.031774	-3.456964
H	5.174591	1.903993	-0.508154	C	2.564797	-3.234503	-2.356404	H	-2.518126	-3.751726	-3.038983
H	6.222924	-0.274866	-0.025741	H	2.258373	-2.521784	-3.130662	C	-3.102999	-3.592135	-0.370512
C	-2.489443	0.110696	-0.961518	H	3.628020	-3.455102	-2.509067	H	-2.544163	-4.504775	-0.606015
C	-3.070390	1.376965	-0.734334	H	2.001606	-4.162146	-2.511851	H	-2.929387	-3.351561	0.681146
C	-3.224945	-1.093638	-0.913109	C	2.657435	-3.753881	0.119850	H	-4.166496	-3.819788	-0.508099
C	-4.428028	1.402202	-0.391171	H	3.685542	-4.120242	0.016580	Au	0.000085	-0.000912	1.520837
C	-4.578577	-0.998461	-0.567407	H	2.521797	-3.370164	1.134558	Cl	0.348714	2.328705	1.525695
C	-5.172128	0.230555	-0.298040	H	1.991895	-4.615167	-0.003109	Cl	0.000195	-0.002157	3.871312
H	-4.908413	2.355558	-0.199278	C	-2.313048	2.687685	-0.931963	Cl	-0.348559	-2.330541	1.523151
H	-5.175270	-1.902478	-0.509320	H	-1.243312	2.486756	-0.831741	N	1.085765	-0.049276	-1.348370
H	-6.222943	0.276315	-0.025156	C	-2.634644	-2.450538	-1.291019	N	-1.085925	0.050288	-1.348217
C	2.633771	2.451915	-1.289376	H	-1.547279	-2.389487	-1.191023	C	-0.000036	0.000100	-0.534522

Cl_2

Cl	0.0	0.0	1.021364	Cl	0.0	0.0	-1.021364

5. References

[1] For recent reviews on gold-catalyzed organic reactions, see: (a) A. Arcadi, *Chem. Rev.*, 2008, **108**, 3266; (b) A. S. Hashmi and M. Rudolph, *Chem. Soc. Rev.*, 2008, **37**, 1766; (c) Z. Li, C. Brouwer and C. He, *Chem. Rev.*, 2008, **108**, 3239; (d) N. Marion and S. P. Nolan, *Chem. Soc. Rev.*, 2008, **37**, 1776; (e) N. T. Patil and Y. Yamamoto, *Chem. Rev.*, 2008, **108**, 3395; (f) A. Corma, A. Leyva-Pérez and M. J. Sabater, *Chem. Rev.*, 2011, **111**, 1657; (g) H. Huang, Y. Zhou and H. Liu, *Beilstein J. Org. Chem.*, 2011, **7**, 897; (h) M. Rudolph and A. S. K. Hashmi, *Chem. Soc. Rev.*, 2012, **41**, 2448; (i) G. Abbiati, F. Marinelli, E. Rossi and A. Arcadi, *Isr. J. Chem.*, 2013, **53**, 856; (j) M. Chiarucci and M. Bandini, *Beilstein J. Org. Chem.*, 2013, **9**, 2586; (k) F. López and J. L. Mascareñas, *Beilstein J. Org. Chem.*, 2013, **9**, 2250; (l) L. Nunes dos Santos Comprido and A. S. K. Hashmi, *Isr. J. Chem.*, 2013, **53**, 883; (m) H. Ohno, *Isr. J. Chem.*, 2013, **53**, 869; (n) G. Abbiati and E. Rossi, *Beilstein J. Org Chem*, 2014, **10**, 481; (o) M. E. Muratore, A. Homs, C. Obradors and A. M. Echavarren, *Chem.– Asian J.*, 2014, **9**, 3066; (p) J. Xie, C. Pan, A. Abdukader and C. Zhu, *Chem. Soc. Rev.*, 2014, **43**, 5245; (q) W. Yang and A. S. K. Hashmi, *Chem. Soc. Rev.*, 2014, **43**, 2941.

[2] For recent accounts on gold-catalyzed reactions, see: (a) E. Soriano and J. Marco-Contelles, *Acc. Chem. Res.*, 2009, **42**, 1026; (b) S. Gaillard, C. S. J. Cazin and S. P. Nolan, *Acc. Chem. Res.*, 2012, **45**, 778; (c) B. Alcaide and P. Almendros, *Acc. Chem. Res.*, 2014, **47**, 939; (d) L. Fensterbank and M. Malacria, *Acc. Chem. Res.*, 2014, **47**, 953; (e) A. Fürstner, *Acc. Chem. Res.*, 2014, **47**, 925; (f) A. S. K. Hashmi, *Acc. Chem. Res.*, 2014, **47**, 864; (g) C. Obradors and A. M. Echavarren, *Acc. Chem. Res.*, 2014, **47**, 902; (h) Y.-M. Wang, A. D. Lackner and F. D. Toste, *Acc. Chem. Res.*, 2014, **47**, 889; (i) H.-S. Yeom and S. Shin, *Acc. Chem. Res.*, 2014, **47**, 966; (j) D.-H. Zhang, X.-Y. Tang and M. Shi, *Acc. Chem. Res.*, 2014, **47**, 913; (k) L. Zhang, *Acc. Chem. Res.*, 2014, **47**, 877.

[3] For ligand effects in gold-catalyzed reactions, see: (a) D. J. Gorin, B. D. Sherry and F. D. Toste, *Chem. Rev.*, 2008, **108**, 3351; (b) M. Alcarazo, T. Stork, A. Anoop, W. Thiel and A. Fürstner, *Angew. Chem., Int. Ed.*, 2010, **49**, 2542; (c) S. P. Nolan, *Acc. Chem. Res.*, 2011, **44**, 91; (d) G. Cera and M. Bandini, *Isr. J. Chem.*, 2013, **53**, 848; (e) D. Gatineau, J.-P. Goddard, V. Mouriès-Mansuy and L. Fensterbank, *Isr. J. Chem.*, 2013, **53**, 892.

[4] For selected reviews on gold-catalyzed oxidative C–C coupling reactions, see: (a) M. N. Hopkinson, A. D. Gee and V. Gouverneur, *Chem.– Eur, J.*, 2011, **17**, 8248; (b) H. A. Wegner and M. Auzias, *Angew. Chem., Int. Ed.*, 2011, **50**, 8236; (c) J. P. Brand, Y. Li and J. Waser, *Isr. J. Chem.*, 2013, **53**, 901.

[5] For recent examples of oxidative heteroarylation of alkene through gold(I)/gold(III) catalytic cycle, see: (a) G. Zhang, Y. Peng, L. Cui and L. Zhang, *Angew. Chem., Int. Ed.*, 2009, **48**, 3112; (b) L. T. Ball, M. Green, G. C. Lloyd-Jones and C. A. Russell, *Org. Lett.*, 2010, **12**, 4724; (c) W. E. Brenzovich, Jr., D. Benitez, A. D. Lackner, H. P. Shunatona, E. Tkatchouk, W. A. Goddard, III and F. D. Toste, *Angew. Chem., Int. Ed.*, 2010, **49**, 5519; (d) W. E. Brenzovich, Jr., J.-F. Brazeau and F. D. Toste, *Org. Lett.*, 2010, **12**, 4728; (e) M. N. Hopkinson, A. Tessier, A. Salisbury, G. T. Giuffredi, L. E. Combettes, A. D. Gee and V. Gouverneur, *Chem.– Eur. J.*, 2010, **16**, 4739; (f) A. D. Melhado, W. E. Brenzovich, Jr., A. D. Lackner and F. D. Toste, *J. Am. Chem. Soc.*, 2010, **132**, 8885; (g) G. Zhang, L. Cui, Y. Wang and L. Zhang, *J. Am. Chem. Soc.*, 2010, **132**, 1474; (h) G. Zhang, Y. Luo, Y. Wang and L. Zhang, *Angew. Chem., Int. Ed.*, 2011, **50**, 4450; (i) L. T. Ball, G. C. Lloyd-Jones and C. A. Russell, *Chem.– Eur. J.*, 2012, **18**, 2931; (j) R. Zhang, Q. Xu, K. Chen, P. Gu and M. Shi, *Eur. J. Org. Chem.*, 2013, 7366; (k) S. Zhu, L. Ye, W. Wu and H. Jiang, *Tetrahedron*, 2013, **69**, 10375.

[6] For recent examples of gold-catalyzed C–C bond forming oxidative coupling reaction, see: (a) C. Jones, D. Taube, V. R. Ziatdinov, R. A. Periana, R. J. Nielsen, J. Oxgaard and W. A. Goddard, III, *Angew. Chem., Int. Ed.*, 2004, **43**, 4626; (b) H. A. Wegner, S. Ahles and M. Néuburger, *Chem.– Eur. J.*, 2008, **14**, 11310; (c) J. P. Brand, J. Charpentier and J. Waser, *Angew. Chem., Int. Ed.*, 2009, **48**, 9346; (d) L. Cui, G. Zhang and L. Zhang, *Bioorg. Med. Chem. Lett.*, 2009, **19**, 3884; (e) Y. Peng, L. Cui, G. Zhang and L. Zhang, *J. Am. Chem. Soc.*, 2009, **131**, 5062; (f) J. P. Brand and J. Waser, *Angew. Chem., Int. Ed.*, 2010, **49**, 7304; (g) T. de Haro and C. Nevado, *J. Am. Chem. Soc.*, 2010, **132**, 1512; (h) M. N. Hopkinson, J. E. Ross, G. T. Giuffredi, A. D. Gee and V. Gouverneur, *Org. Lett.*, 2010, **12**, 4904; (i) D. Qian and J. Zhang, *Beilstein. J Org. Chem.*, 2011, **7**, 808; (j) J. P. Brand, C. Chevalley, R. Scopelliti and J. Waser, *Chem.– Eur. J*, 2012, **18**, 5655; (k) M. D. Levin and F. D. Toste, *Angew. Chem., Int. Ed.*, 2014, **53**, 6211; (l) Y. Ma, S. Zhang, S. Yang, F. Song and J. You, *Angew. Chem., Int. Ed.*, 2014, **53**, 7870; (m) H. Peng, Y. Xi, N.

Ronaghi, B. Dong, N. G. Akhmedov and X. Shi, *J. Am. Chem. Soc.*, 2014, **136**, 13174.

[7] For gold-catalyzed oxidative C–H arylation of arenes, see: (a) L. T. Ball, G. C. Lloyd-Jones and C. A. Russell, *Science*, 2012, **337**, 1644; (b) L. T. Ball, G. C. Lloyd-Jones and C. A. Russell, *J. Am. Chem. Soc.*, 2014, **136**, 254; (c) A. Kar, N. Mangu, H. M. Kaiser, M. Beller and M. K. Tse, *Chem. Commun.*, 2008, 386; (d) A. Kar, N. Mangu, H. M. Kaiser and M. K. Tse, *J. Organomet. Chem.*, 2009, **694**, 524; (e) Q. Wu, C. Du, Y. Huang, X. Liu, Z. Long, F. Song and J. You, *Chem. Sci.*, 2015, **6**, 288.

[8] For selected mechanistic investigations on gold(I)/gold(III) redox processes, see: (a) N. P. Mankad and F. D. Toste, *J. Am. Chem. Soc.*, 2010, **132**, 12859; (b) E. Tkatchouk, N. P. Mankad, D. Benitez, W. A. Goddard, III and F. D. Toste, *J. Am. Chem. Soc.*, 2011, **133**, 14293; (c) M. Hofer and C. Nevado, *Eur. J. Inorg. Chem.*, 2012, 1338; (d) X. C. Cambeiro, T. C. Boorman, P. Lu and I. Larrosa, *Angew. Chem., Int. Ed.*, 2013, **52**, 1781; (e) M. Hofer and C. Nevado, *Tetrahedron*, 2013, **69**, 5751; (f) M. Hofer, E. Gomez-Bengoa and C. Nevado, *Organometallics*, 2014, **33**, 1328; (g) M. S. Winston, W. J. Wolf and F. D. Toste, *J. Am. Chem. Soc.*, 2014, **136**, 7777; (h) W. J. Wolf, M. S. Winston and F. D. Toste, *Nat. Chem*, 2014, **6**, 159.

[9] For the synthesis and DFT calculation of pyridylidene, see: (a) H. G. Raubenheimer, J. G. Toerien, G. J. Kruger, R. Otte, W. van Zyl and P. Olivier, *J. Organomet. Chem.*, 1994, **466**, 291; (b) C. E. Strasser, E. Stander-Grobler, O. Schuster, S. Cronje and H. G. Raubenheimer, *Eur. J. Inorg. Chem.*, 2009, 1905; (c) M. Roselló-Merino, J. Díez and S. Conejero, *Chem. Commun.*, 2010, **46**, 9247; (d) O. Holloczki and L. Nyulászi, *J. Org. Chem.*, 2008, **73**, 4794; (e) M. Z. Kassaee, F. A. Shakib, M. R. Momeni, M. Ghambarian and S. M. Musavi, *Tetrahedron*, 2009, **65**, 10093; (f) A. A. Tukov, A. T. Normand and M. S. Nechaev, *Dalton Trans.*, 2009, 7015.

[10] For our contributions to the synthesis and complexation of pyridylidene ligands, see: (a) K. Hata, Y. Segawa and K. Itami, *Chem. Commun.*, 2012, **48**, 6642; (b) T. Yoshidomi, Y. Segawa and K. Itami, *Chem. Commun.*, 2013, **49**, 5648.

[11] For the synthesis and characterization of nonclassical carbenes, see: (a) Y. Canac, M. Soleilhavoup, S. Conejero and G. Bertrand, *J. Organomet. Chem.*, 2004, **689**,

3857; (b) M. Melaimi, M. Soleilhavoup and G. Bertrand, *Angew. Chem., Int. Ed.*, 2010, **49**, 8810; (c) D. Martin, M. Melaimi, M. Soleilhavoup and G. Bertrand, *Organometallics*, 2011, **30**, 5304.

[12] For nonclassical carbene-gold complexes in catalytic reactions, see: (a) X. Zeng, G. D. Frey, R. Kinjo, B. Donnadieu and G. Bertrand, *J. Am. Chem. Soc.*, 2009, **131**, 8690; (b) R. Kinjo, B. Donnadieu and G. Bertrand, *Angew. Chem., Int. Ed.*, 2011, **50**, 5560; (c) M. J. López-Gómez, D. Martin and G. Bertrand, *Chem. Commun.*, 2013, **49**, 4483; (d) X. Hu, D. Martin, M. Melaimi and G. Bertrand, *J. Am. Chem. Soc.*, 2014, **136**, 13594; (e) L. Jin, D. S. Weinberger, M. Melaimi, C. E. Moore, A. L. Rheingold and G. Bertrand, *Angew. Chem., Int. Ed.*, 2014, **53**, 9059.

[13] Electron-rich arenes show the reactivity toward dehydrogenative homo- and cross-coupling reaction under oxidative conditions without metal oxidants. For related examples, see: (a) H. Ito, K. Ueda and K. Itami, in *From C–H to C–C Bonds: Cross-Dehydrogenative-Coupling*, ed. C.-J. Li, The Royal Society of Chemistry, 2015, pp. 153; (b) A. Jean, J. Cantat, D. Bérard, D. Bouchu and S. Canesi, *Org. Lett.*, 2007, **9**, 2553; (c) Y. Kita, K. Morimoto, M. Ito, C. Ogawa, A. Goto and T. Dohi, *J. Am. Chem. Soc.*, 2009, **131**, 1668; (d) K. Morimoto, N. Yamaoka, C. Ogawa, T. Nakae, H. Fujioka, T. Dohi and Y. Kita, *Org. Lett.*, 2010, **12**, 3804.

[14] For palladium-catalyzed C–H arylation of isoxazole, see: (a) H. A. Chiong and O. Daugulis, *Org. Lett.*, 2007, **9**, 1449; (b)Y. Fall, C. Reynaud, H. Doucet and M. Santelli, *Eur. J. Org. Chem.*, 2009, 4041; (c) J. Roger, F. Požgan and H. Doucet, *Adv. Synth. Catal.*, 2010, **352**, 696.

[15] Higher volatility of products resulted in the lower isolated yields.

[16] Synthesis and characterization of $AuCl_3$(IPr) complex has been reported by Nolan. S. Gaillard, X. Bantreil, A. M. Z. Slawin and S. P. Nolan, *Dalton Trans.*, 2009, 6967.

[17] Crystallographic data reported in this manuscript have been deposited with Cambridge Crystallographic Data Centre as supplementary publication No. CCDC-1045812 [$AuCl_3$(PyC)]. Copies of the data can be obtained free of charge via http://www.ccdc.cam.ac.uk/conts/retrieving.html.

[18] K. Funaki, T. Sato and S. Oi, *Org. Lett.*, 2012, **14**, 6186.

[19] A. Altomare, M. C. Burla, M. Camalli, G. L. Cascarano, C. Giacovazza, A. Guagliardi, A. G. G. Moliterni, G. Polidori and R. Spagna, *J. Appl. Crystallogr.*, 1999, **32**, 115.

[20] G. M. Sheldrick, University of Göttingen: Göttingen, Germany 1997.

[21] M. J. Frisch, G. W. Trucks, H. B. Schlegel, G. E. Scuseria, M. A. Robb, J. R. Cheeseman, G. Scalmani, V. Barone, B. Mennucci, G. A. Petersson, H. Nakatsuji, M. Caricato, X. Li, H. P. Hratchian, A. F. Izmaylov, J. Bloino, G. Zheng, J. L. Sonnenberg, M. Hada, M. Ehara, K. Toyota, R. Fukuda, J. Hasegawa, M. Ishida, T. Nakajima, Y. Honda, O. Kitao, H. Nakai, T. Vreven, J. A. Montgomery, Jr., J. E. Peralta, F. Ogliaro, M. Bearpark, J. J. Heyd, E. Brothers, K. N. Kudin, V. N. Staroverov, R. Kobayashi, J. Normand, K. Raghavachari, A. Rendell, J. C. Burant, S. S. Iyengar, J. Tomasi, M. Cossi, N. Rega, J. M. Millam, M. Klene, J. E. Knox, J. B. Cross, V. Bakken, C. Adamo, J. Jaramillo, R. Gomperts, R. E. Stratmann, O. Yazyev, A. J. Austin, R. Cammi, C. Pomelli, J. W. Ochterski, R. L. Martin, K. Morokuma, V. G. Zakrzewski, G. A. Voth, P. Salvador, J. J. Dannenberg, S. Dapprich, A. D. Daniels, O. Farkas, J. B. Foresman, J. V. Ortiz, J. Cioslowski, and D. J. Fox, Gaussian 09, Revision D.01, Gaussian, Inc., Wallingford CT, 2013.

[22] P. Fuentealba, H. Preuss, H. Stoll and, L. Von Szentpály, *Chem. Phys. Lett.,* 1982, **89**, 418.